Thermally stable C2-Symmetric α-Diimine Nickel Precatalysts for ethylene polymerization: semicrystalline to amorphous PE with high tensile and elastic properties

Xiaoxu Li,[a,†] Zexu Hu,[a,†] Qaiser Mahmood,[a,*] Yizhou Wang,[b] Sunny Sohail,[a,b] Song Zou,[b] Tongling Liang,[b] Wen-Hua Sun[a,b,*]

[a]Chemistry and Chemical Engineering Guangdong Laboratory, Shantou, 515031, China.
[b]Key Laboratory of Engineering Plastics, Institute of Chemistry, Chinese Academy of Sciences, Beijing, 100190.
[†]These authors equally contributed.
*Corresponding authors; Email address: qaiser@ccelab.com.cn (Q. Mahmood); whsun@iccas.ac.cn (W.-H. Sun)

Contents

1	General conditions
2	Synthesis of imino-ketone and L-iPr$_3$ ligand
3	X-ray crystallographic studies
4	Crystal data and structural refinements for complexes
5	Typical procedure for ethylene polymerization
6	^{1}H and ^{13}C spectra of organic compounds
7	^{1}H NMR spectra of obtained polyethylene using different nickel complexes at different temperatures
8	^{13}C NMR spectrum of polyethylene obtained at 40 ℃ temperature using NiBr-iPr
9	GPC curves of obtained polyethylene using NiBr-iPr at different temperatures
10	DSC curves of obtained polyethylene using different nickel complexes at different temperatures
11	Wide-angle X-ray diffraction (WAXD) spectra of the polyethylene
12	ESI-MS spectra of ligands, and their nickel complexes
13	References

1. General conditions

All manipulations involving air and/or moisture sensitive compounds were performed under an atmosphere of nitrogen using standard Schlenk techniques. Methylaluminoxane (MAO, 1.67 M in toluene) and modified methylaluminoxane (MMAO, 1.93 M in heptane) were purchased from Anhui Botai Electronic Materials Co. Dimethylaluminum chloride (Me_2AlCl, 0.9 M in heptane) and diethylaluminum chloride (Et_2AlCl, 2.0 M in hexane) were supplied from Shanghai Macklin Biochemical Co., Ltd. High-purity ethylene was purchased from Guangdong Jieyang Petrochemical Company and used as received. Acenaphthylene-1,2-dione was bought from Macklin with 98% purity. The common aniline 2,6-$iPr_2C_6H_3$ were obtained from, Heowns and Macklin with 98% purity. $ZnCl_2$ used as catalyst during the synthesis of bulky aniline was obtained from Macklin with 98% purity. $(DME)NiBr_2$ with 97% purity was obtained from Leyan. *p*-Toluenesulfonic acid monohydrate used as catalysts during synthesis of ligands was obtained from Dingjiuding Chemicals with 98% purity. Toluene was obtained from Xihua, with purity ≥ 99.5 with $H_2O\% \leq$ 0.03% which was distilled over sodium before use. Other reagents were purchased from Aldrich, Acros or local suppliers. The Bulk aniline was prepared using the literature route [1]. ^1H and ^{13}C NMR spectroscopic measurements for the organic compounds were performed using a Bruker AVANCE III 600WB spectrometer at 599.92 MHz with 1024 and 16 scans respectively. Operating conditions used for ^1H and ^{13}C spectra: spectral width 15.0 kHz; acquisition time 2.1845 s; relaxation delay 2.0 s. Chemical shifts are measured in ppm for the ^1H and ^{13}C NMR spectra and are relative to TMS as an internal standard. Elemental analyses were conducted on a Flash EA 1112 microanalyzer. FT-IR spectra were carried out using a PerkinElmer System 2000 FT-IR spectrometer. The sample is grinded with KBr to prepare a homogeneous KBr pellet for scanning. The concentration of the sample in KBr was maintained in the range of 0.2% to 1%. The frequency ranges were measured as wave numbers typically over the range 4000–400 cm^{-1} using, OMNIC software. Molecular weights (M_w) and molecular weight distributions ($Đ$) of the polyethylenes were determined using a PL-GPC220 instrument at 150 °C with 1,2,4-trichlorobenzene as the solvent. The flow rate of TCB was kept at 1.00 ml/min with injection volume 200.0 µl and column length was settled at 650 mm. The columns used has specifications 2 × PLgel MIXED-B 10µm 300 × 7.5 mm. Sample concentration was kept at 0.1 mg/ml. Narrow standards for calibration were used. The melting

temperatures of the polyethylenes were measured from the second scanning run on a PerkinElmer TA-Q2000 DSC analyzer under a nitrogen atmosphere. In the procedure, a sample of about 4.0–6.0 mg was heated to 150 °C at a heating rate of 20 °C min^{-1} and kept for 5 min at 150 °C to remove the thermal history and then cooled at a rate of 20 °C min^{-1} to 25 °C. The ^{1}H NMR spectra of the polyethylenes were recorded on a Bruker DMX 300 MHz instrument at 110 °C and ^{13}C at 110 °C in deuterated tetrachloroethane with TMS as an internal standard and peaks were integrated using deconvolution method. Operating conditions used for ^{1}H spectra: spectral width 15 kHz; acquisition time 2.1889 s; relaxation delay 2.0 s. Operating conditions used for ^{13}C spectra: spectral frequency 125.70 MHz; pulse width 10.0 Ms; spectral width 21.3675 kHz; acquisition time 0.7668 s; relaxation delay 5.0 s; number of scans 2048. The chemical shift values (δ) are reported in parts per million (ppm). The stress–strain curves were obtained using a universal tester (Instron 1122, UK). To make sure the results are consistent, every sample is test five times for fracture test. [Sample size: width 5 mm, thickness 1 mm, length 30 mm, shape: rectangle]. Twice for cyclic tensile test. [Sample size: width 2.5 mm, thickness 1 mm, length 15 mm, shape: rectangle] In the fracture test, the program is set to a constant speed of 50mm/min, and in the cyclic tensile test, the constant speed of 50mm/min is continued, and the cycle is carried out when the strain reaches 300%. The electrospray (ESI) mass spectra for the complexes and the high resolution mass spectra for all new organic compounds were measured using Bruker 9.4 T Solarix (FT-ICR-MS) instrument.

2. Synthesis of imino-ketone and L-iPr$_3$ ligand

Synthesis of imino-ketone: To a solution of acenaphthenequinone (1.01 g, 5.56 mmol) in ethanol (100 mL), a solution of 2,4-bis(bis(4-fluorophenyl)methyl)-6-isopropylaniline (3.0 g, 5.56 mmol) in dichloromethane (100 mL) was added, followed by para-toluenesulfonic acid (0.19 g, 1.11 mmol, 20%) as a catalyst was added. After 24 h of stirring at room temperature, volatiles were removed under vacuum, and the residue was purified by alumina column chromatography using petroleum ether/ethyl acetate/triethylamine (500:40:3), affording the red crystalline imino-ketone (1.71 g, 43%). The product was used in the next step without further analysis.

Synthesis of L-iPr$_3$: To a solution of imino-ketone (1.71 g, 2.43 mmol) and p-toluenesulfonic acid (20 mol%) in dry toluene (100 mL) was added dropwise 2,6-diisopropylaniline (0.29 g, 2.43 mmol and the reaction mixture stirred and heated to

reflux for 12 h using a Dean-Stark trap. After cooling to room temperature, the solvent was removed under reduced pressure. The residue was purified by alumina column chromatography using petroleum ether/ethyl acetate/triethylamine (500:10:3) as the eluent affording **L-iPr$_3$** as a deep yellow crystalline solid (0.58 g, 30%). ^{1}H NMR (600 MHz, Chloroform-d) δ 7.81 (d, J = 8.2 Hz, 1H), 7.78 (d, J = 8.2 Hz, 1H), 7.33 – 7.29 (m, 2H), 7.12 (t, J = 7.7 Hz, 1H), 7.09 – 6.96 (m, 9H), 6.90 (dd, J = 8.6, 5.4 Hz, 2H), 6.85 (t, J = 8.6 Hz, 2H), 6.78 (dd, J = 8.3, 5.3 Hz, 2H), 6.54 (d, J = 7.2 Hz, 1H), 6.49 (d, J = 1.9 Hz, 1H), 6.20 (d, J = 7.2 Hz, 1H), 6.16 (t, J = 8.5 Hz, 2H), 5.67 (s, 1H), 5.51 (s, 1H), 3.24 – 3.13 (m, 1H), 2.87 (dq, J = 13.7, 6.8 Hz, 2H), 1.31 (d, J = 6.8 Hz, 4H), 1.19 (d, J = 6.8 Hz, 3H), 1.14 (d, J = 6.8 Hz, 3H), 1.09 (d, J = 6.9 Hz, 3H), 0.91 (d, J = 6.7 Hz, 4H).^{13}C NMR (151 MHz, Chloroform-*d*) δ 162.94, 162.61, 160.99, 147.51, 147.14, 140.68, 140.19, 136.13, 135.80, 135.61, 131.48, 131.43, 131.01, 130.95, 130.90, 130.86, 129.36, 129.16, 128.78, 128.00, 127.25, 125.42, 124.88, 124.00, 123.84, 123.57, 115.52, 115.50, 115.38, 115.36, 115.10, 114.96, 114.90, 114.76, 55.30, 51.26, 29.04, 29.00, 28.69, 24.59, 23.97, 23.59, 23.38, 23.23, 22.87.FTIR (KBr, cm^{-1}): 744 (w), 787 (m), 834 (s), 925 (w), 1015 (w), 1094 (w), 1157 (m), 1225 (s), 1434 (w), 1457 (w), 1506 (s), 1599 (m), 1650 (m), 1676 (ν(C=N), w), 3053 (w). Anal. Calcd. for $C_{59}H_{50}F_4N_2$ (863.06): C, 82.11; H, 5.84; N, 3.25. Found: C, 81.66; H, 6.00; N, 2.97. MS-ESI (m/z): calcd. for $[(C_{59}H_{50}F_4N_2)+H]^+$: 863.39829, found: 863.39870.

Synthesis of NiBr-iPr$_3$: To a solution of **L-iPr$_3$** (0.3 g, 0.34 mmol) in dichloromethane (10 mL) was added (DME)$NiBr_2$ (0.099 g, 0.32 mmol) under a nitrogen atmosphere. The reaction mixture was stirred for 24 h at ambient temperature. The most of the solvent was removed under reduced pressure and excess diethyl ether was added to precipitate the product. The product was collected by filtration, washed with diethyl ether (3 × 5 mL) and then dried under reduced pressure to give **NiBr-iPr$_3$** as a deep red solid (0.31 g, 85%). FTIR (KBr, cm^{-1}): 708 (w), 779 (m), 833 (s), 935 (w), 1016 (w), 1098 (w), 1158 (m), 1224 (s), 1435 (w), 1463 (w), 1507 (s), 1601 (m), 1620 (ν(C=N), w), 3064 (w). Anal. Calcd. for $C_{59}H_{50}Br_2F_4N_2Ni$ (1081.56): C, 65.52; H, 4.66; N, 2.59. Found: C, 64.29; H, 4.86; N, 2.32. MS-ESI (m/z): calcd. for $[(C_{59}H_{50}F_4N_2)NiBr+CH_2Cl_2]^+$: 1083.19750, found: 1083.29501.

3. X-ray crystallographic studies

The single-crystal X-ray diffraction analysis of **NiBr-iPr** and **NiBr-Cl** complexes were conducted using a Rigaku Sealed Tube CCD (Saturn 724+) diffractometer,

Japan. The diffractometer employed graphite-monochromated Cu-Kα radiation with a wavelength (λ) of 0.71073 Å. The measurements were performed at a temperature of 170 (±10) K. The cell parameters were determined by globally refining the positions of all collected reflections. The intensities obtained from the X-ray diffraction analysis were corrected for Lorentz and polymerization effects; an empirical absorption correction was carried out as well. The structures of complexes **NiBr-iPr** and **NiBr-Cl** were identified via direct methods and further refined via full-matrix least squares fitting on F2. The non-hydrogen atoms in each complex were refined anisotropically. The positions of all hydrogen atoms were determined based on calculated positions. The structural solution and refinement for each complex were carried out using SHELXT (Sheldrick) software.[2] The crystal data and processing parameters for **NiBr-iPr** and **NiBr-Cl** are presented in Table S1.

4. Crystal data and structural refinements for complexes

Table S1. Crystal data and structural refinements for **NiBr-iPr,** and **NiBr-Cl**

	NiBr-iPr	**NiBr-Cl**
CCDC numbers	2378621	2378622
Bond precision	C-C = 0.0028 A	C-C = 0.0065 A
	Wavelength = 1.54184	Wavelength = 0.71073
Empirical formula	$C_{86}H_{64}Br_2F_8N_2Ni$	$C_{82}H_{59}Br_2Cl_2F_9N_4Ni$
Formula weight	1495.967	1560.76
Temperature/K	169.99(10)	170.00(10)
Crystal system	monoclinic	monoclinic
Space group	$P2_{1/c}$	$P2_1/n$
a/Å	18.0709(1)	16.2292(9)
b/Å	19.9898(2)	21.7914(10)
c/Å	20.4029(1)	20.6488(9)
α /°	90	90
β /°	97.382(1)	110.249(5)
γ /°	90	90
Volume/Å^3	7309.13(9)	6851.3(6)
Z	4	4
ρ_{calc}g/cm^3	1.359	1.513
μ /mm^{-1}	2.214	1.602

F(000)	3048.2	3168.0
F000’	2934.70	2881.52
Crystal size/mm^3	0.3 × 0.25 × 0.1	0.3 × 0.25 × 0.18
Radiation	Cu K α (λ = 1.54184)	Mo K α (λ = 0.71073)
θ range	4.94 to 154.86	3.264 to 62.154
h,k,lmax	22,25,25	23,30,29
Index ranges	-22 ⩽ h ⩽ 22, -25 ⩽ k ⩽ 24, -22 ⩽ l ⩽ 25	-19 ⩽ h ⩽ 23, -23 ⩽ k ⩽ 30, -29 ⩽ l ⩽ 28
Reflections collected	56972	65997
Independent reflections	14872[R_{int} =0.0341, R_{sigma} = 0.0306]	18600[R_{int} =0.0399, R_{sigma} = 0.0516]
Data/restraints/parameters	14872/0/861	18600/0/820
Goodness-of-fit on F^2	1.026	1.044
Data completeness	0.958	-
Theta(max)	77.430	31.077
Final *R* indexes [I>=2 σ (*I*)]	R_1 = 0.0353, wR_2 = 0.0972	R_1 = 0.0815, wR_2 = 0.2560
Final *R* indexes [all data]	R_1 = 0.0393, wR_2 = 0.1000	R_1 = 0.1137, wR_2 = 0.2749
Largest diff. peak/hole/e $Å^{-3}$	0.34/-0.52	1.93/-1.56
S	1.026	1.044
Npar	861	820

5. Typical procedure for ethylene polymerization

The polymerization process at 1MPa ethylene pressure was conducted in a 250 mL stainless steel autoclave equipped with an ethylene pressure control system, a mechanical stirrer, and a temperature controller. Initially, the autoclave was dried, then purged twice with nitrogen and once with ethylene under reduced pressure to ensure an inert environment. Then, the complex (2.0 μmol) was dissolved in 30 mL of toluene and injected into the autoclave at the required reaction temperature. An additional 30 mL of toluene was added for washing purposes. Next, the appropriate amount of co-catalyst (MAO, MMAO, Me_2AlCl, Et_2AlCl) and more toluene were added successively to reach a total volume of 100 mL. The autoclave was

immediately pressurized with 1 MPa of ethylene, and stirring was initiated. After the desired reaction time, the ethylene pressure was released, and the reaction was quenched by adding 10% hydrochloric acid in ethanol. The resulting polymer was collected, washed with ethanol, dried under reduced pressure at room temperature, and then weighed.

6. ^{1}H and ^{13}C NMR spectra of organic compounds

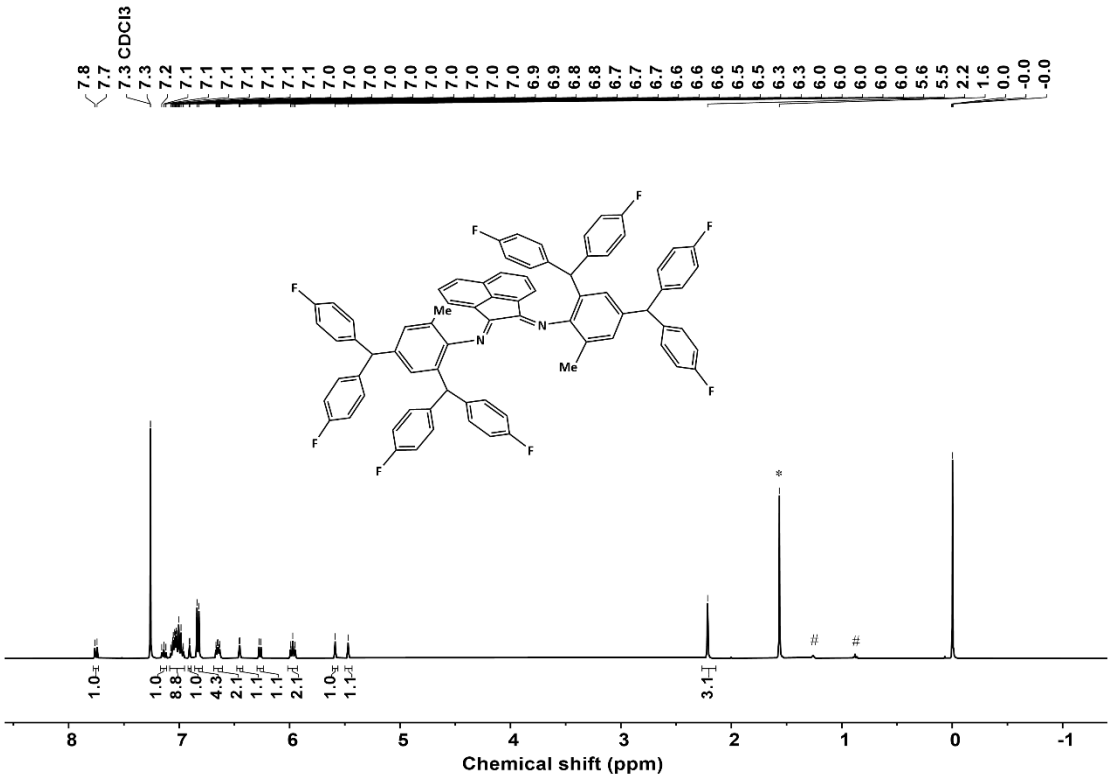

Figure S1. ^{1}H NMR spectrum (in $CDCl_3$) of **NiBr-Me** [* water and # hexane].

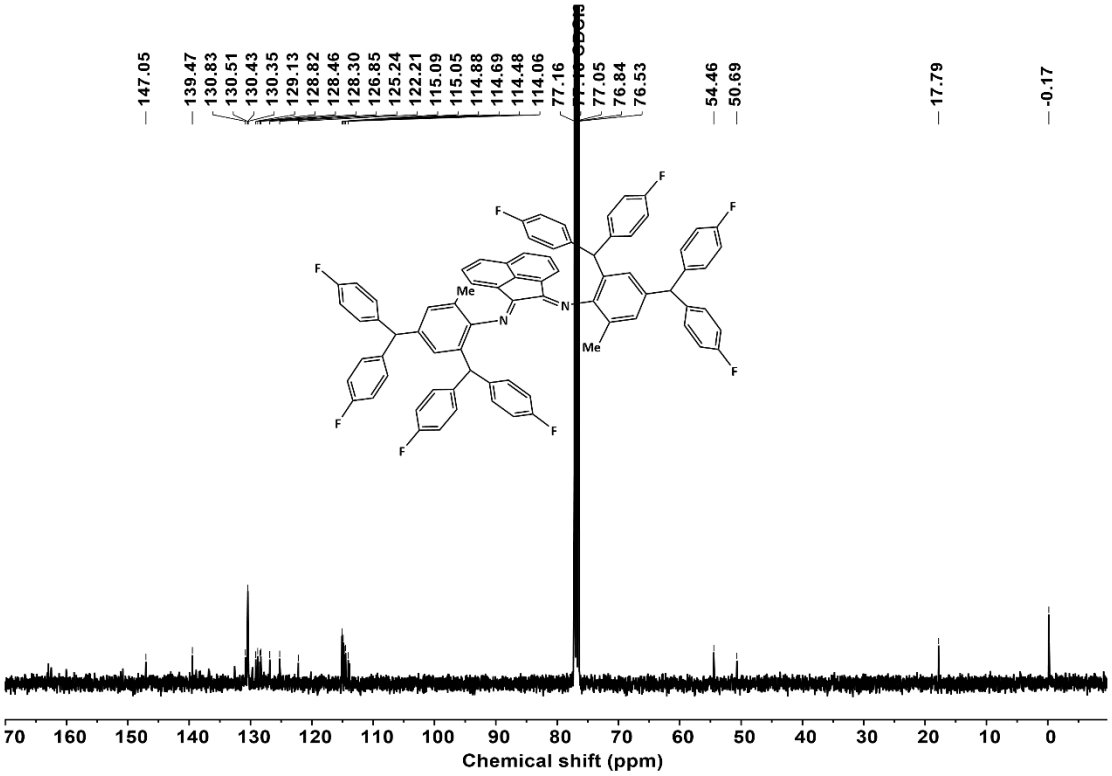

Figure S2. ^{13}C NMR spectrum (in $CDCl_3$) of **NiBr-Me**.

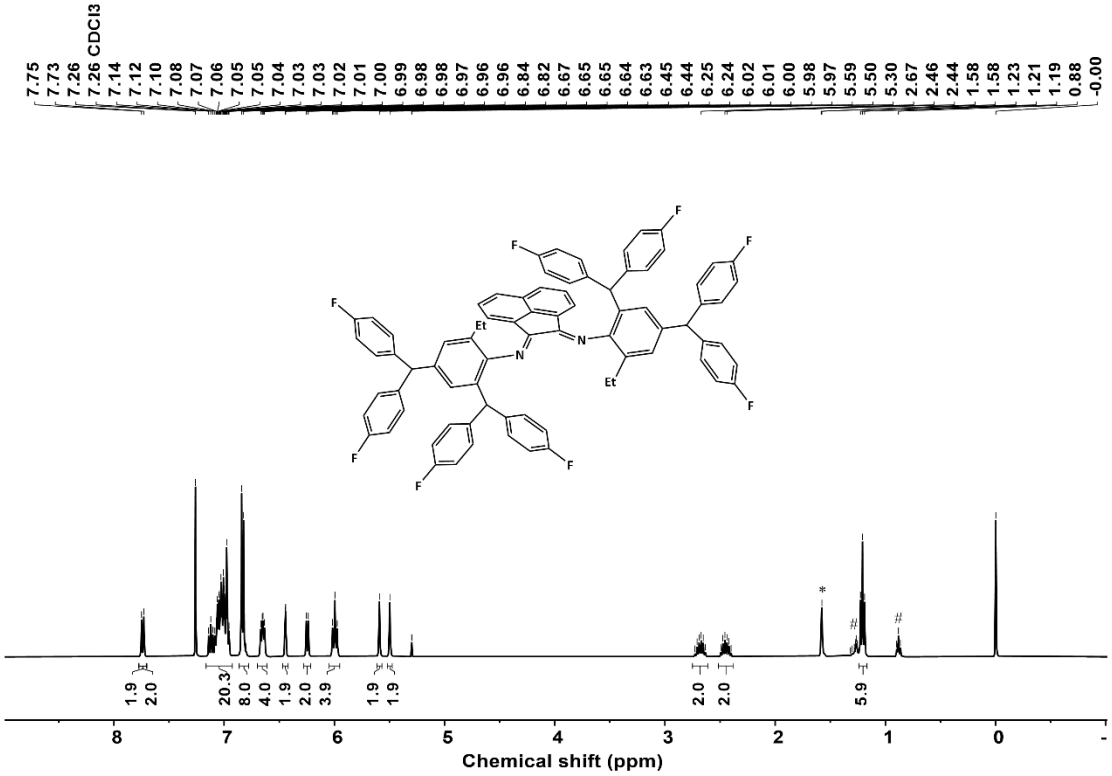

Figure S3. ^{1}H NMR spectrum (in $CDCl_3$) of **NiBr-Et** [* water and # hexane].

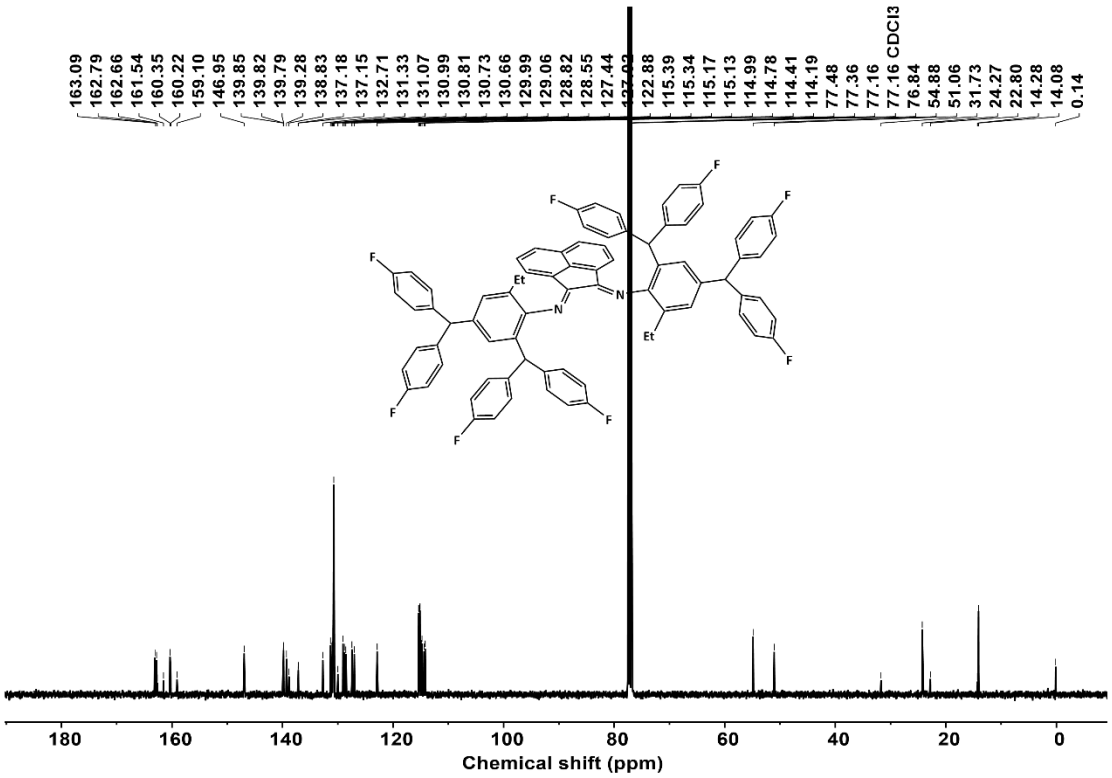

Figure S4. ^{13}C NMR spectrum (in $CDCl_3$) of **NiBr-Et**.

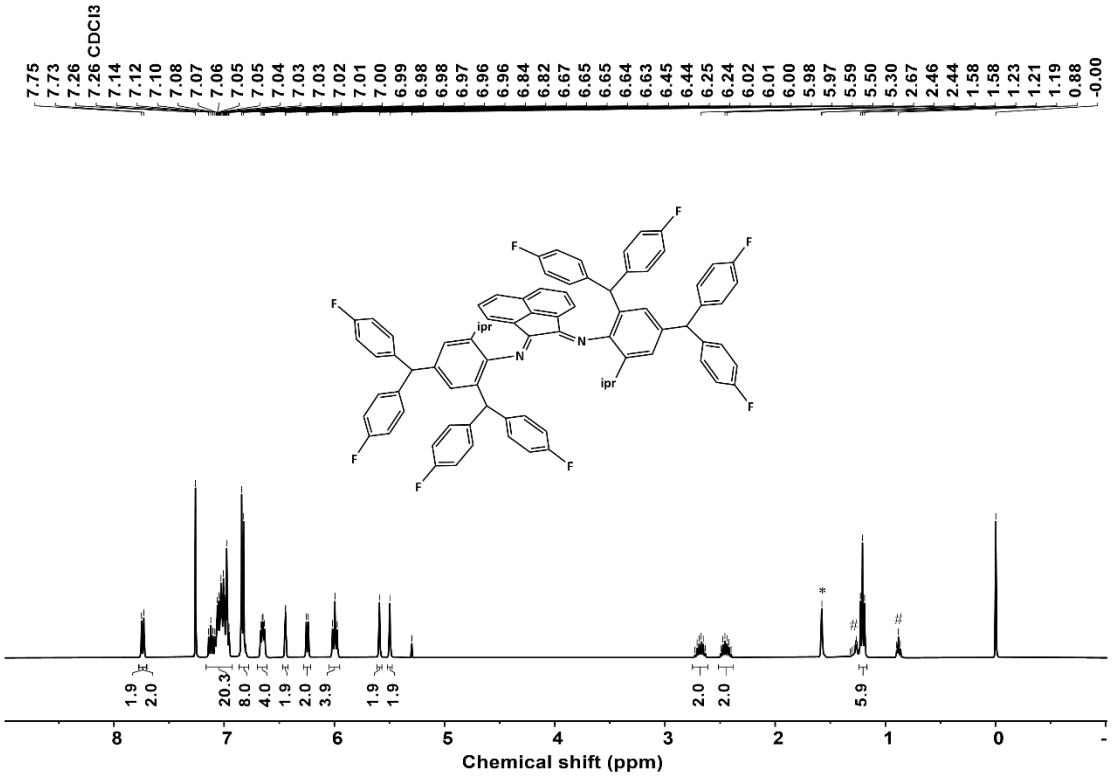

Figure S5. ^{1}H NMR spectrum (in $CDCl_3$) of **NiBr-iPr** [* water and # hexane].

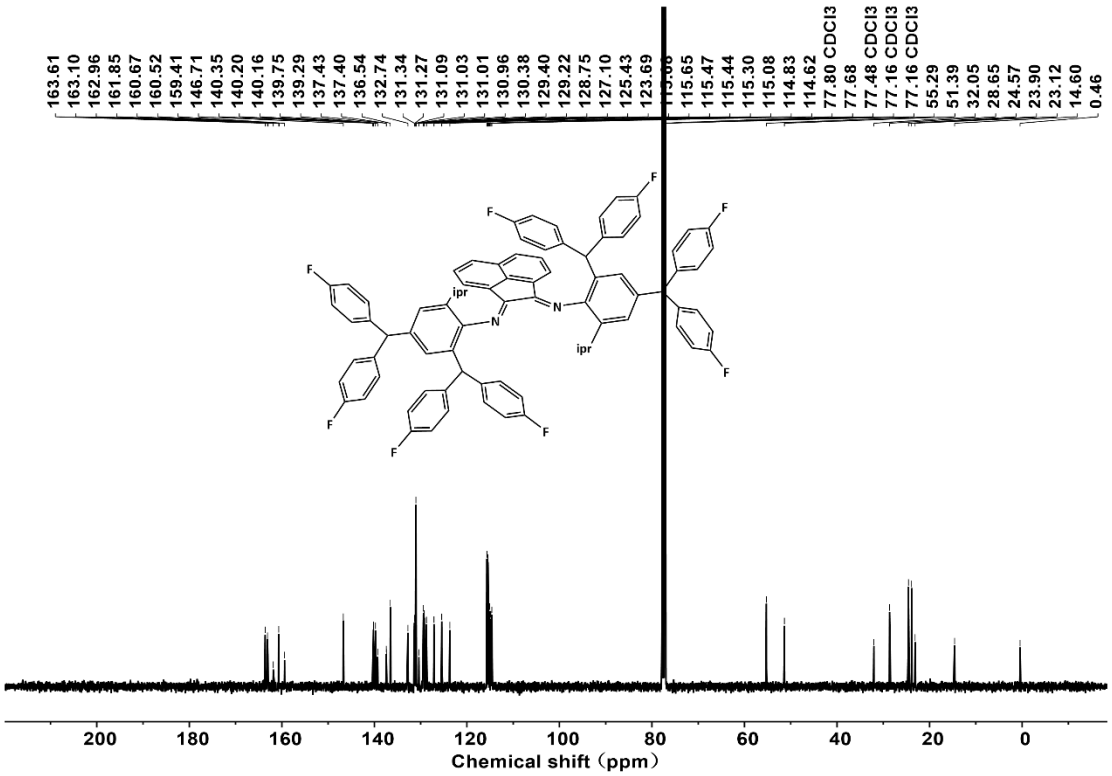

Figure S6. ^{13}C NMR spectrum (in $CDCl_3$) of **NiBr-iPr**.

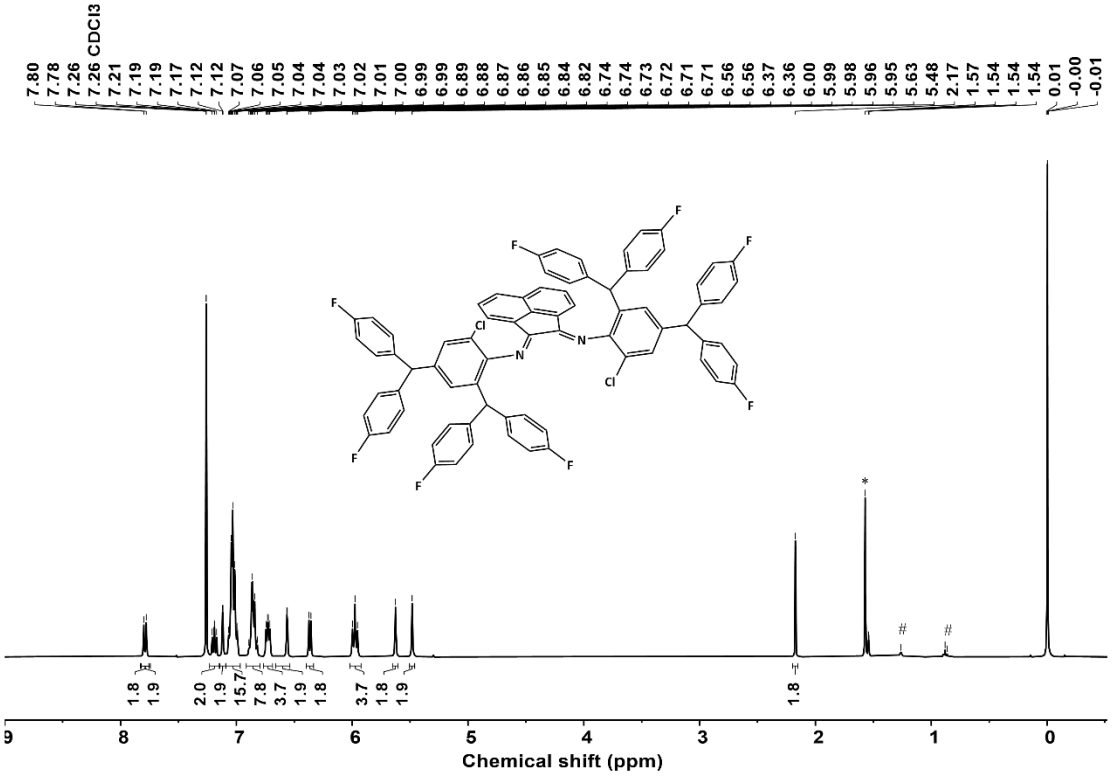

Figure S7. ^{1}H NMR spectrum (in $CDCl_3$) of **NiBr-Cl** [* water and # hexane].

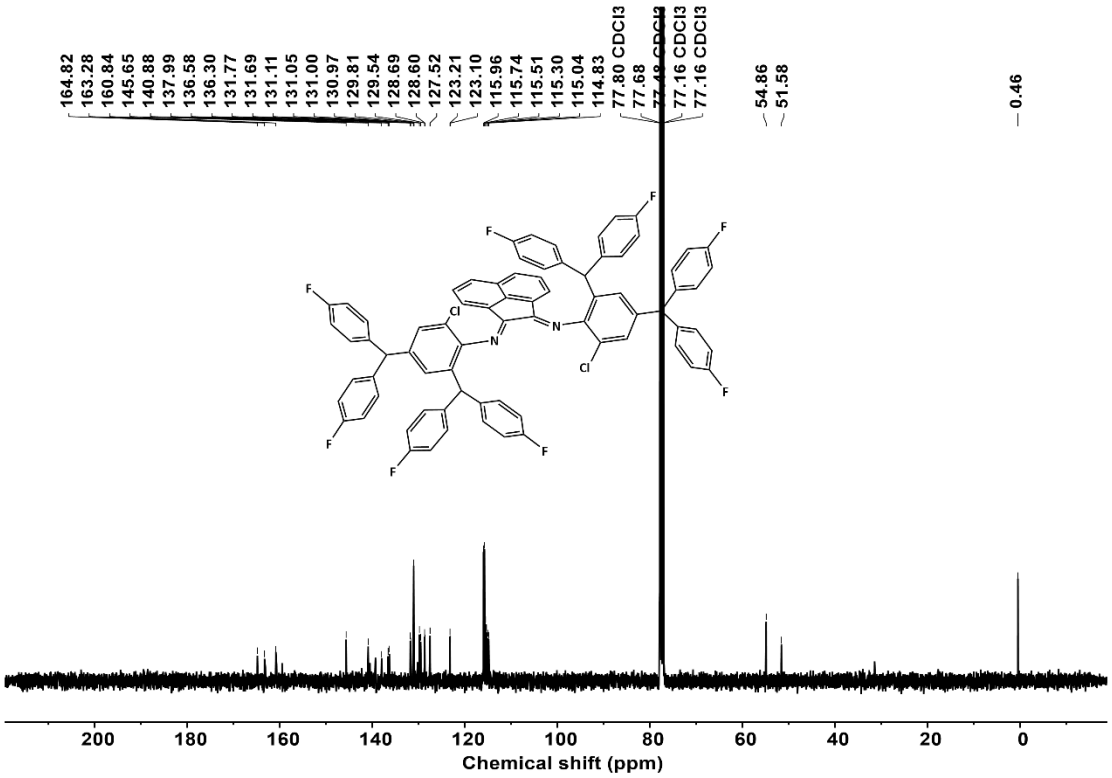

Figure S8. ^{13}C NMR spectrum (in $CDCl_3$) of **NiBr-Cl**.

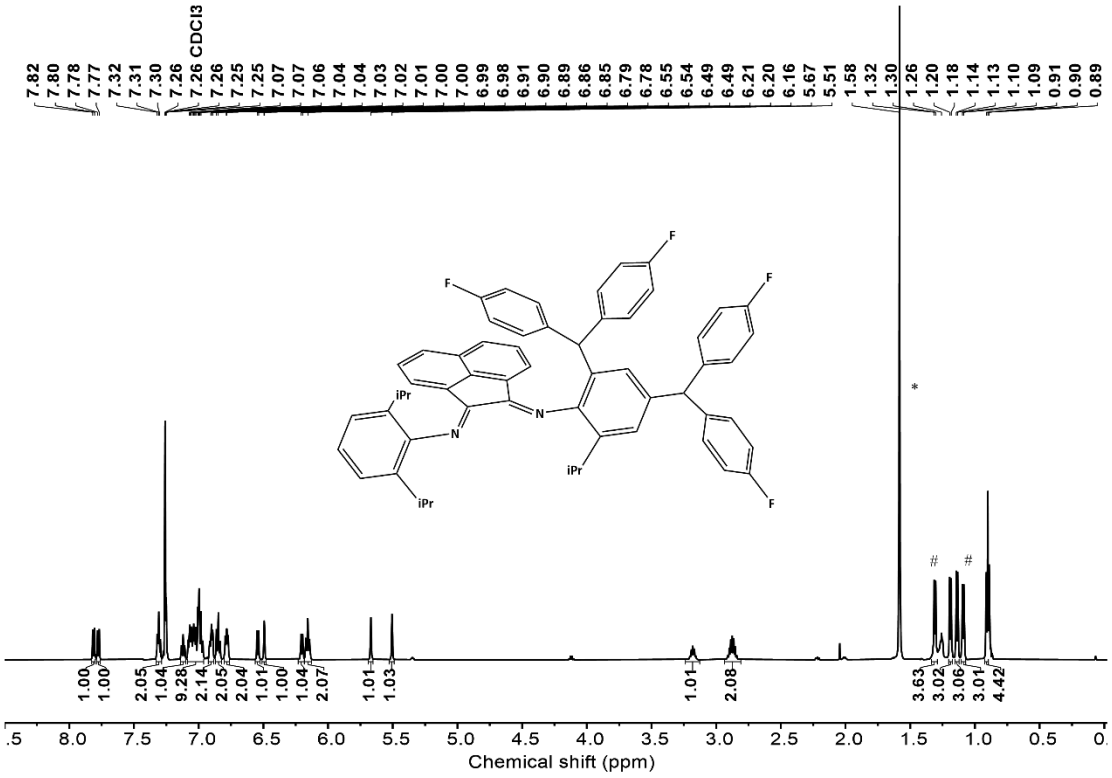

Figure S9. ^{1}H NMR spectrum (in $CDCl_3$) of **NiBr-iPr$_3$** [* water and # hexane].

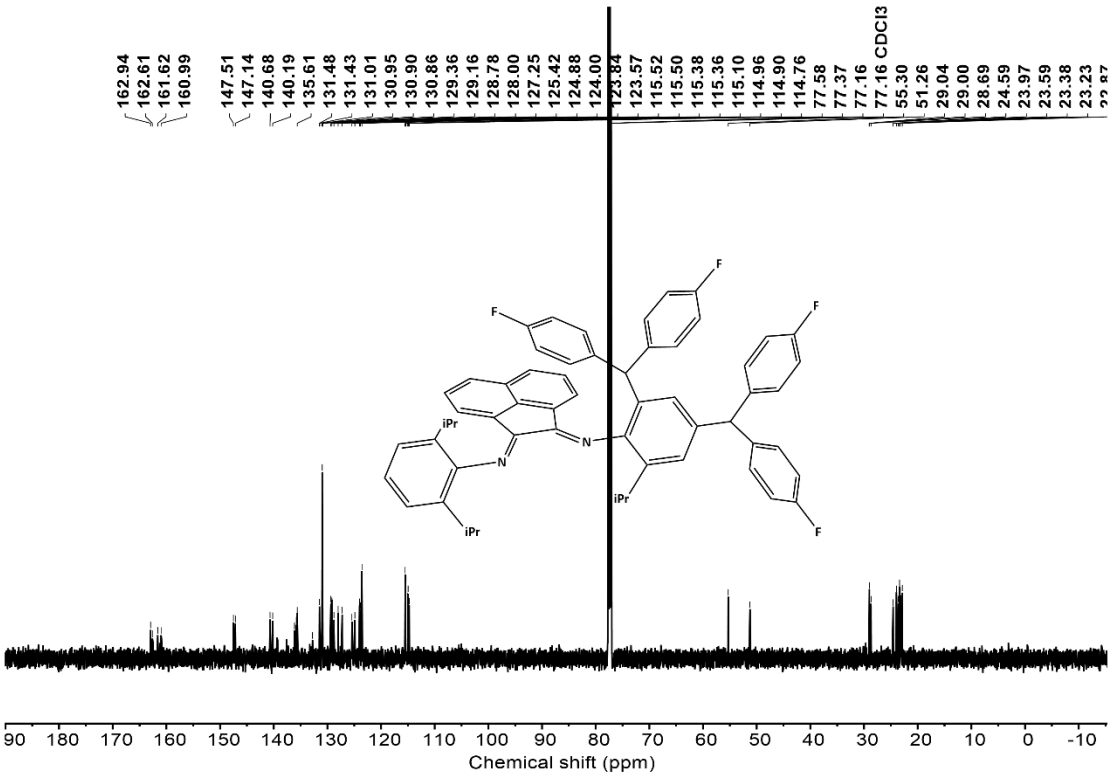

Figure S10. ^{13}C NMR spectrum (in $CDCl_3$) of **NiBr-iPr$_3$**.

7. ^{1}H NMR spectra of obtained polyethylene using different nickel complexes at different temperatures.

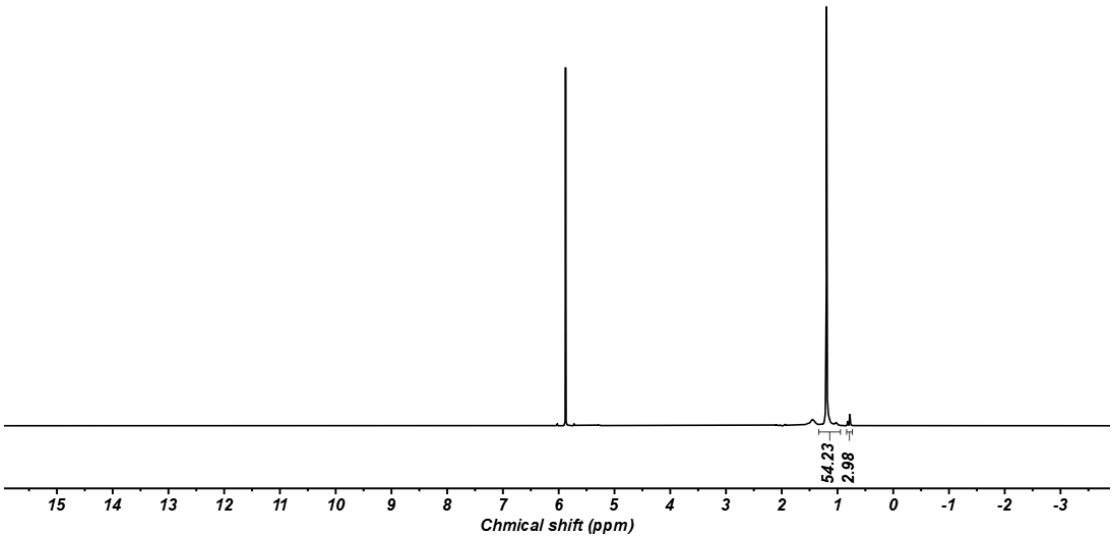

Figure S11. ^{1}H NMR spectrum of polyethylene produced using **NiBr-iPr** at 30 °C (entry 1, Table 2).

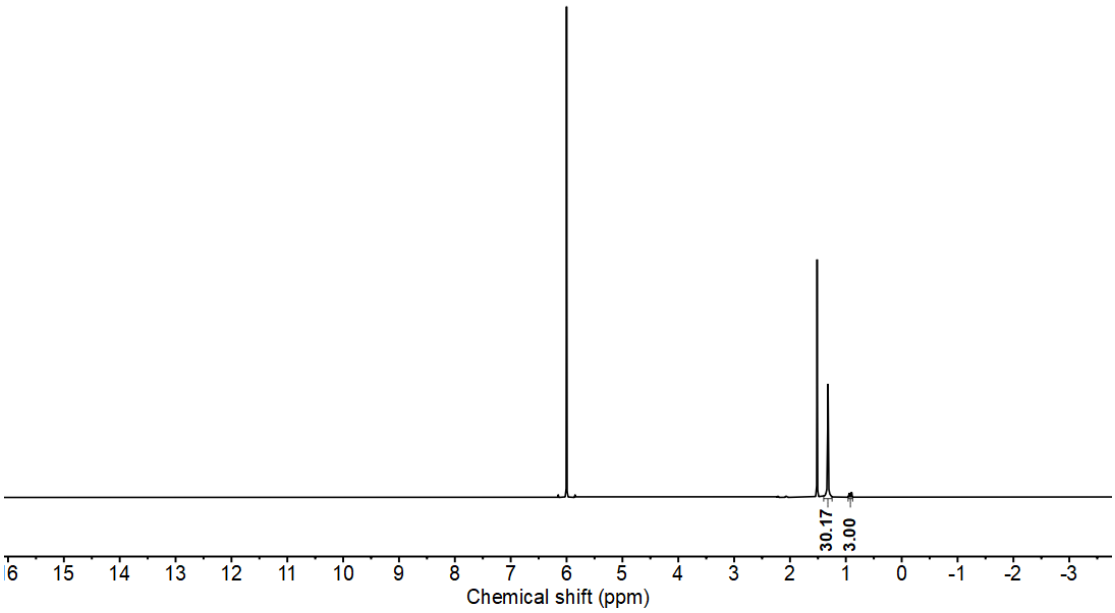

Figure S12. ^{1}H NMR spectrum of polyethylene produced using **NiBr-iPr** at 40 °C (entry 2, Table 2).

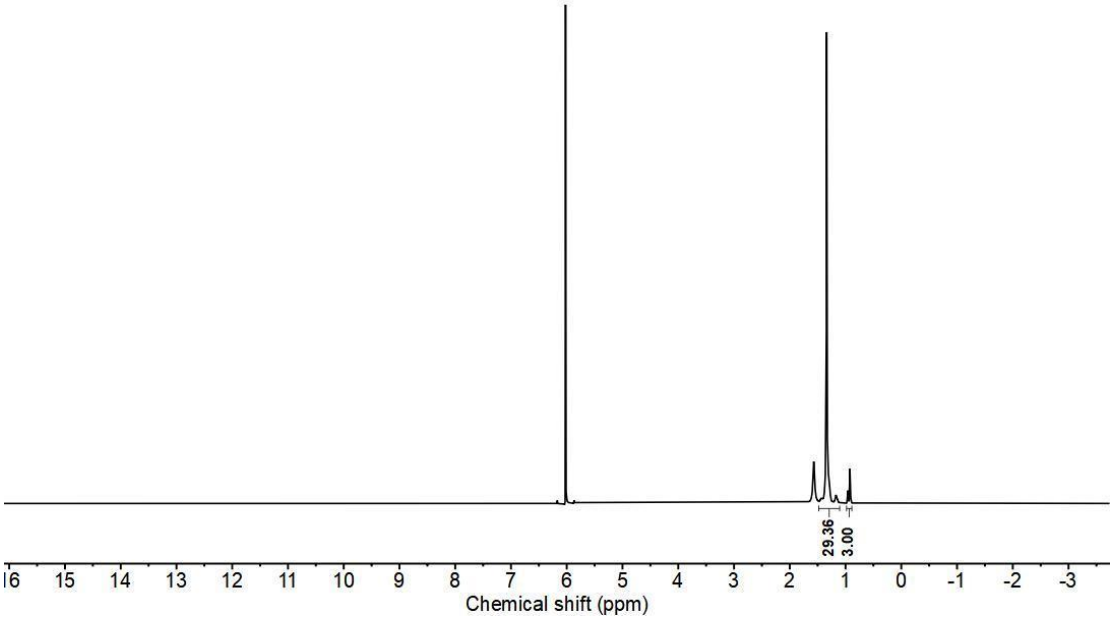

Figure S13. ^{1}H NMR spectrum of polyethylene produced using **NiBr-iPr** at 50 °C (entry 3, Table 2).

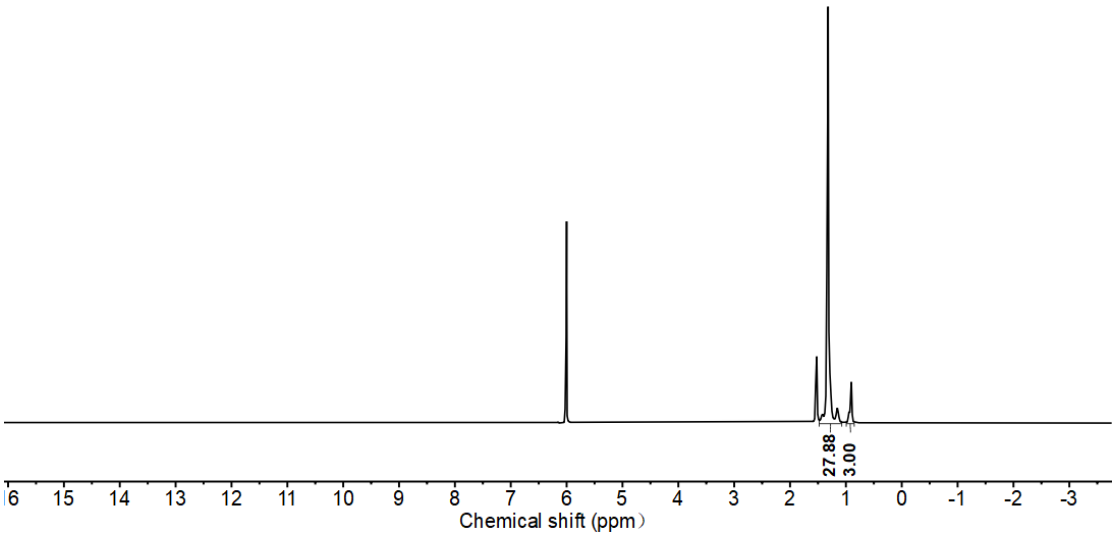

Figure S14. ^{1}H NMR spectrum of polyethylene produced using **NiBr-iPr** at 60 °C (entry 4, Table 2).

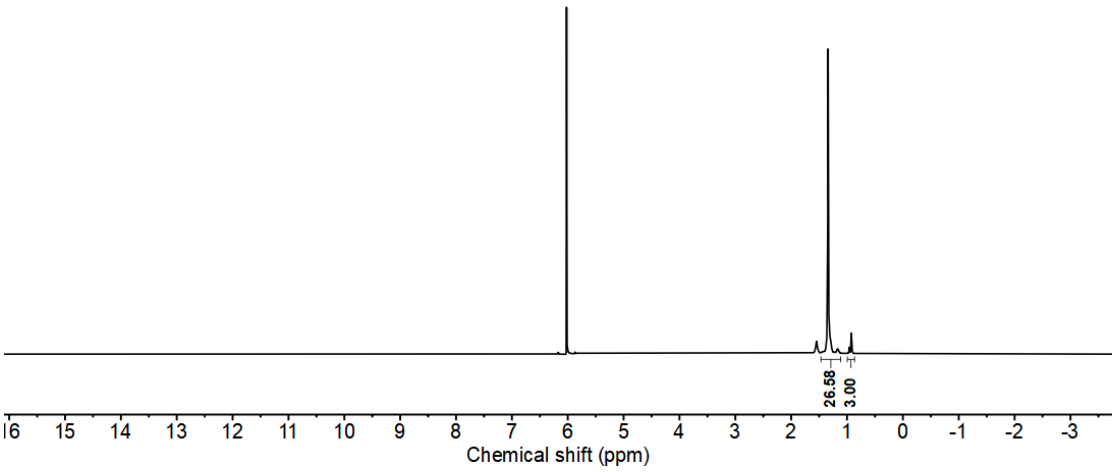

Figure S15. ^{1}H NMR spectrum of polyethylene produced using **NiBr-iPr** at 70 °C (entry 5, Table 2).

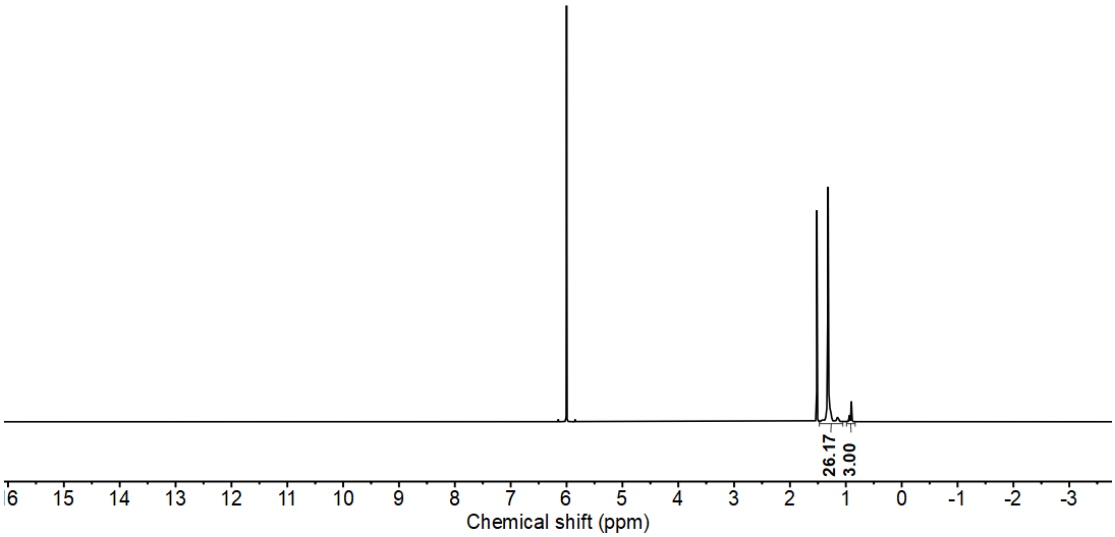

Figure S16. ^{1}H NMR spectrum of polyethylene produced using **NiBr-iPr** at 80 °C (entry 6, Table 2).

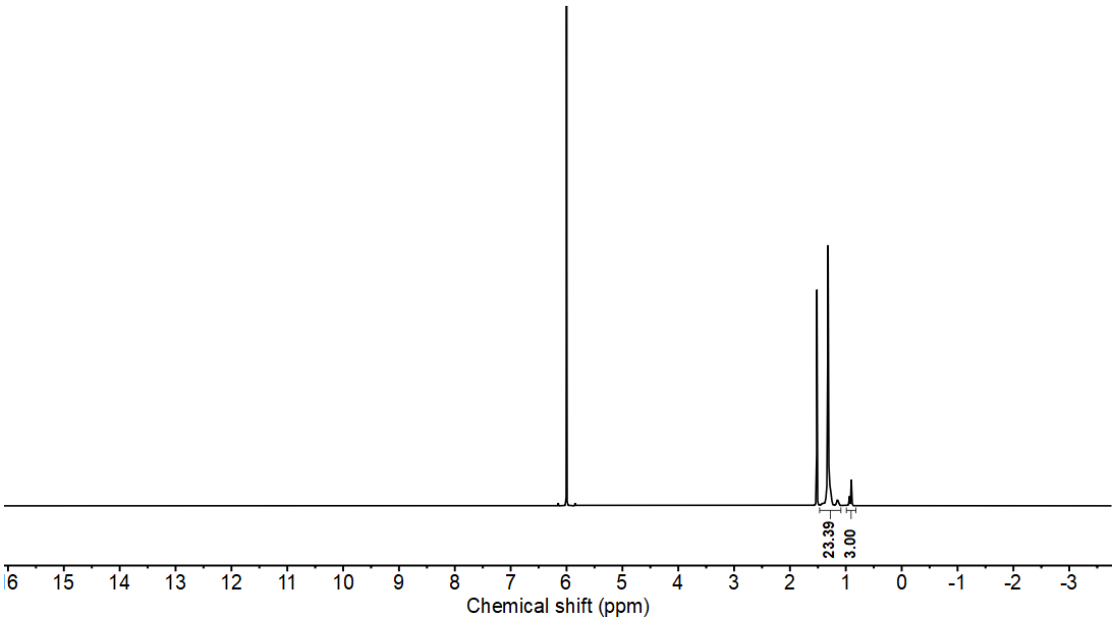

Figure S17. ^{1}H NMR spectrum of polyethylene produced using **NiBr-iPr** at 100 °C (entry 7, Table 2).

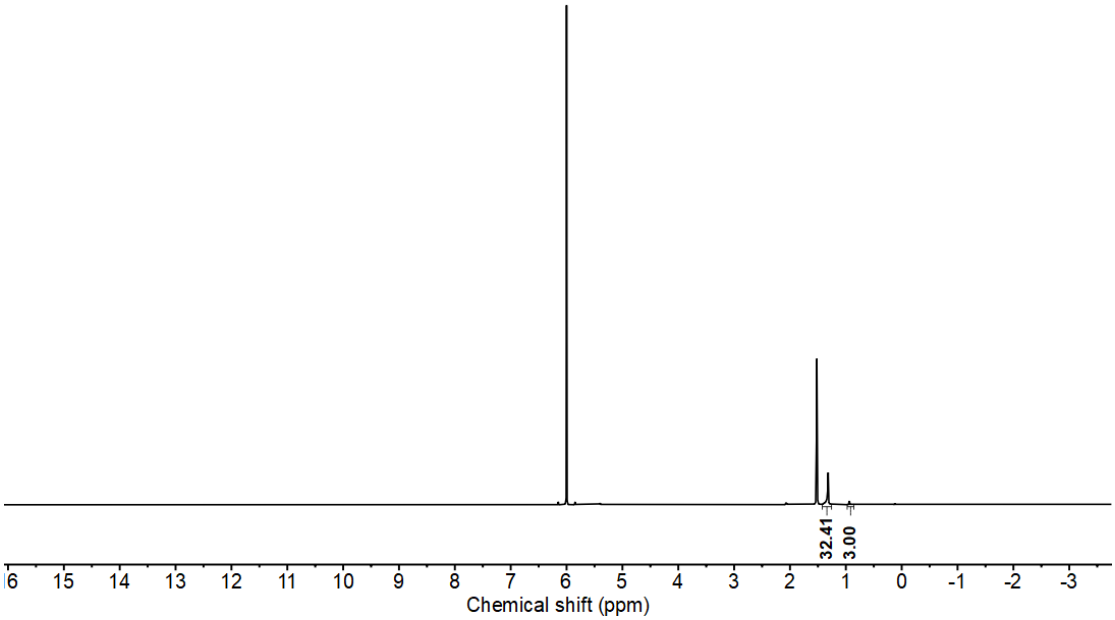

Figure S18. ^{1}H NMR spectrum of polyethylene produced using **NiBr-Et** at 40 °C (entry 8, Table 2).

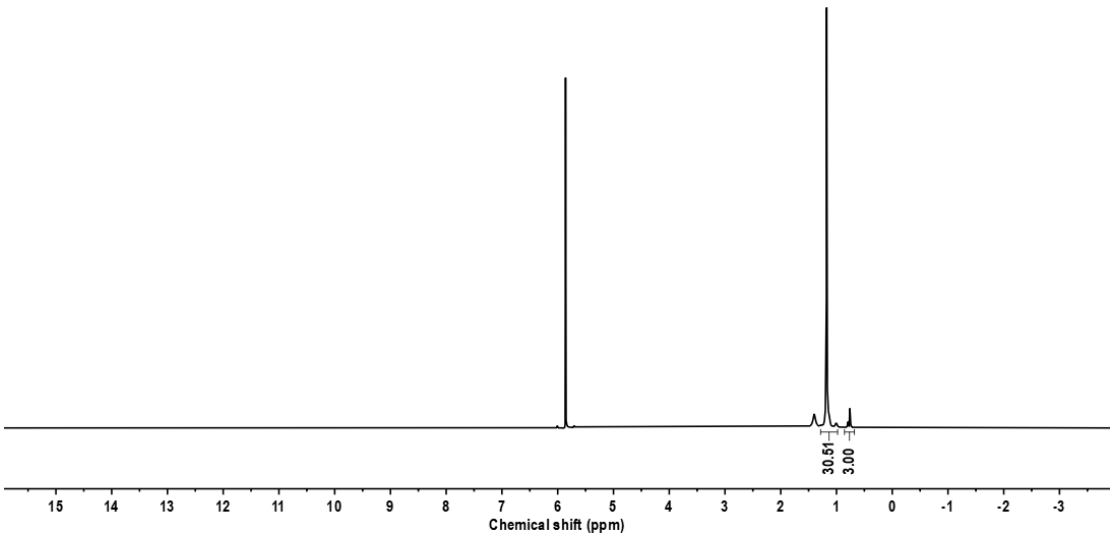

Figure S19. ^{1}H NMR spectrum of polyethylene produced using **NiBr-Et** at 60 °C (entry 9, Table 2).

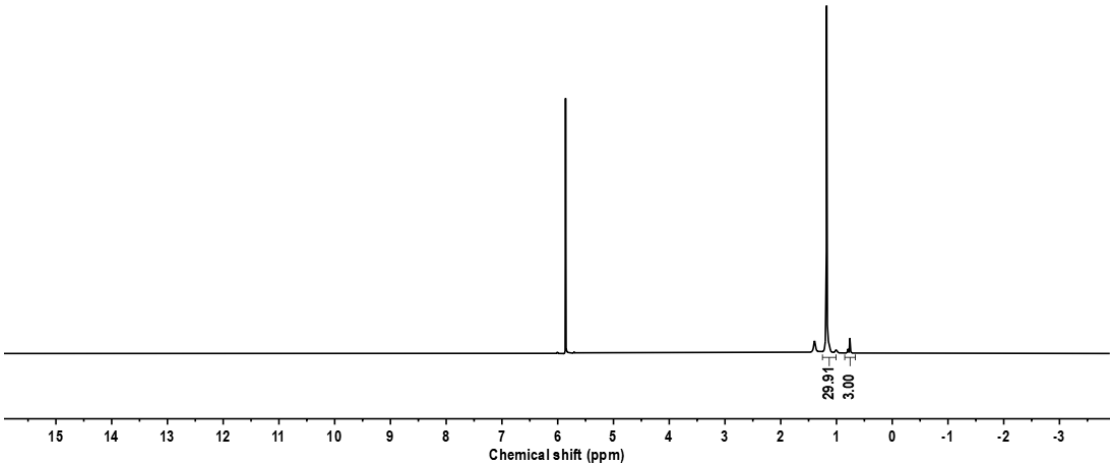

Figure S20. ^{1}H NMR spectrum of polyethylene produced using **NiBr-Et** at 80 °C (entry 10, Table 2).

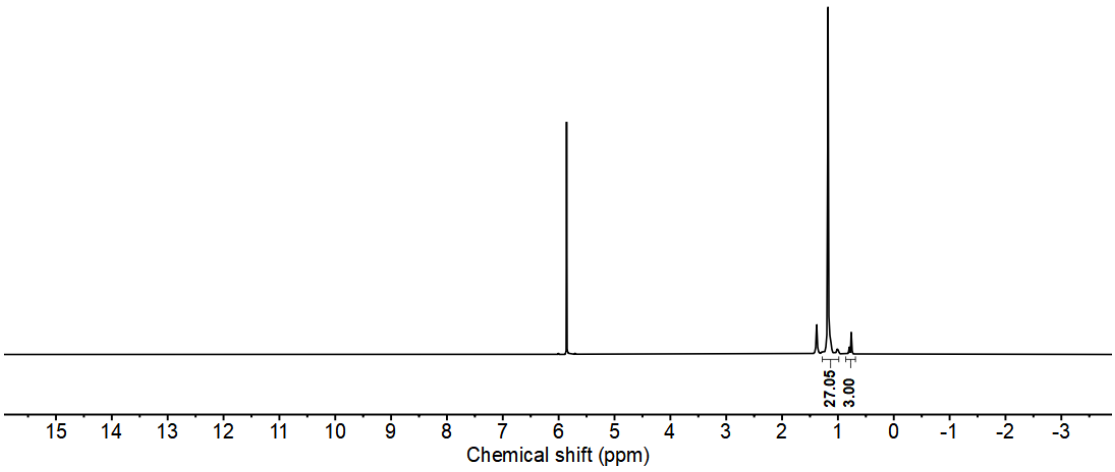

Figure S21. ^{1}H NMR spectrum of polyethylene produced using **NiBr-Et** at 100 °C (entry 11, Table 2).

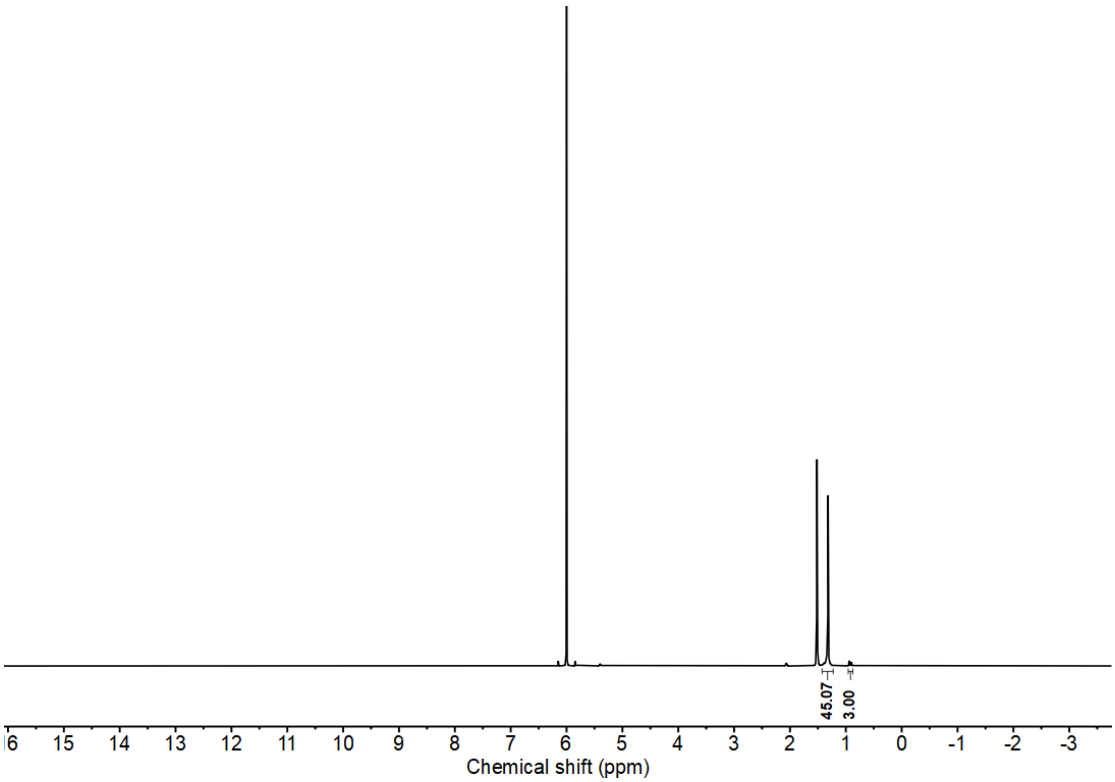

Figure S22. ^{1}H NMR spectrum of polyethylene produced using **NiBr-Me** at 40 °C (entry 12, Table 2).

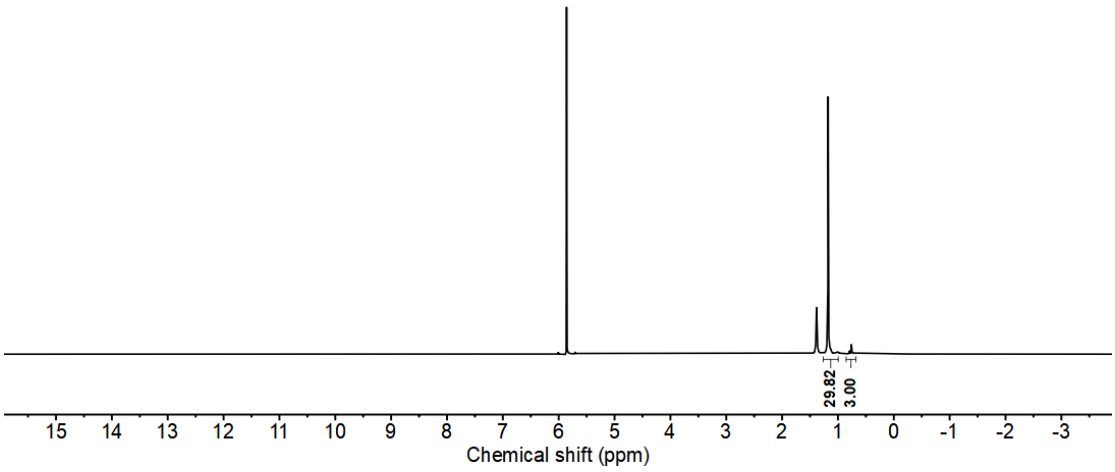

Figure S23. ^{1}H NMR spectrum of polyethylene produced using **NiBr-Me** at 60 °C (entry 13, Table 2).

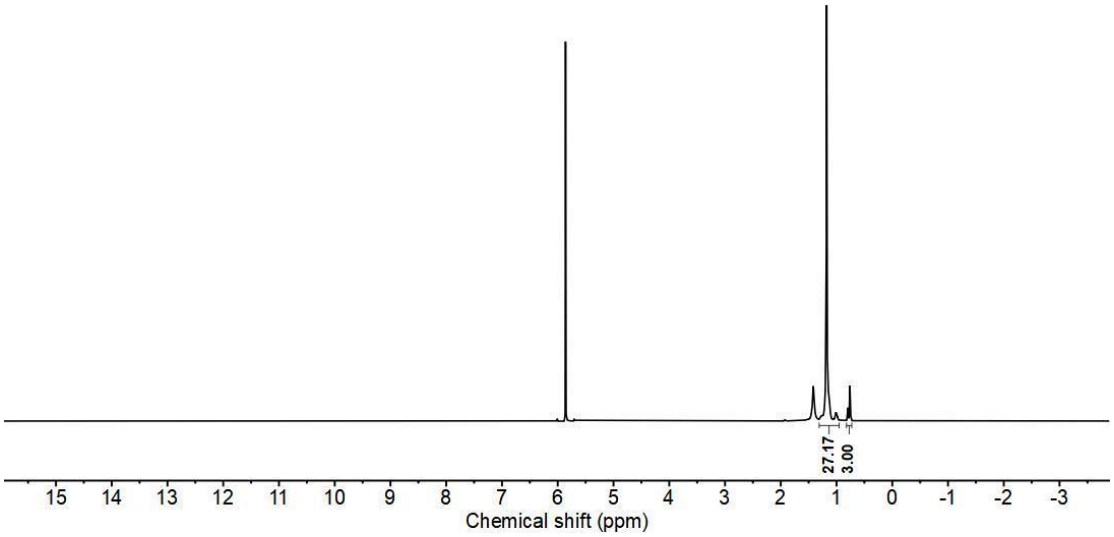

Figure S24. ^{1}H NMR spectrum of polyethylene produced using **NiBr-Me** at 80 °C (entry 14, Table 2).

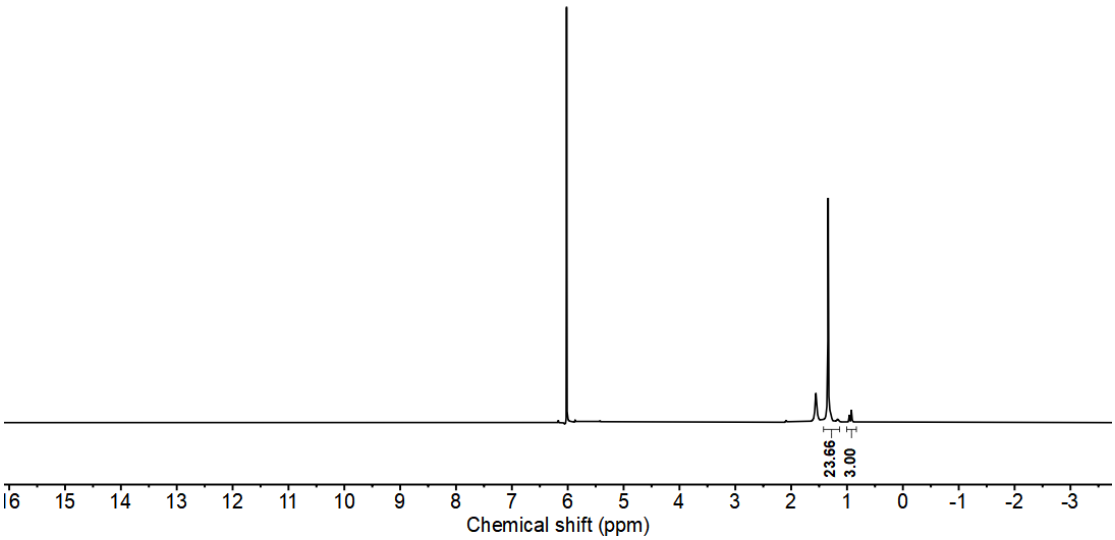

Figure S25. ^{1}H NMR spectrum of polyethylene produced using **NiBr-Me** at 100 °C (entry 15, Table 2).

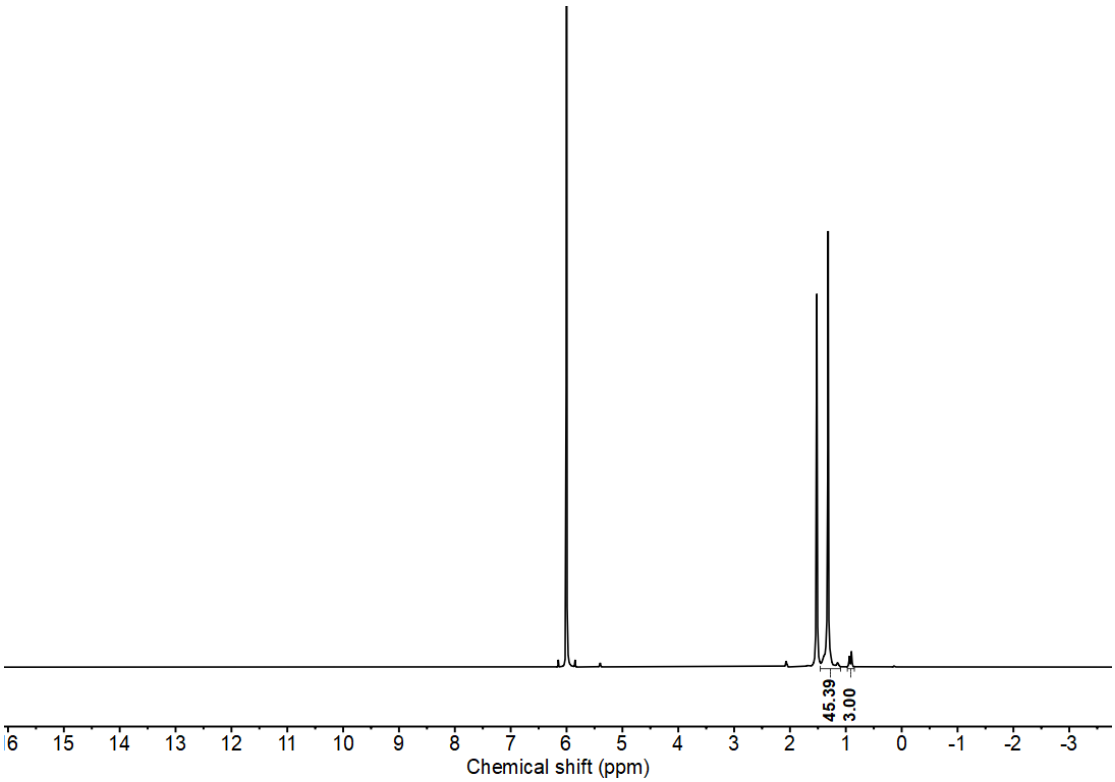

Figure S26. ^{1}H NMR spectrum of polyethylene produced using **NiBr-Cl** at 40 °C (entry 16, Table 2).

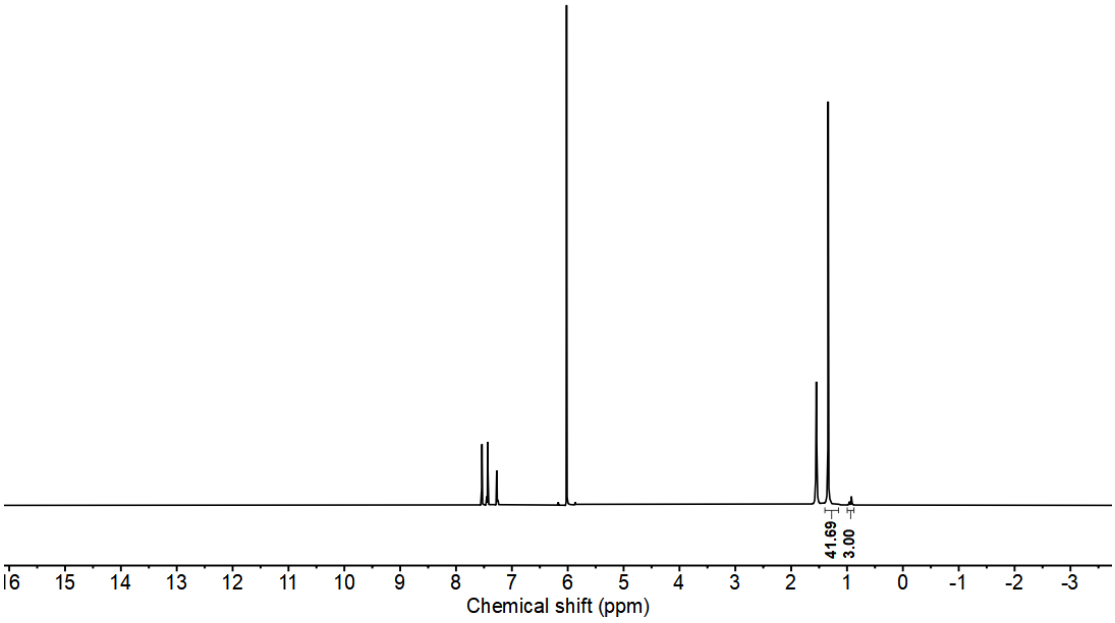

Figure S27. ^{1}H NMR spectrum of polyethylene produced using **NiBr-Cl** at 60 °C (entry 17, Table 2).

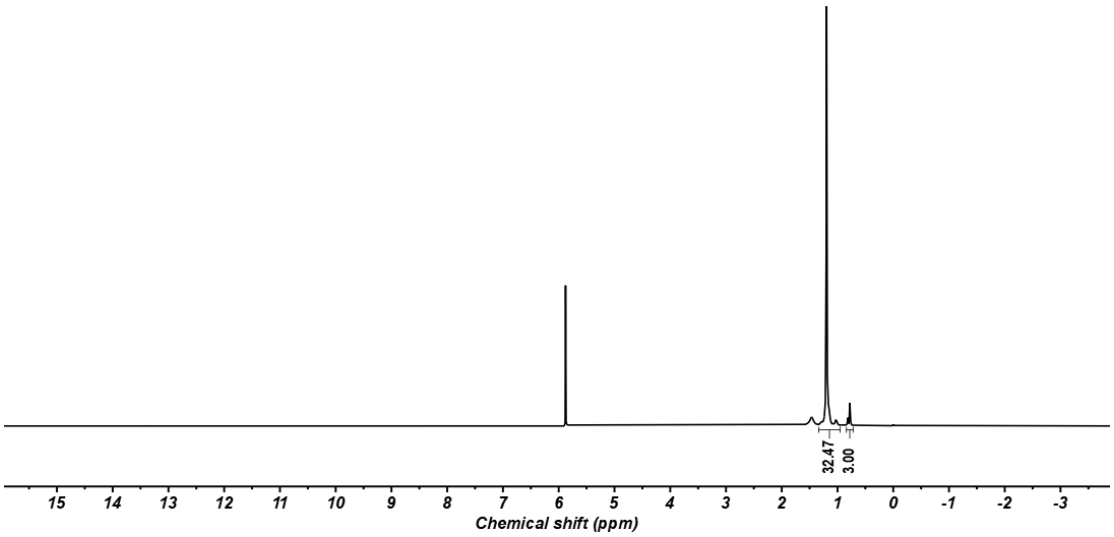

Figure S28. ^{1}H NMR spectrum of polyethylene produced using **NiBr-Cl** at 80 °C (entry 18, Table 2).

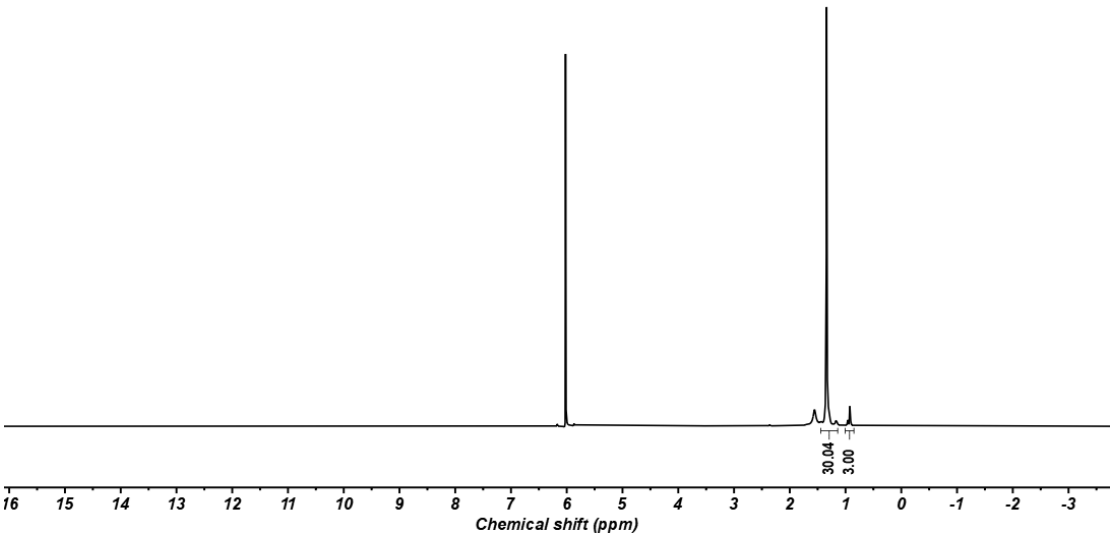

Figure S29. ^{1}H NMR spectrum of polyethylene produced using **NiBr-Cl** at 100 °C (entry 19, Table 2).

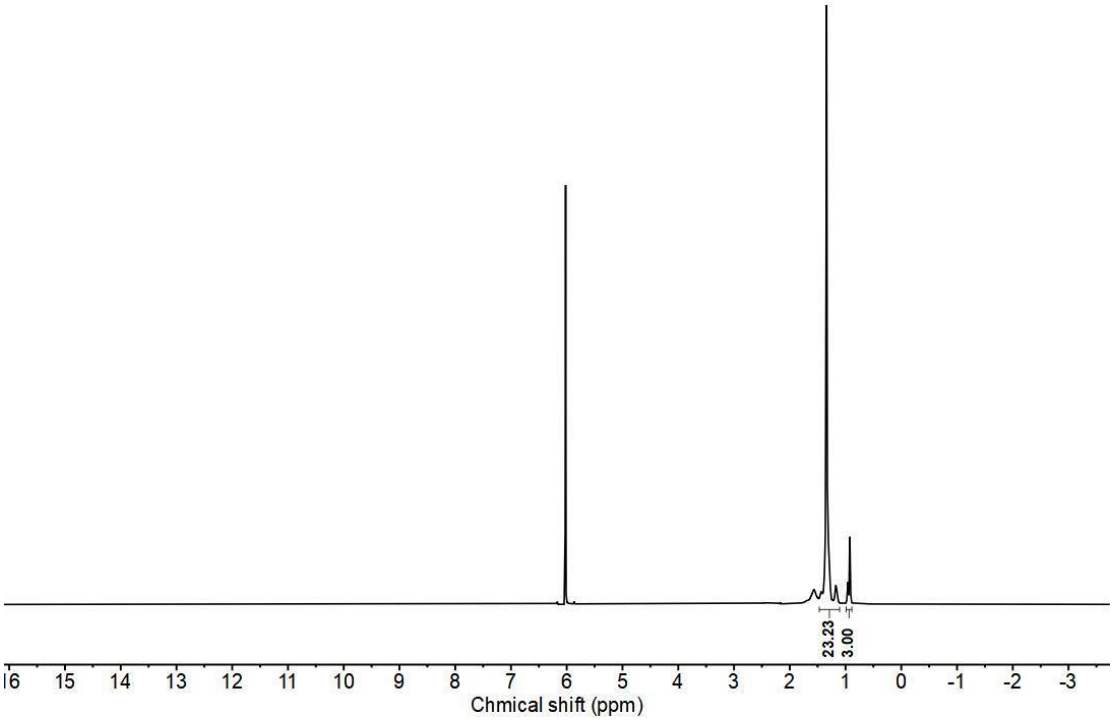

Figure S30. ^{1}H NMR spectrum of polyethylene produced using **NiBr-iPr$_3$** at 40 °C (entry 20, Table 2).

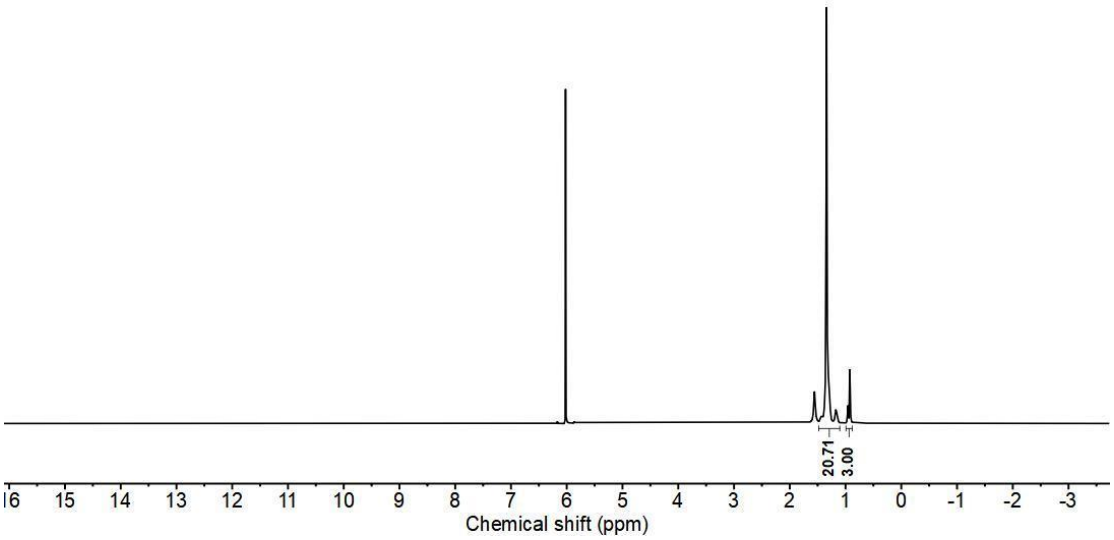

Figure S31. ^{1}H NMR spectrum of polyethylene produced using **NiBr-iPr$_3$** at 60 °C (entry 21, Table 2).

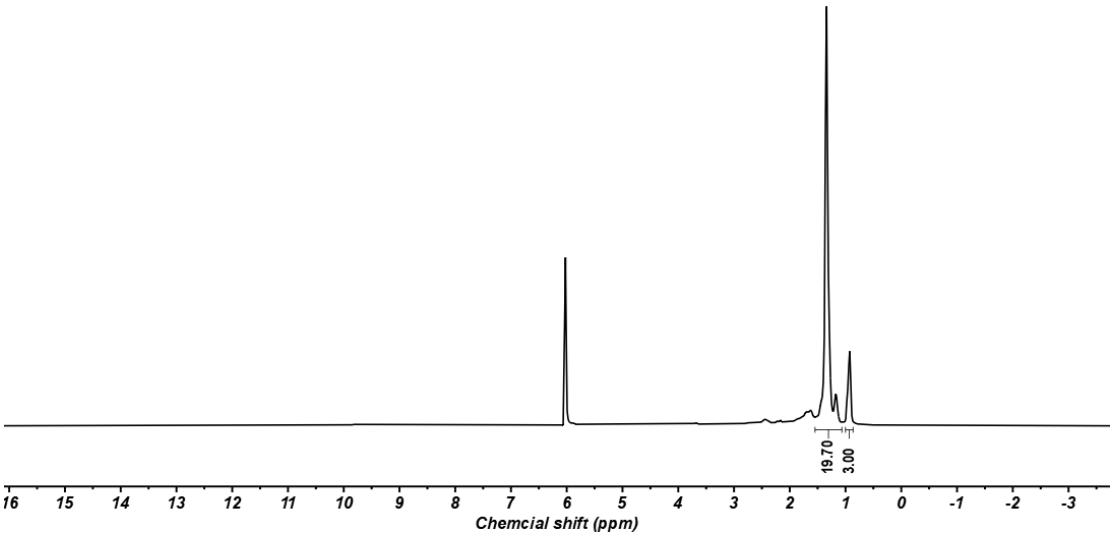

Figure S32. ^{1}H NMR spectrum of polyethylene produced using **NiBr-iPr$_3$** at 80 °C (entry 22, Table 2).

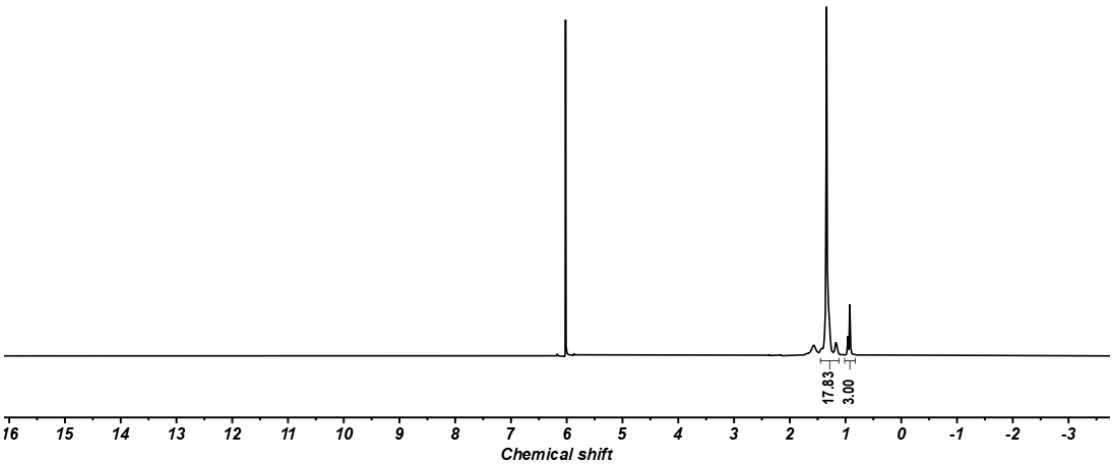

Figure S33. ^{1}H NMR spectrum of polyethylene produced using **NiBr-iPr$_3$** at 100 °C (entry 23, Table 2).

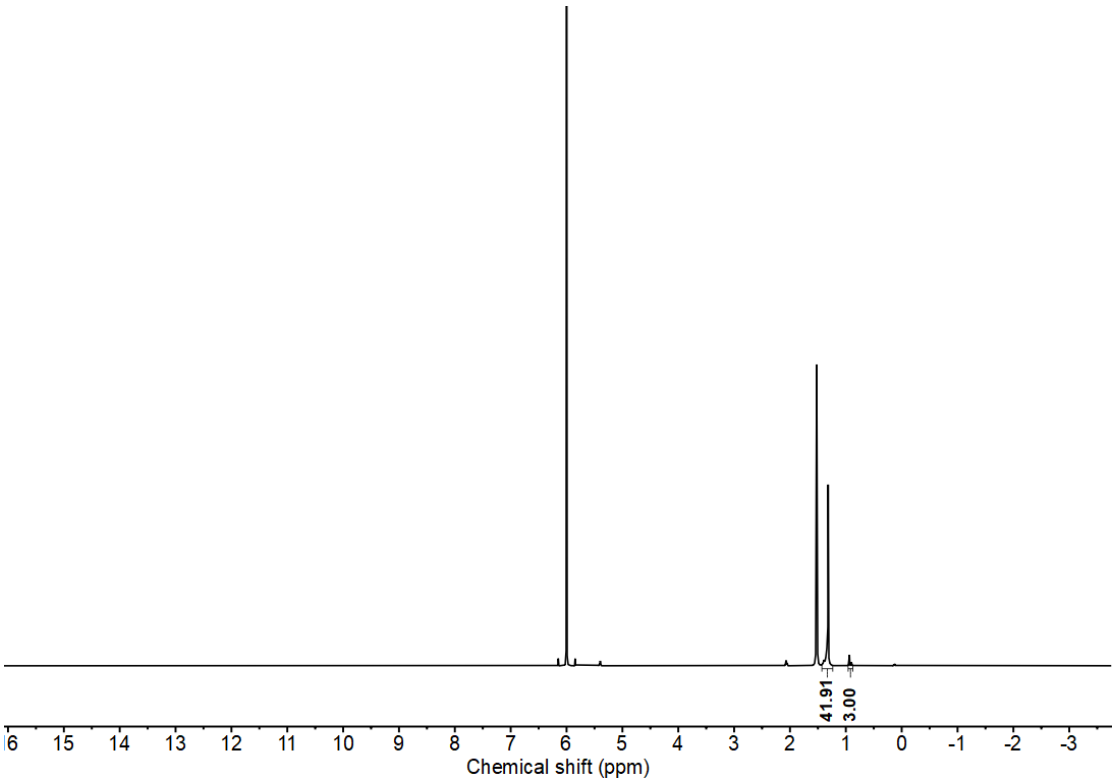

Figure S34. ^{1}H NMR spectrum of polyethylene produced using **NiCl-iPr** at 40 °C (entry 24, Table 2).

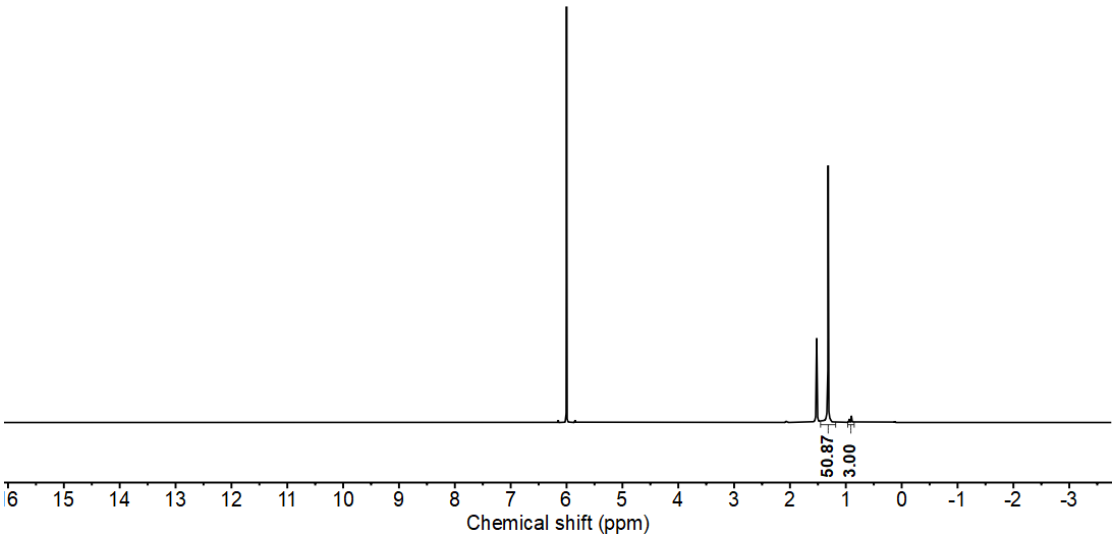

Figure S35. ^{1}H NMR spectrum of polyethylene produced using **NiCl-Et** at 40 °C (entry 25, Table 2).

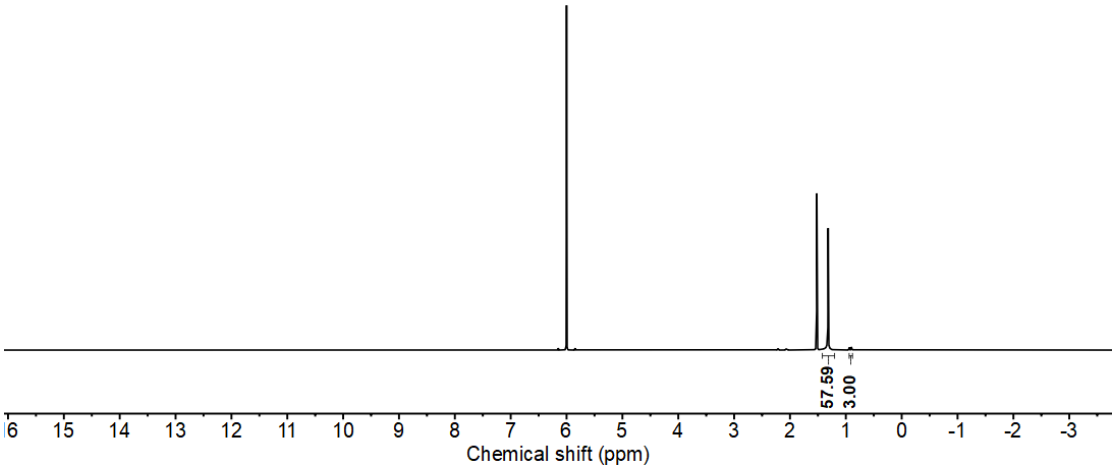

Figure S36. ^{1}H NMR spectrum of polyethylene produced using **NiCl-Me** at 40 °C (entry 26, Table 2).

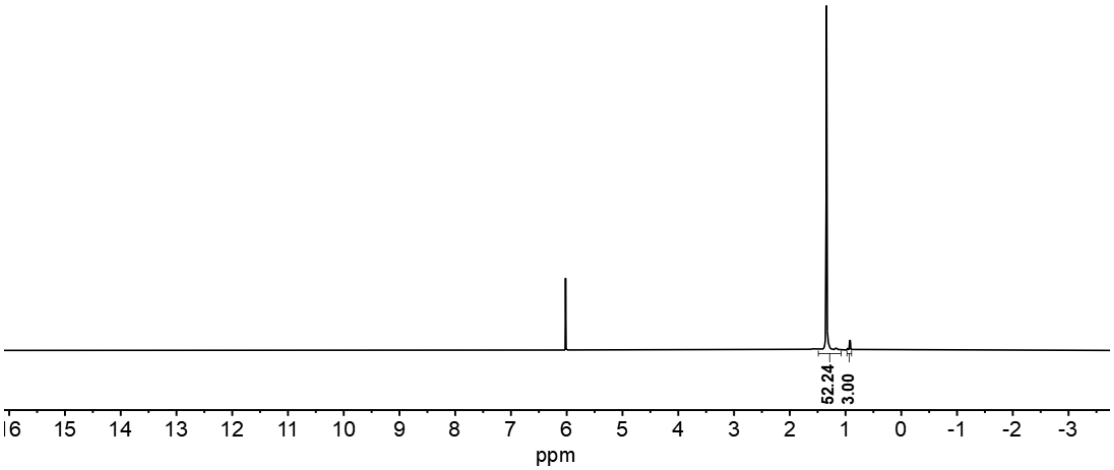

Figure S37. ^{1}H NMR spectrum of polyethylene produced using **NiCl-Cl** at 40 °C (entry 27, Table 2).

8. ^{13}C NMR spectrum of polyethylene obtained at different polymerization temperature using NiBr-iPr

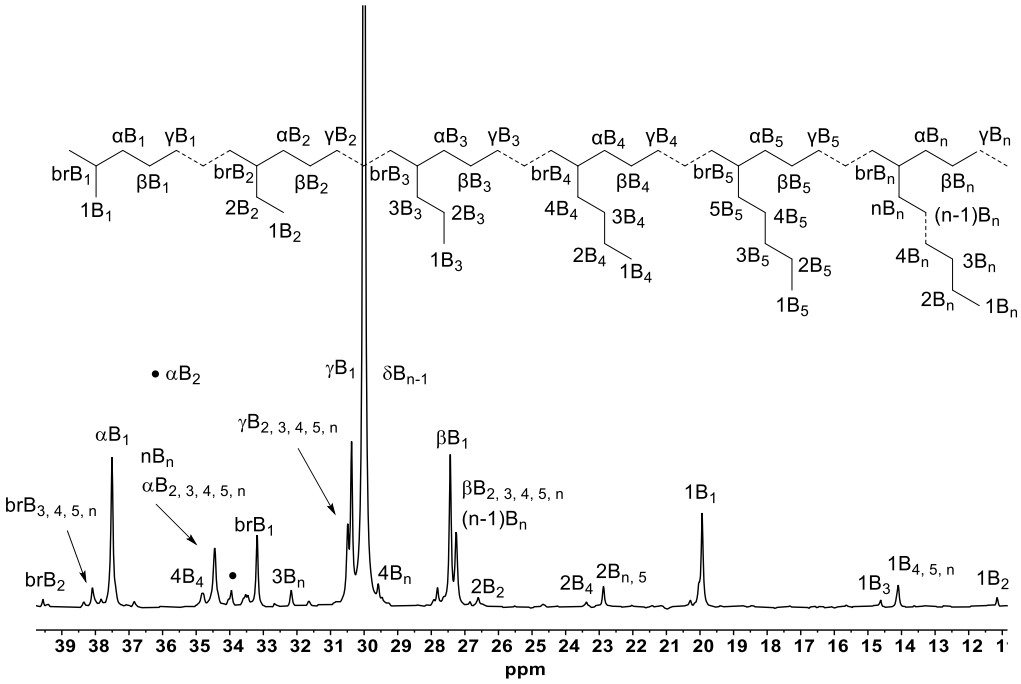

Figure S38. ^{13}C NMR spectrum of polyethylene obtained at polymerization temperature of 40 °C using **NiBr-iPr** (entry 2, Table 2).

9. GPC curves of obtained polyethylene using different catalysts at different temperatures

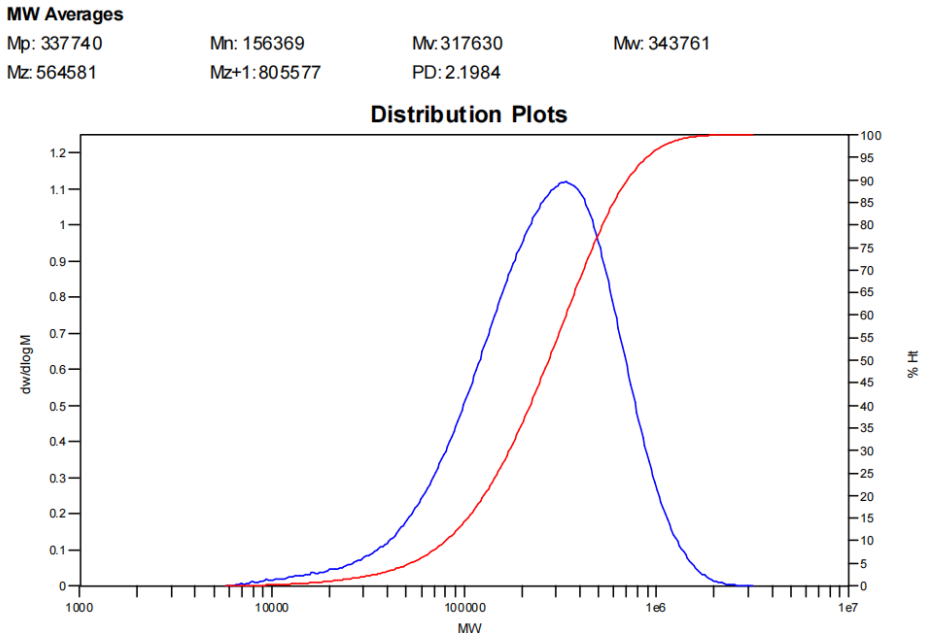

Figure S39. GPC curves of obtained polyethylene using **NiBr-iPr** at 30°C temperatures (entry 1, Table 2).

MW Averages

Mp: 278196	Mn: 136128	Mv: 303683	Mw: 334590
Mz: 613866	Mz+1: 927997	PD: 2.4579	

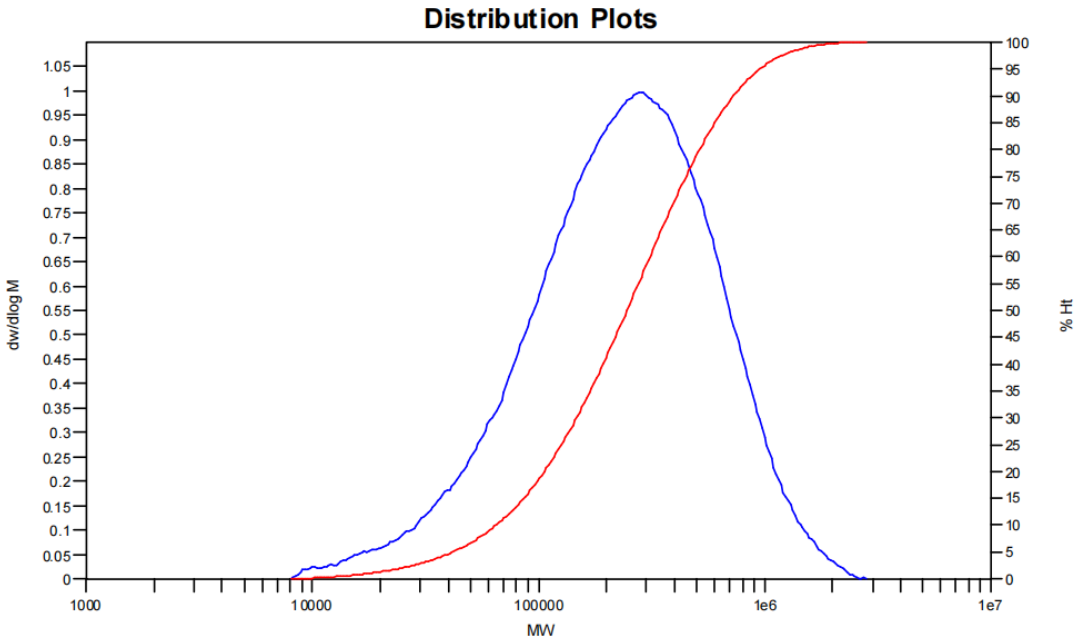

Figure S40. GPC curves of obtained polyethylene using **NiBr-iPr** at 40 ℃ temperatures (entry 2, Table 2).

MW Averages

Mp: 188299	Mn: 117384	Mv: 205383	Mw: 220393
Mz: 345706	Mz+1: 477336	PD: 1.8775	

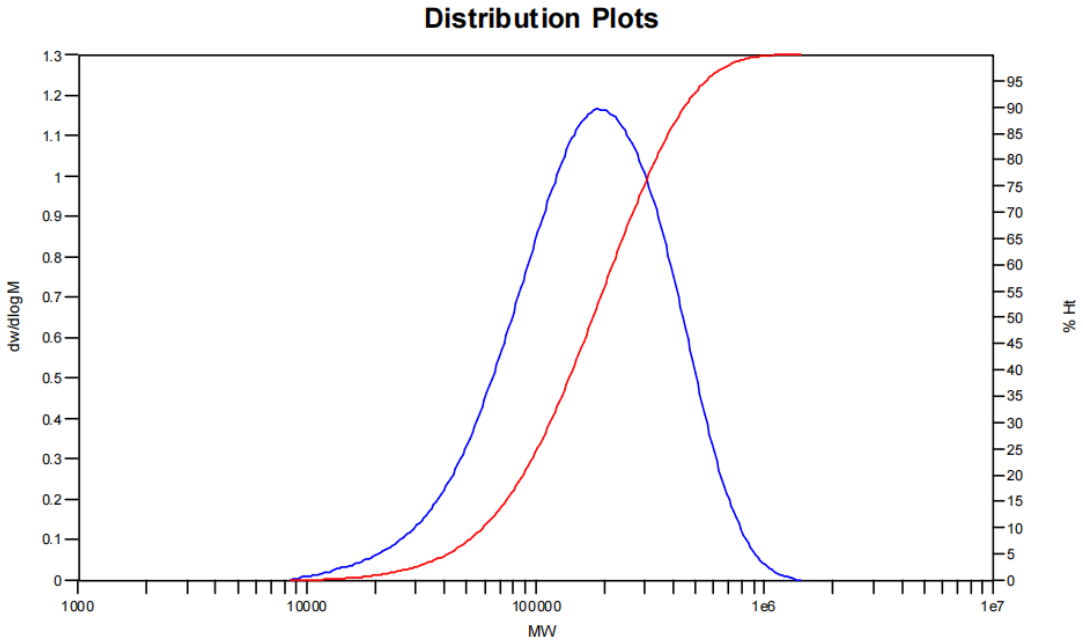

Figure S41. GPC curves of obtained polyethylene using **NiBr-iPr** at 50℃ temperatures (entry 3, Table 2).

MW Averages

Mp: 175037	Mn: 113622	Mv: 199373	Mw: 214834
Mz: 348887	Mz+1: 499520	PD: 1.8908	

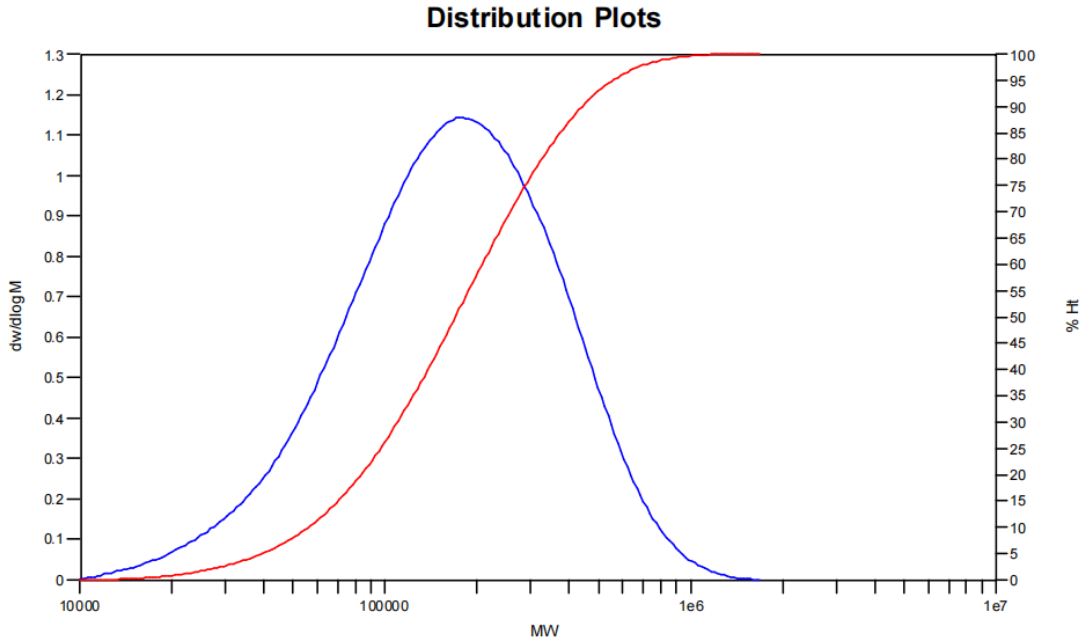

Figure S42. GPC curves of obtained polyethylene using **NiBr-iPr** at 60 ℃ temperatures (entry 4, Table 2).

MW Averages

Mp: 175037	Mn: 94197	Mv: 180019	Mw: 194235
Mz: 315774	Mz+1: 457595	PD: 2.0620	

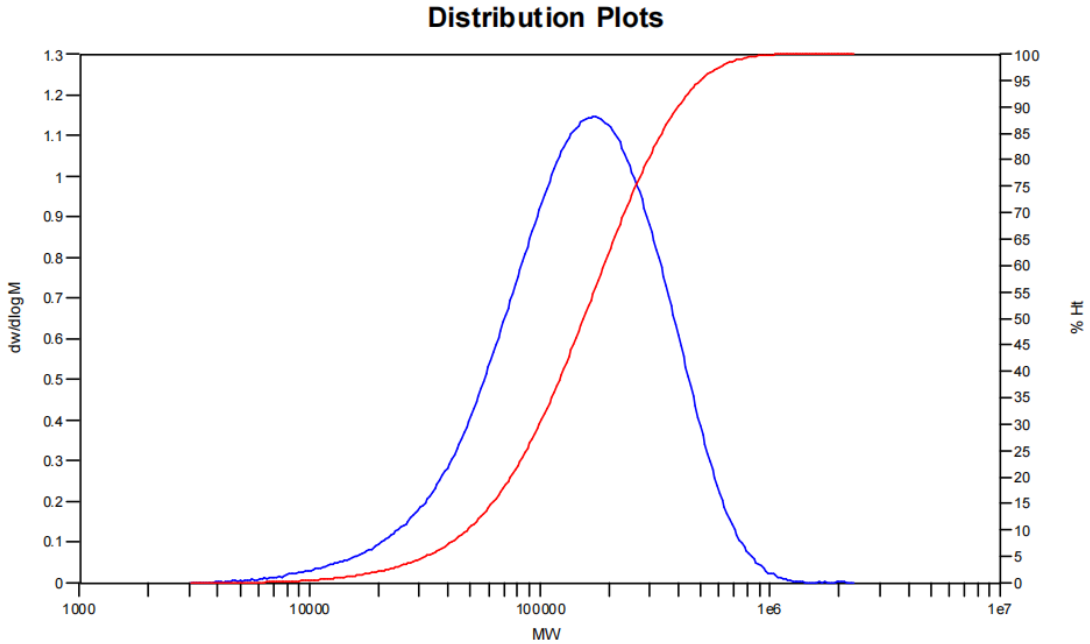

Figure S43. GPC curves of obtained polyethylene using **NiBr-iPr** at 70℃ temperatures (entry 5, Table 2).

MW Averages

Mp: 130696	Mn: 77627	Mv: 140057	Mw: 150713
Mz: 240928	Mz+1: 339180	PD: 1.9415	

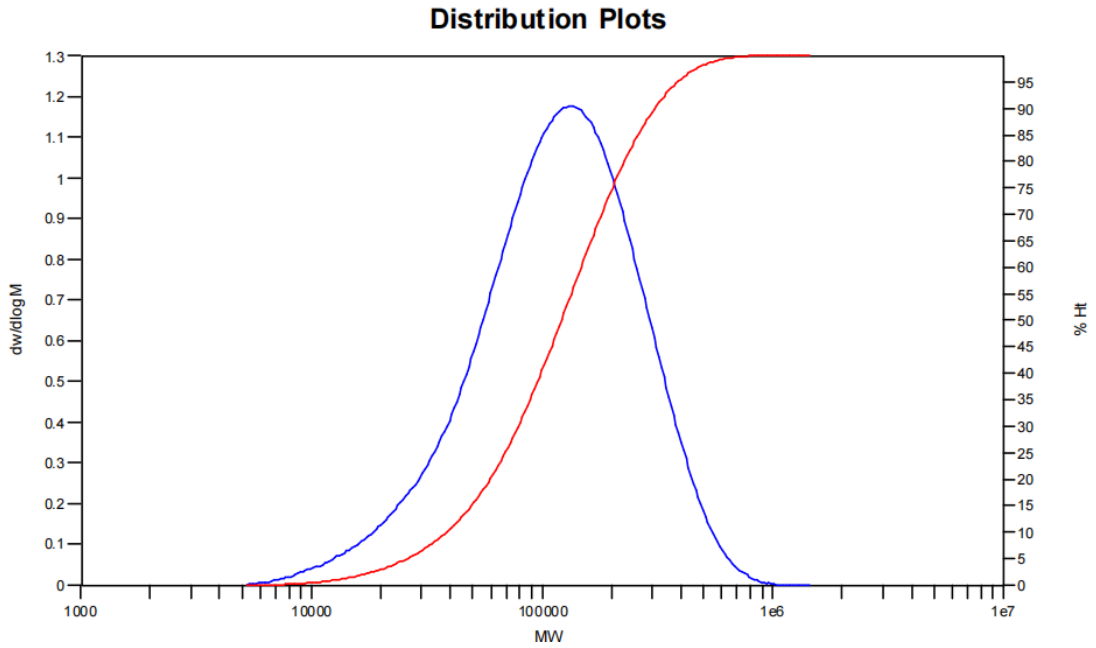

Figure S44. GPC curves of obtained polyethylene using **NiBr-iPr** at 80℃ temperatures (entry 6, Table 2).

MW Averages

Mp: 107568	Mn: 62885	Mv: 110962	Mw: 119180
Mz: 188452	Mz+1: 263256	PD: 1.8952	

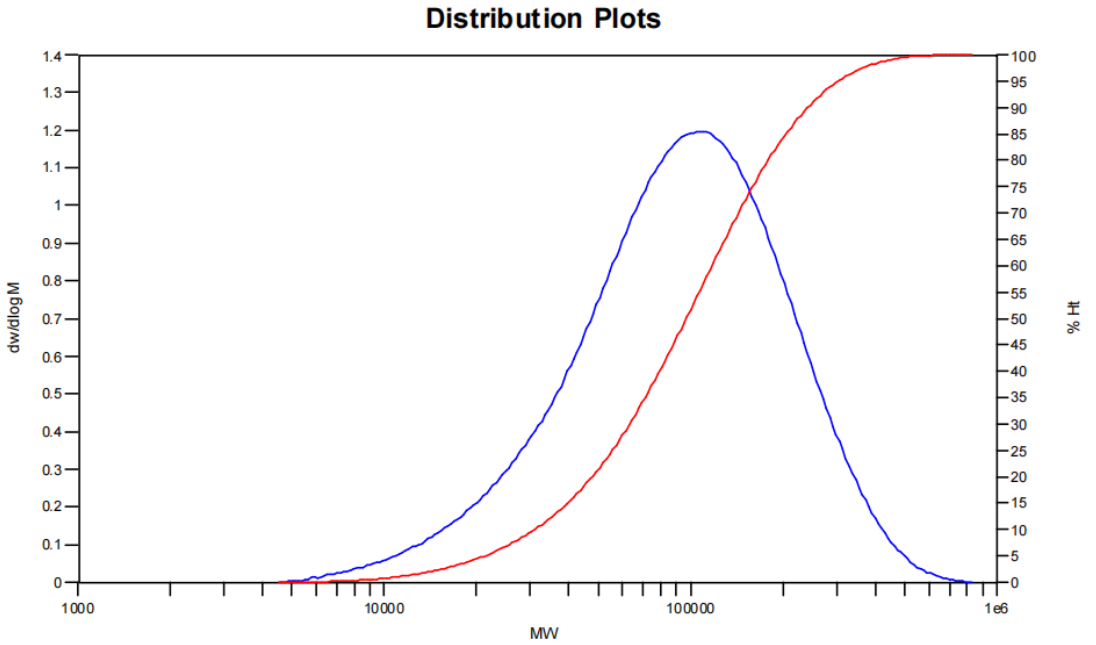

Figure S45. GPC curves of obtained polyethylene using **NiBr-iPr** at 100℃ temperatures (entry 7, Table 2).

MW Averages

Mp: 223282	Mn: 139649	Mv: 235041	Mw: 251663
Mz: 389809	Mz+1: 532531	PD: 1.8021	

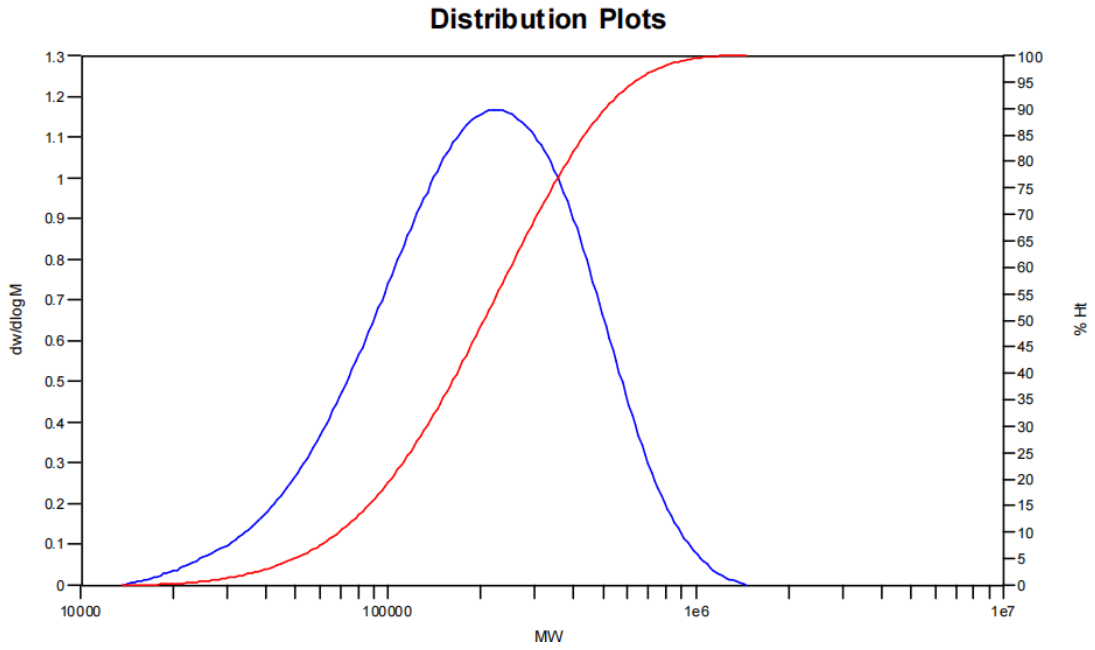

Figure S46. GPC curves of obtained polyethylene using **NiBr-Et** at 40°C temperatures (entry 8, Table 2).

MW Averages

Mp: 151251	Mn: 90592	Mv: 167199	Mw: 180808
Mz: 297023	Mz+1: 419750	PD: 1.9958	

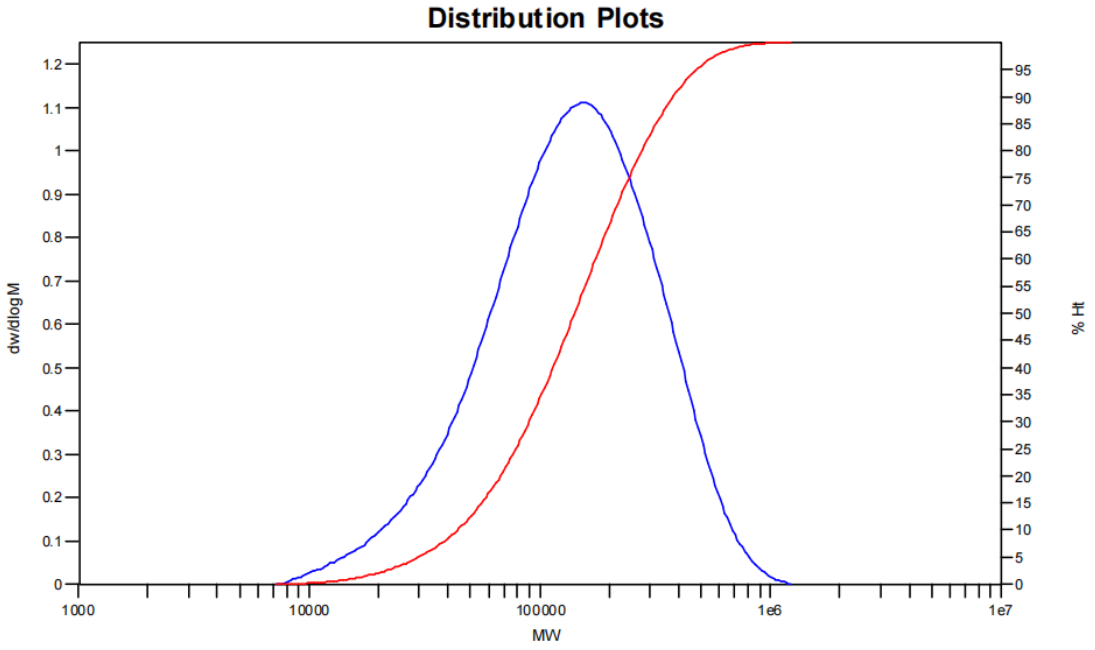

Figure S47. GPC curves of obtained polyethylene using **NiBr-Et** at 60°C temperatures (entry 9, Table 2).

MW Averages

Mp: 137217	Mn: 82252	Mv: 144755	Mw: 155490
Mz: 246514	Mz+1: 346688	PD: 1.8904	

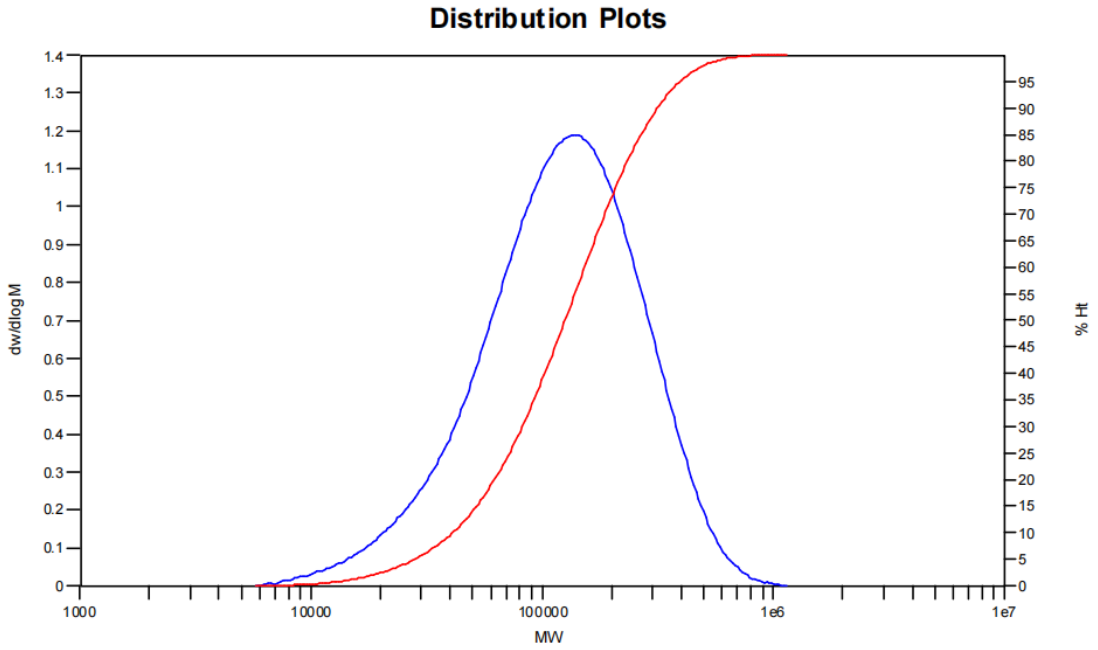

Figure S48. GPC curves of obtained polyethylene using **NiBr-Et** at 80°C temperatures (entry 10, Table 2).

MW Averages

Mp: 90715	Mn: 52962	Mv: 95255	Mw: 102552
Mz: 165887	Mz+1: 242056	PD: 1.9363	

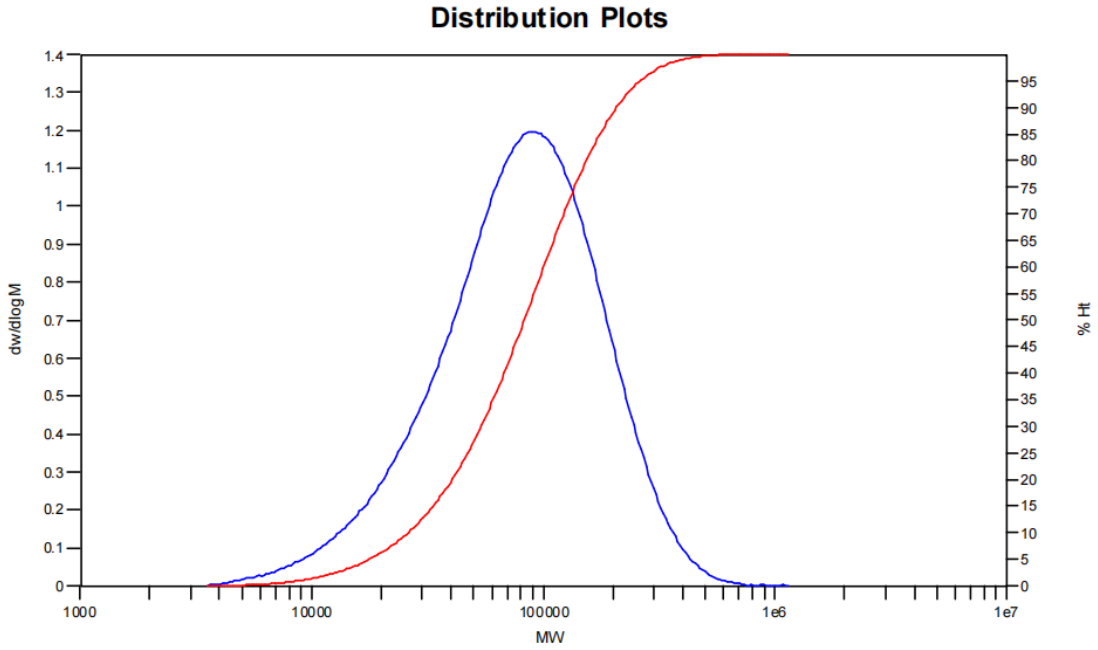

Figure S49. GPC curves of obtained polyethylene using **NiBr-Et** at 100°C temperatures (entry 11, Table 2).

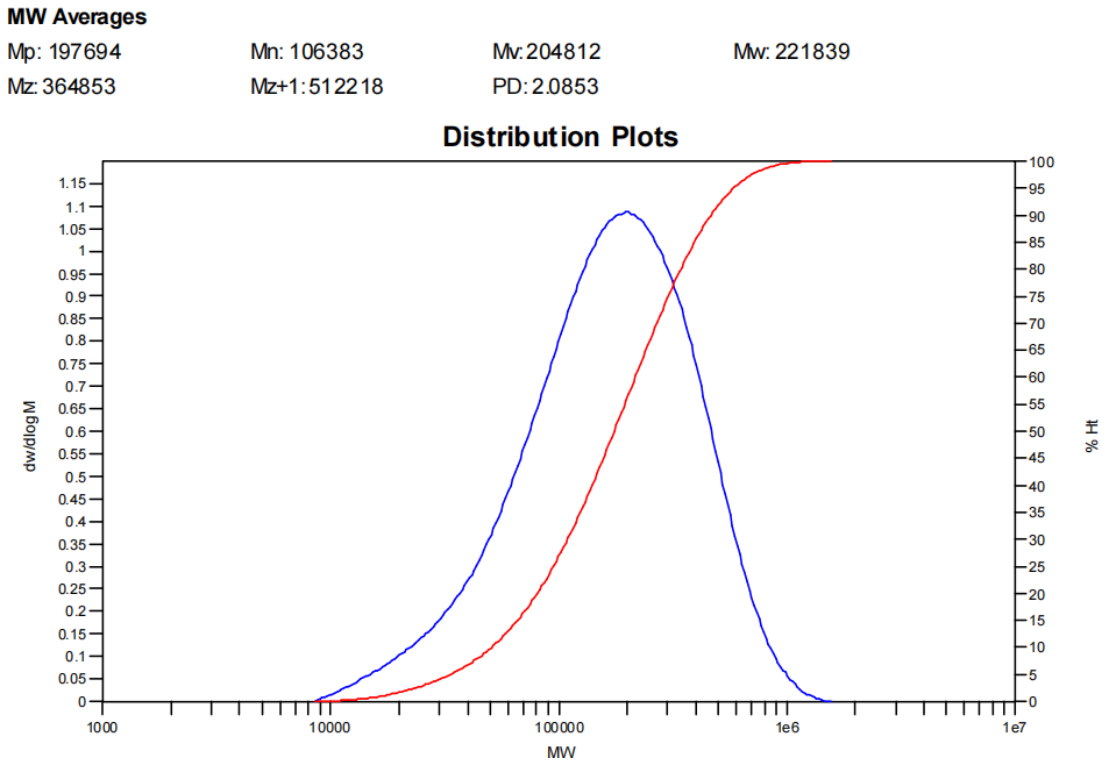

Figure S50. GPC curves of obtained polyethylene using **NiBr-Me** at 40°C temperatures (entry 12, Table 2).

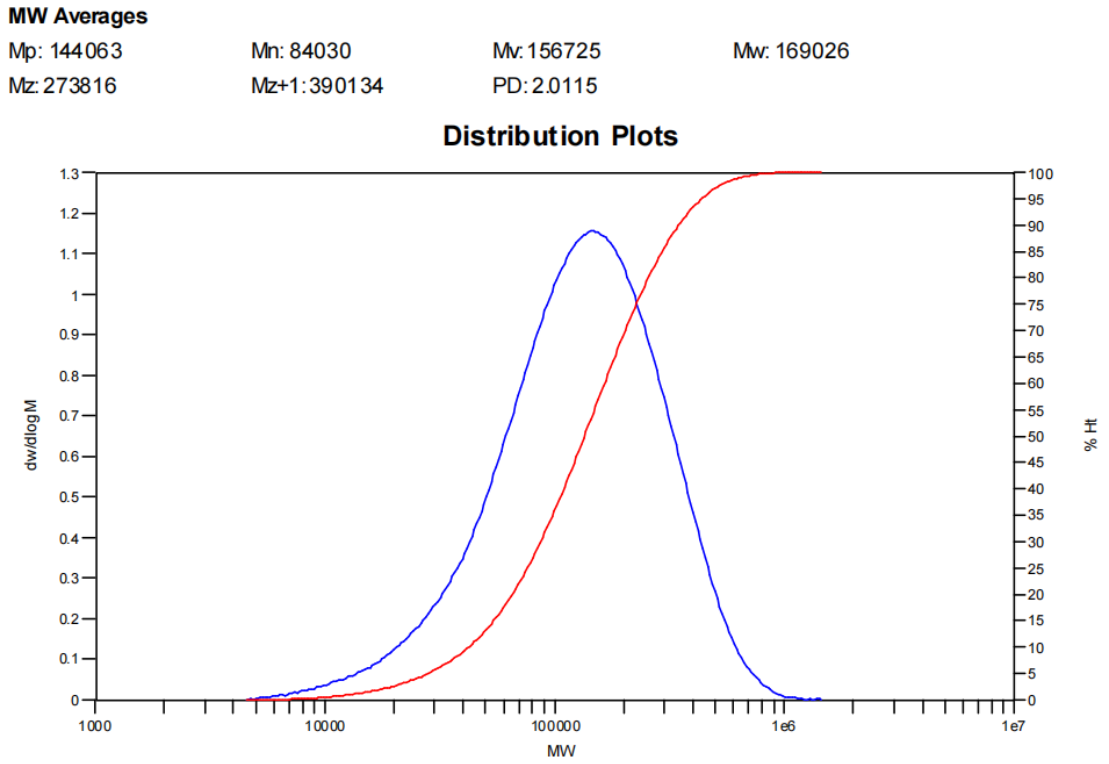

Figure S51. GPC curves of obtained polyethylene using **NiBr-Me** at 60°C temperatures (entry 13, Table 2).

MW Averages

Mp: 99993	Mn: 52052	Mv: 120087	Mw: 133588
Mz: 263881	Mz+1: 423465	PD: 2.5664	

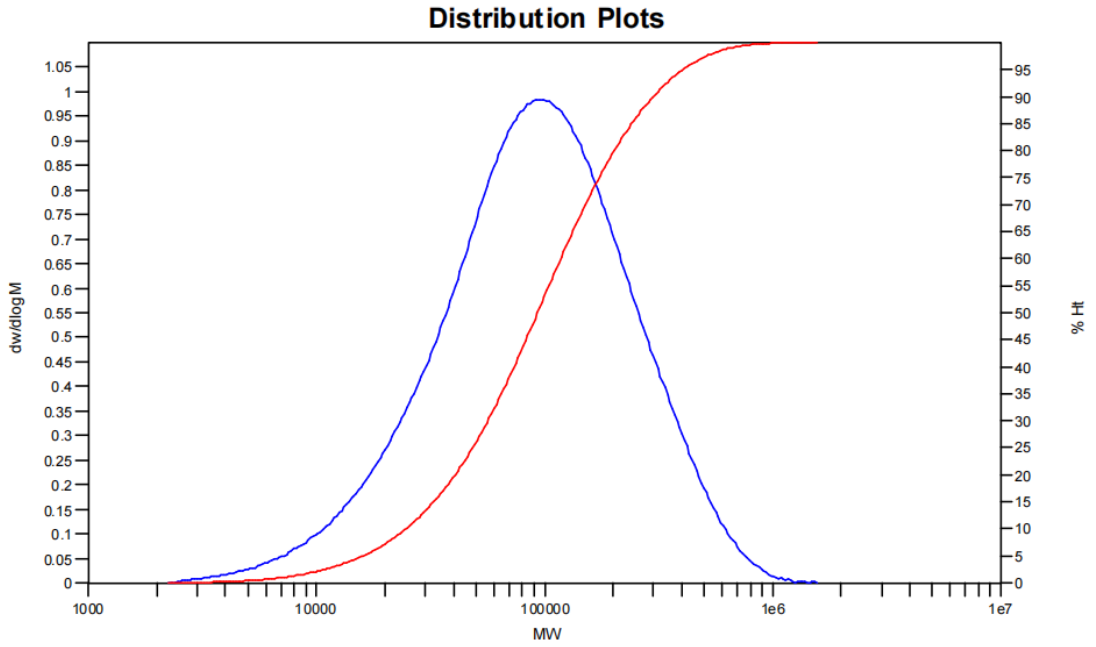

Figure S52. GPC curves of obtained polyethylene using **NiBr-Me** at 80°C temperatures (entry 14, Table 2).

MW Averages

Mp: 86404	Mn: 47027	Mv: 93255	Mw: 101478
Mz: 176968	Mz+1: 275937	PD: 2.1579	

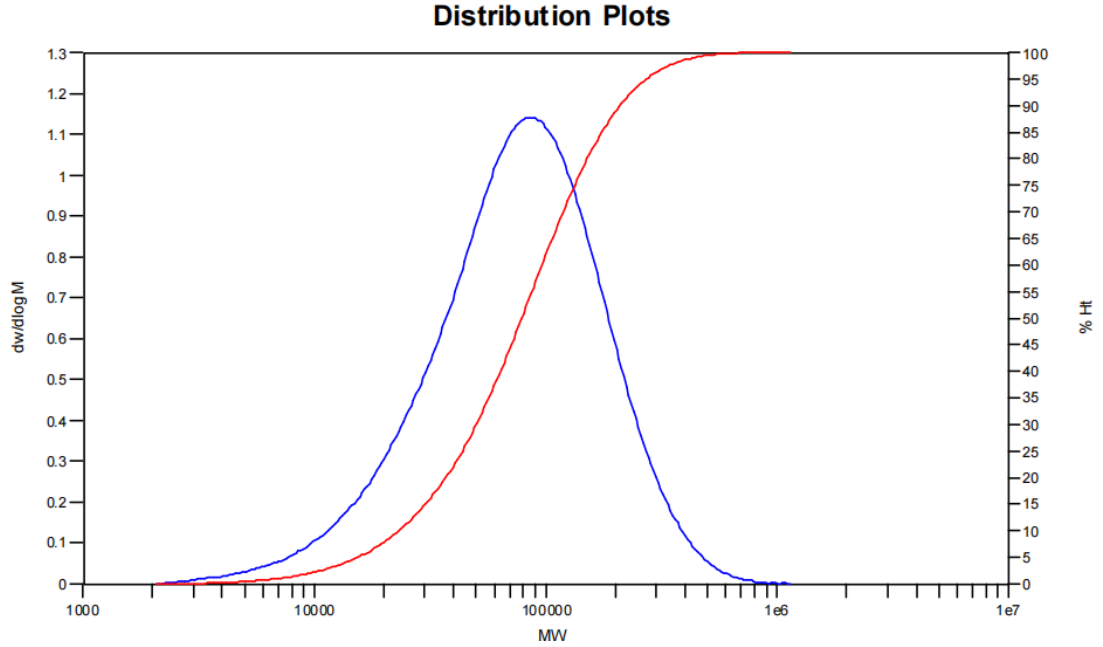

Figure S53. GPC curves of obtained polyethylene using **NiBr-Me** at 100°C temperatures (entry 15, Table 2).

MW Averages

Mp: 107568	Mn: 61872	Mv: 113892	Mw: 123064
Mz: 202181	Mz+1: 289962	PD: 1.9890	

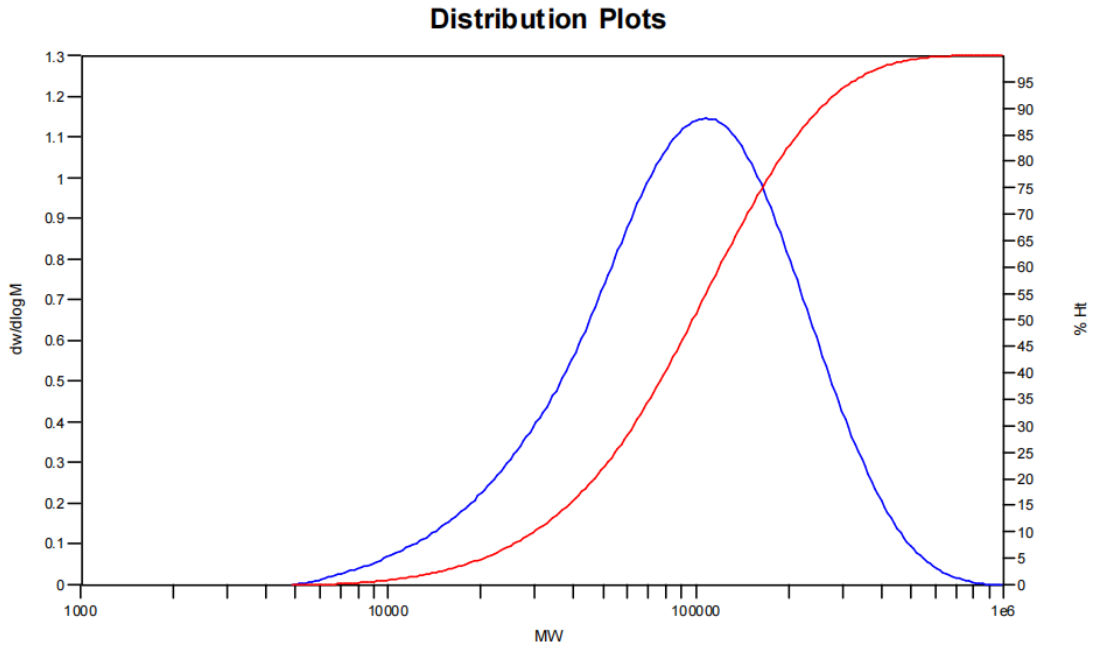

Figure S54. GPC curves of obtained polyethylene using **NiBr-Cl** at 40°C temperatures (entry 16, Table 2).

MW Averages

Mp: 81417	Mn: 44425	Mv: 95836	Mw: 104565
Mz: 184700	Mz+1: 287228	PD: 2.3537	

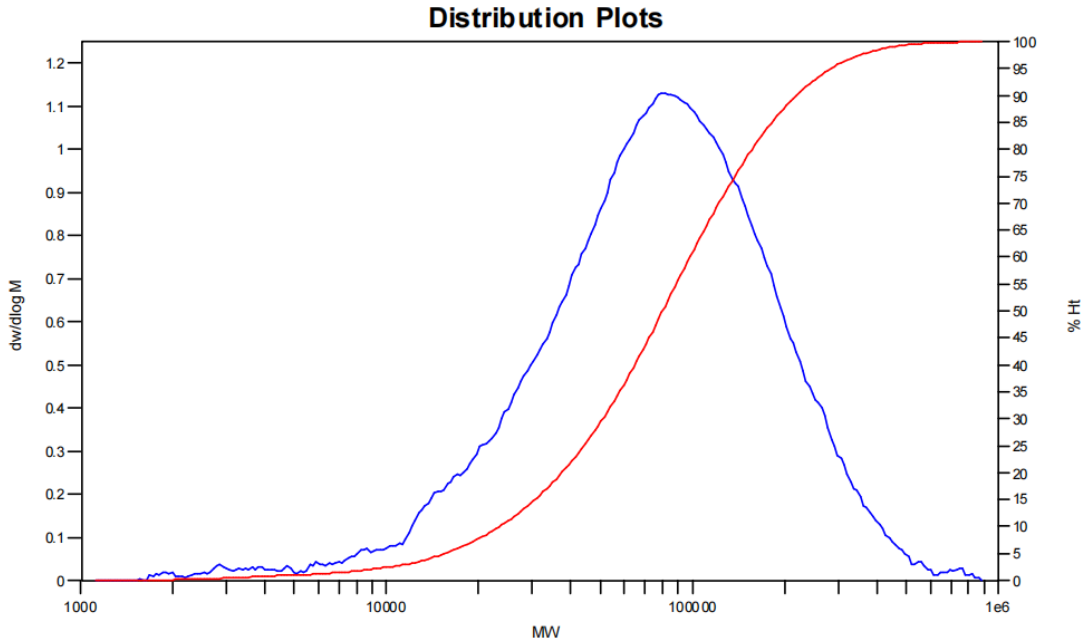

Figure S55. GPC curves of obtained polyethylene using **NiBr-Cl** at 60°C temperatures (entry 17, Table 2).

MW Averages

Mp: 63986	Mn: 43507	Mv: 76272	Mw: 82440
Mz: 136326	Mz+1: 194426	PD: 1.8949	

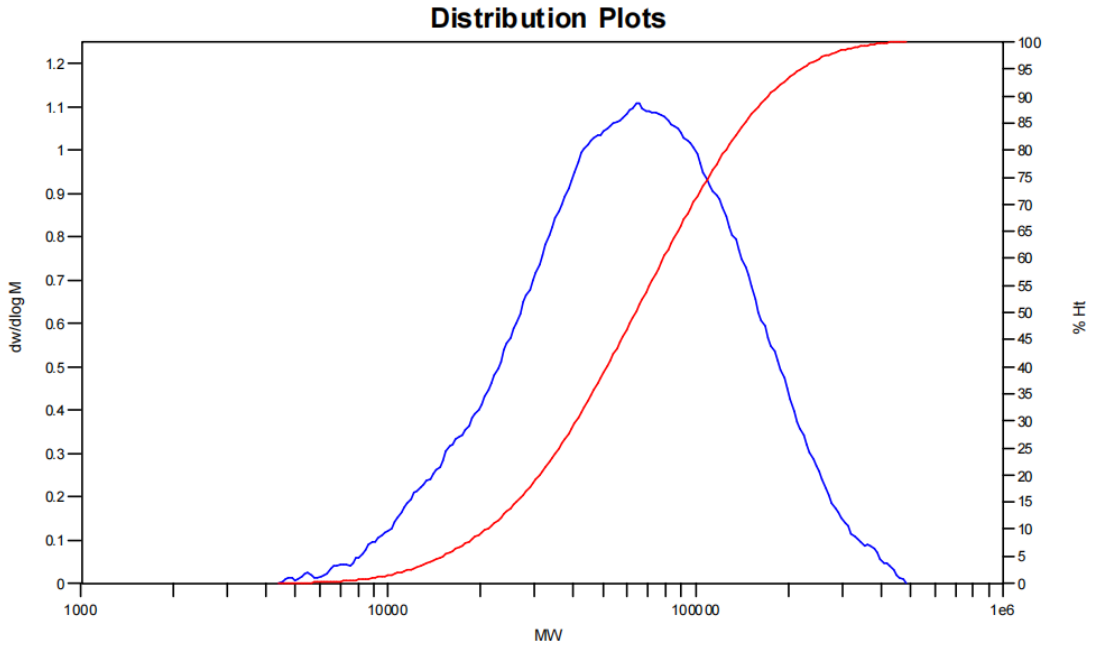

Figure S56. GPC curves of obtained polyethylene using **NiBr-Cl** at 80°C temperatures (entry 18, Table 2).

MW Averages

Mp: 40625	Mn: 22503	Mv: 40065	Mw: 43221
Mz: 71911	Mz+1: 110712	PD: 1.9207	

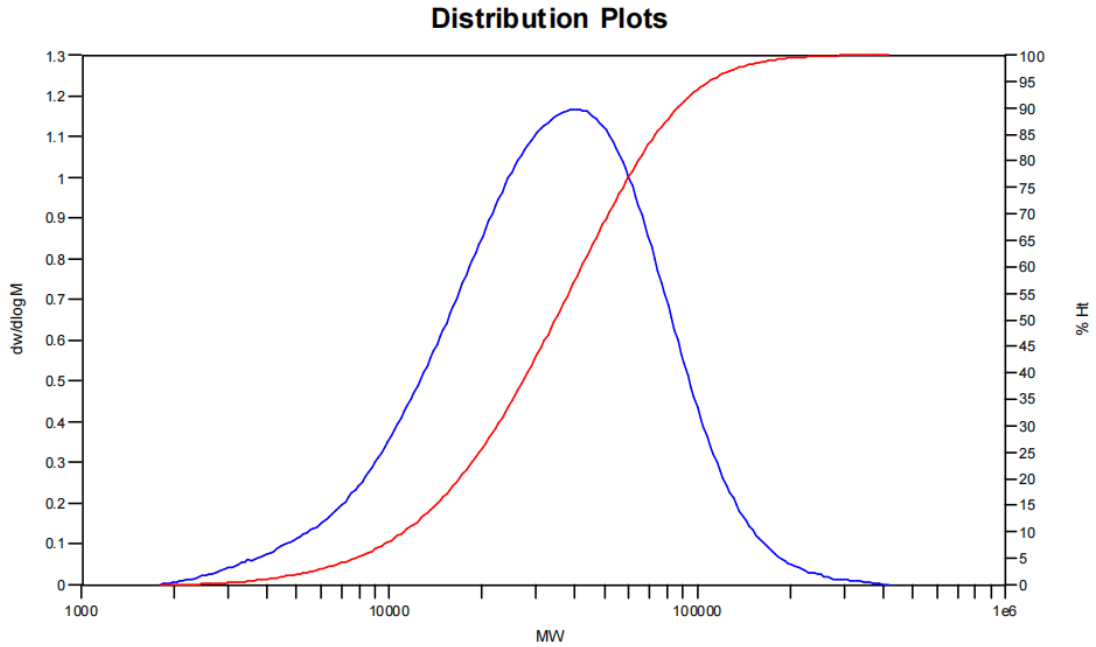

Figure S57. GPC curves of obtained polyethylene using **NiBr-Cl** at 100°C temperatures (entry 19, Table 2).

MW Averages

Mp: 125620	Mn: 66753	Mv: 140940	Mw: 155013
Mz: 278002	Mz+1: 401282	PD: 2.3222	

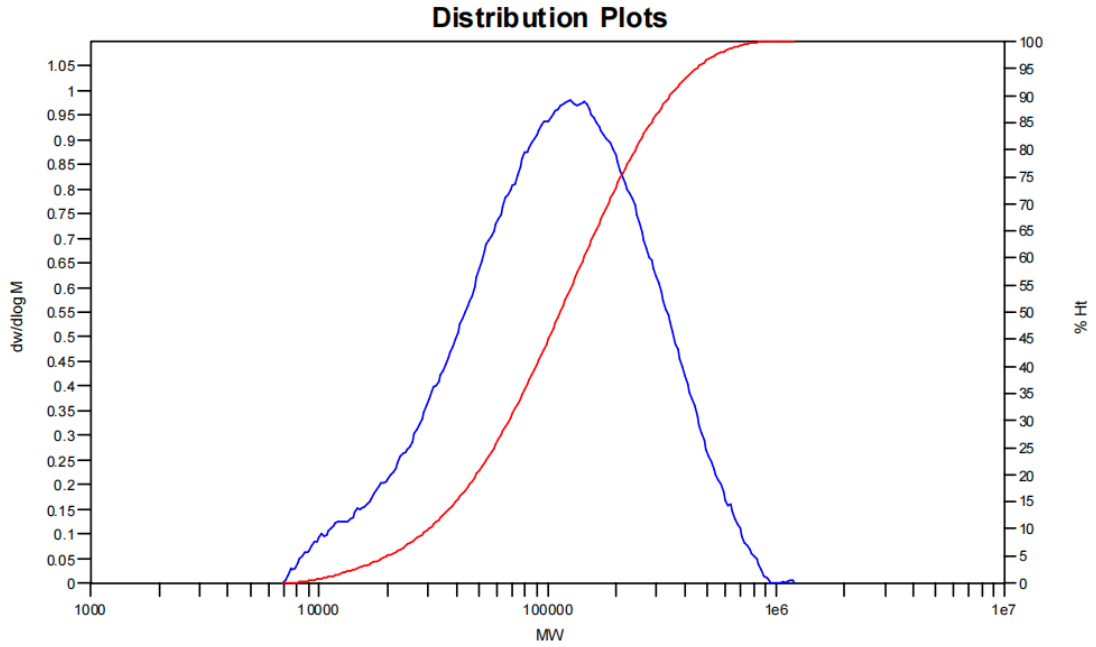

Figure S58. GPC curves of obtained polyethylene using **NiBr-iPr3** at 40°C temperatures (entry 20, Table 2).

MW Averages

Mp: 127553	Mn: 75899	Mv: 134998	Mw: 145051
Mz: 228999	Mz+1: 316650	PD: 1.9111	

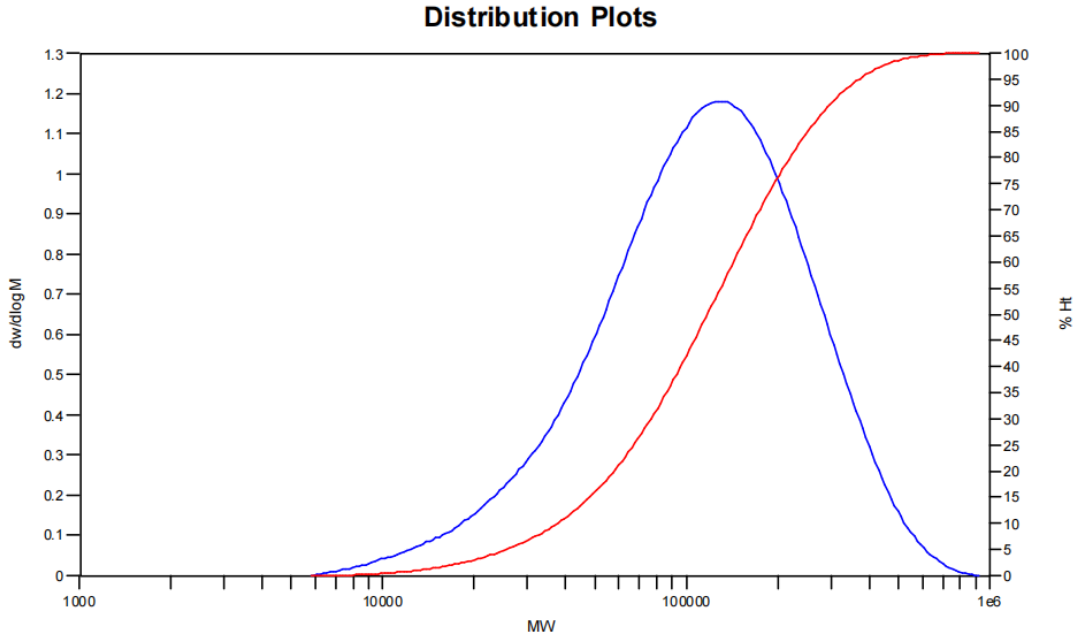

Figure S59. GPC curves of obtained polyethylene using **NiBr-iPr3** at 60°C temperatures (entry 21, Table 2).

MW Averages

Mp: 95241	Mn: 53320	Mv: 114793	Mw: 126394
Mz: 234554	Mz+1: 365155	PD: 2.3705	

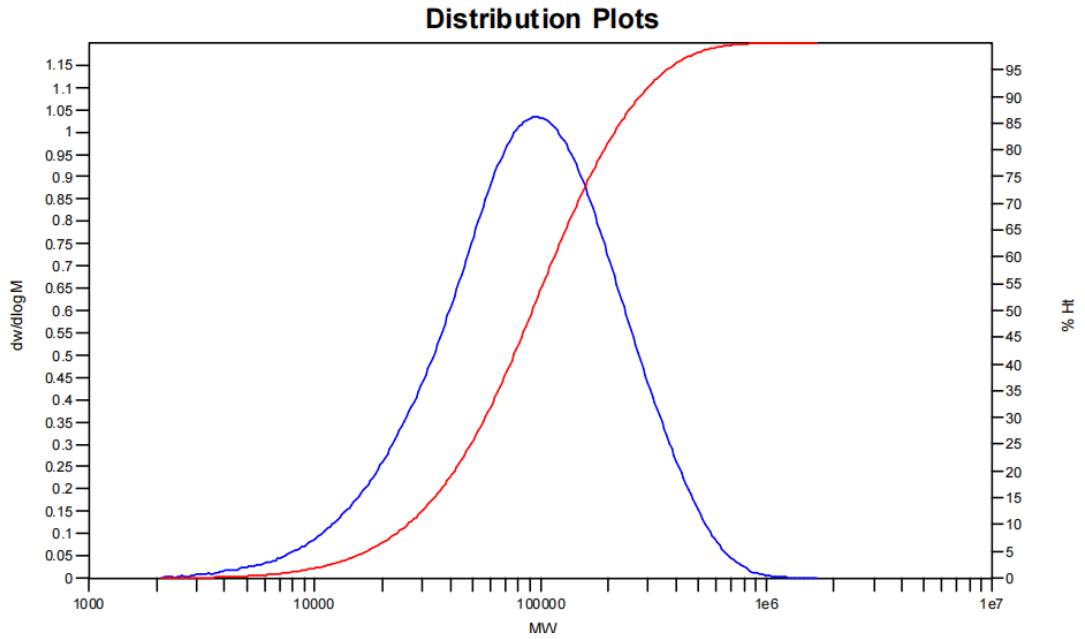

Figure S60. GPC curves of obtained polyethylene using **NiBr-iPr$_3$** at 80°C temperatures (entry 22, Table 2).

MW Averages

Mp: 62964	Mn: 34551	Mv: 61626	Mw: 66402
Mz: 108592	Mz+1: 161173	PD: 1.9219	

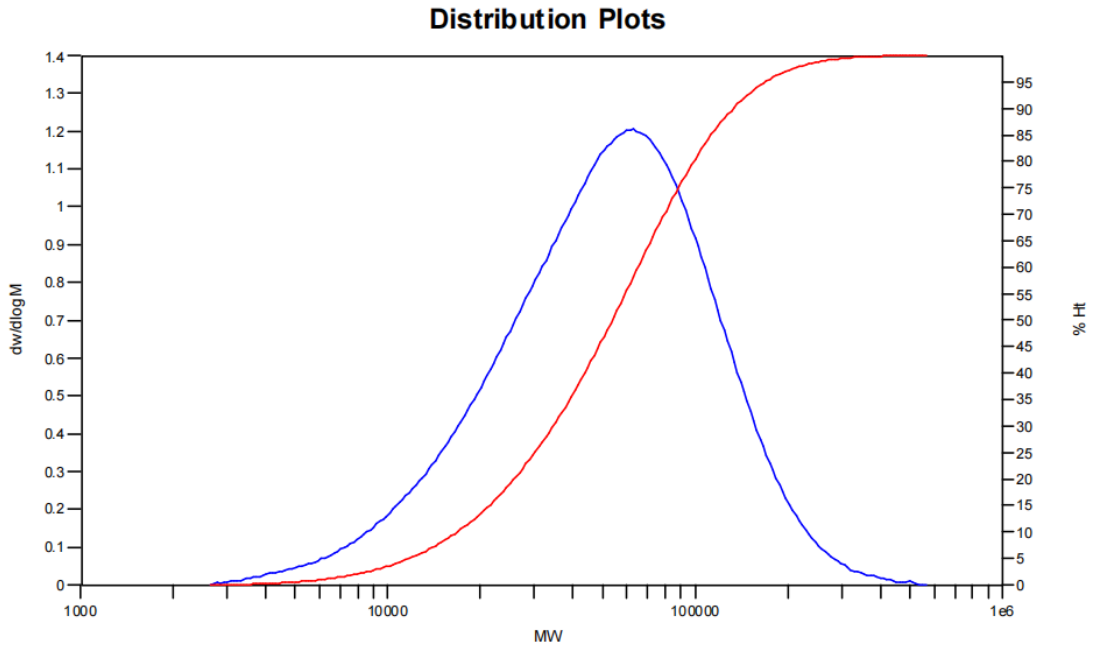

Figure S61. GPC curves of obtained polyethylene using **NiBr-iPr$_3$** at 100°C temperatures (entry 23, Table 2).

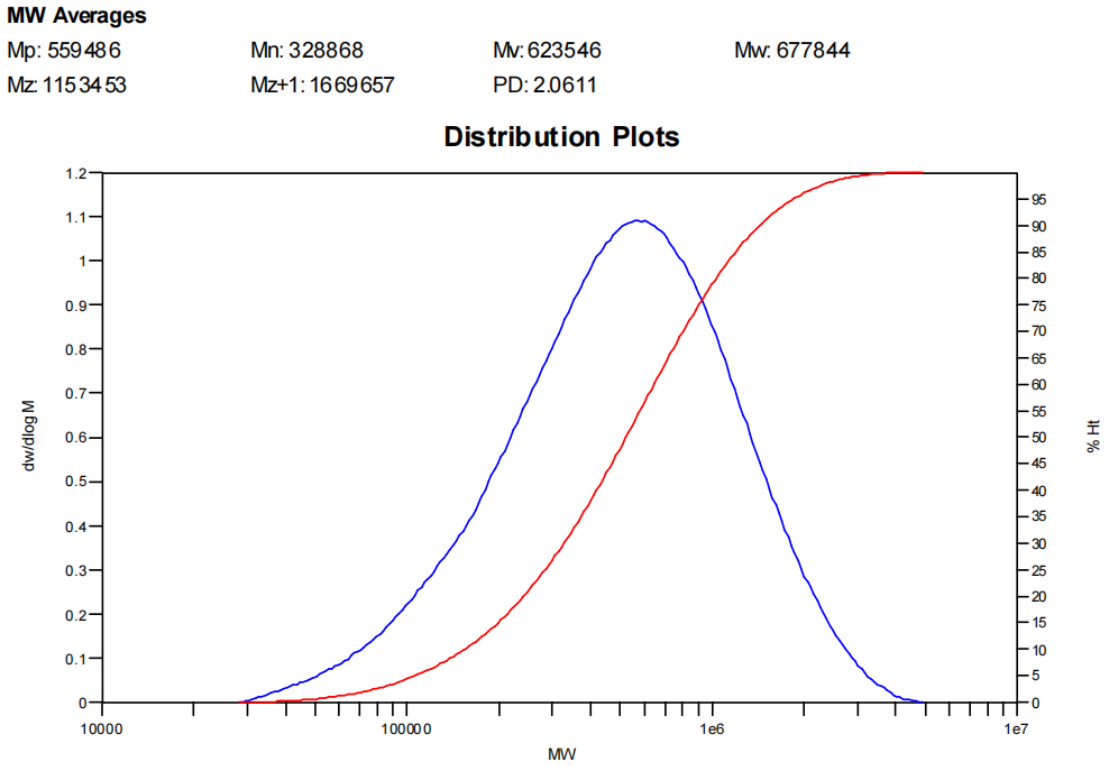

Figure S62. GPC curves of obtained polyethylene using **NiCl-iPr** at 40°C temperatures (entry 24, Table 2).

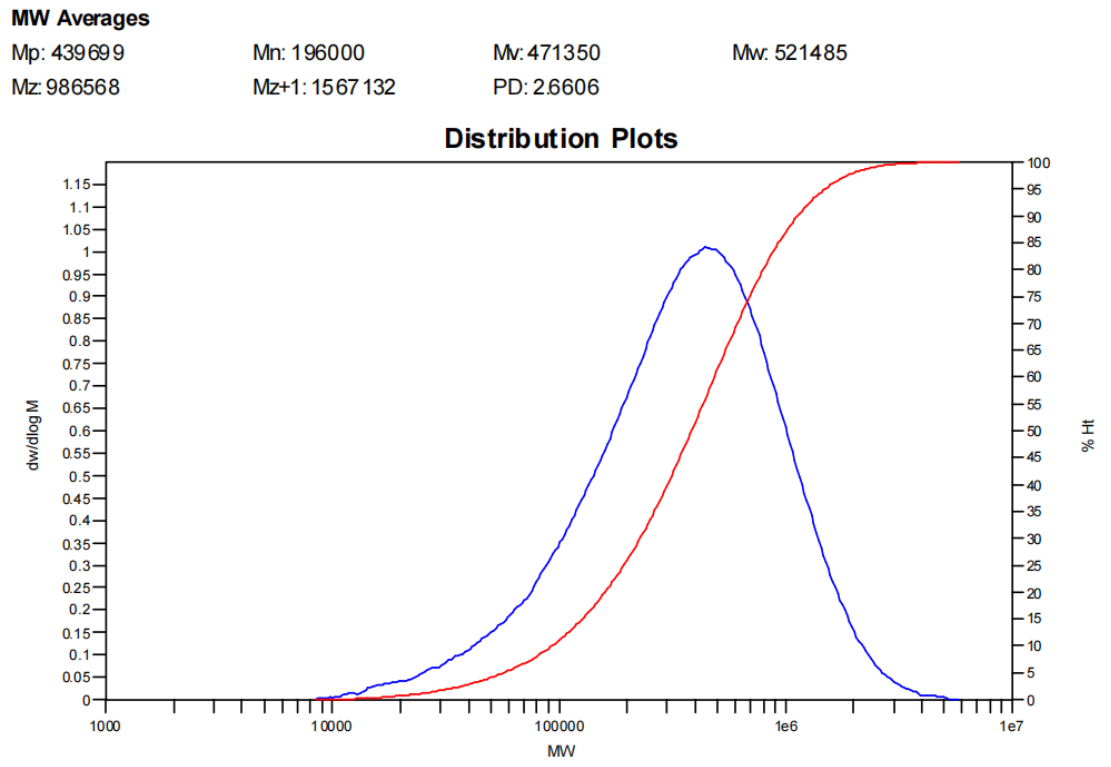

Figure S63. GPC curves of obtained polyethylene using **NiCl-Et** at 40°C temperatures (entry 25, Table 2).

MW Averages

Mp: 508084	Mn: 313014	Mv: 509926	Mw: 543837
Mz: 817796	Mz+1: 1080575	PD: 1.7374	

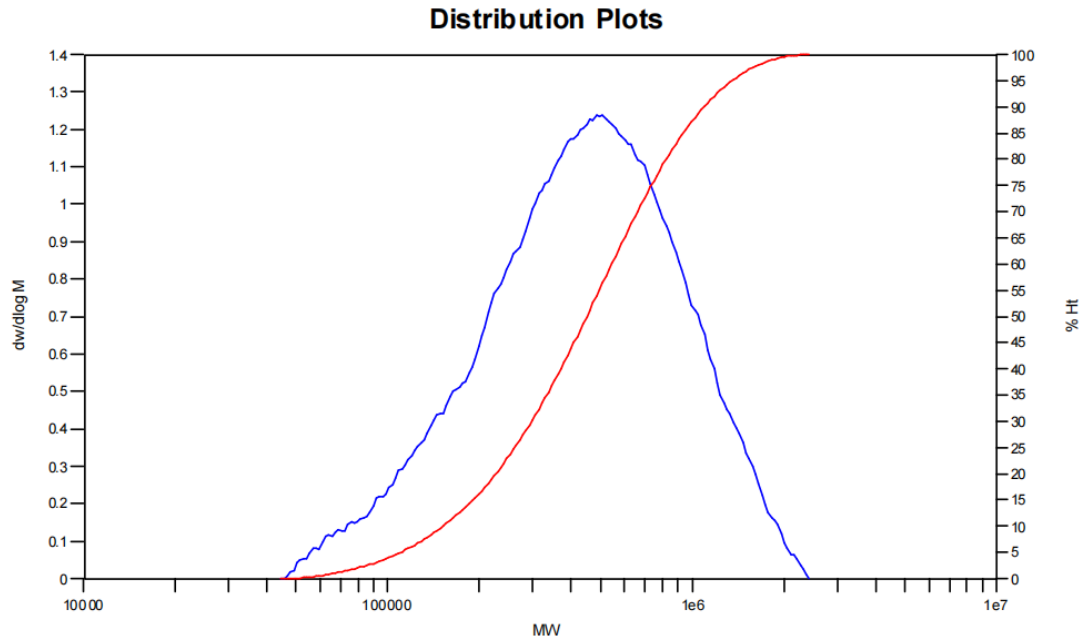

Figure S64. GPC curves of obtained polyethylene using **NiCl-Me** at 40°C temperatures (entry 26, Table 2).

MW Averages

Mp: 154978	Mn: 80064	Mv: 157496	Mw: 170083
Mz: 277610	Mz+1: 404163	PD: 2.1243	

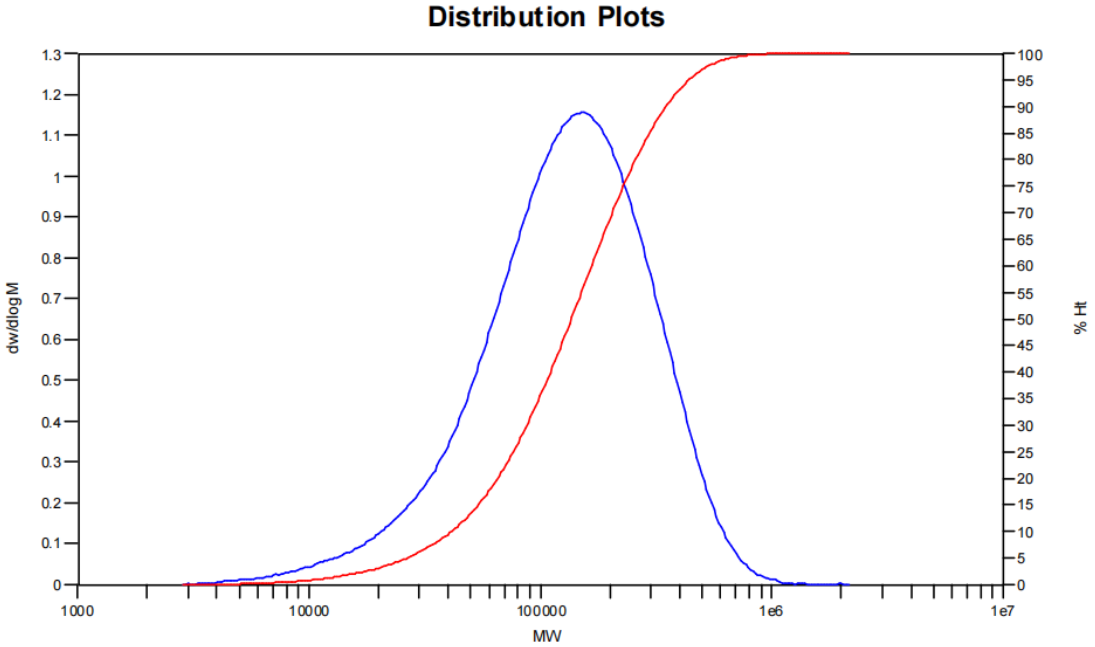

Figure S65. GPC curves of obtained polyethylene using **NiCl-Cl** at 40°C temperatures (entry 27, Table 2).

10. DSC curves of polyethylene using different catalyst at different temperatures

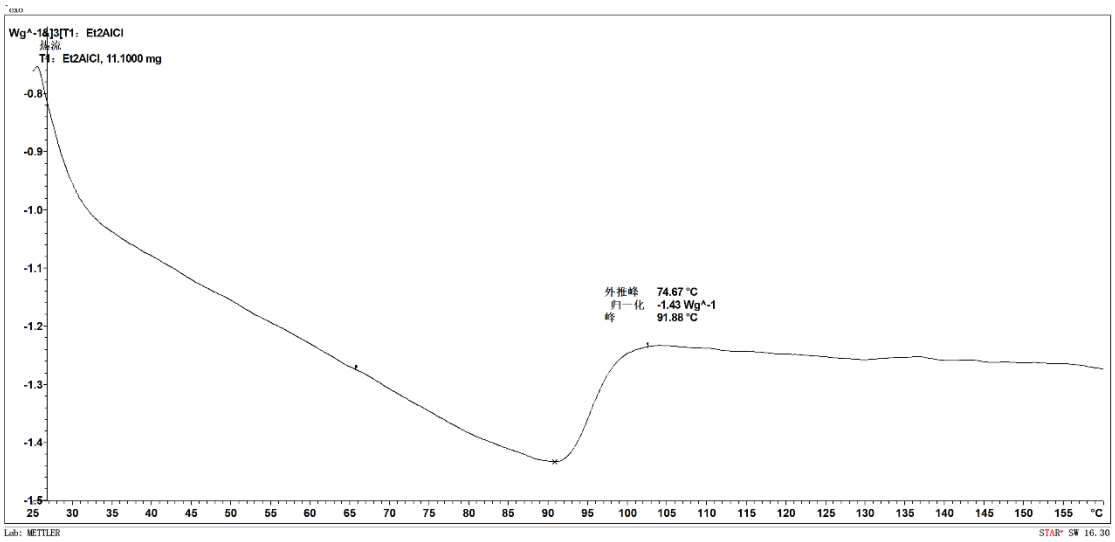

Figure S66. DSC curve of obtained polyethylene using **NiBr-iPr** at 30 °C showing T_m (entry 1, Table 2).

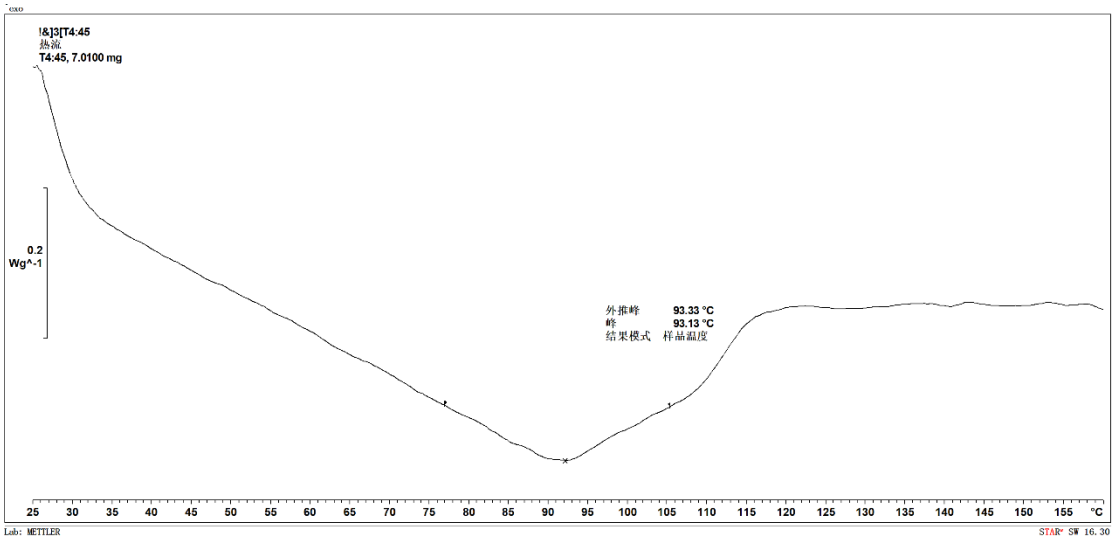

Figure S67. DSC curve of obtained polyethylene using **NiBr-iPr** at 50 °C showing T_m (entry 3, Table 2).

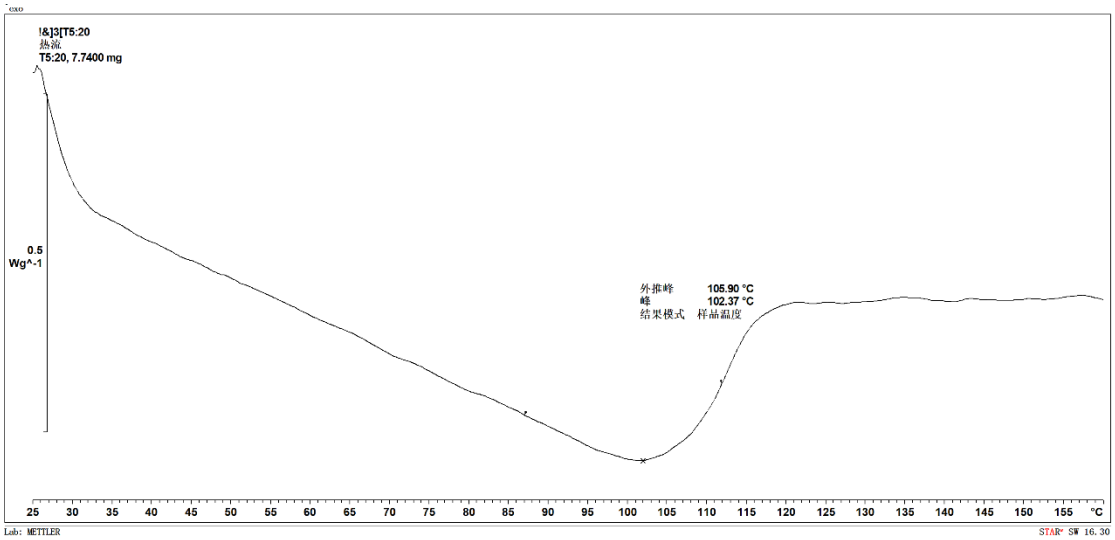

Figure S68. DSC curve of obtained polyethylene using **NiBr-Et** at 40 °C showing T_m (entry 8, Table 2).

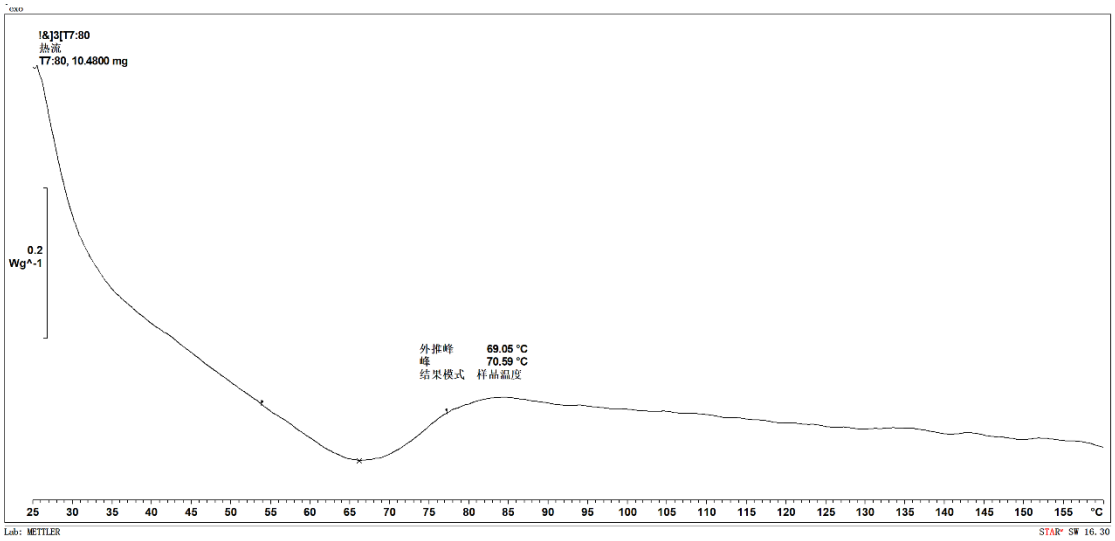

Figure S69. DSC curve of obtained polyethylene using **NiBr-Et** at 80 °C showing T_m (entry 10, Table 2).

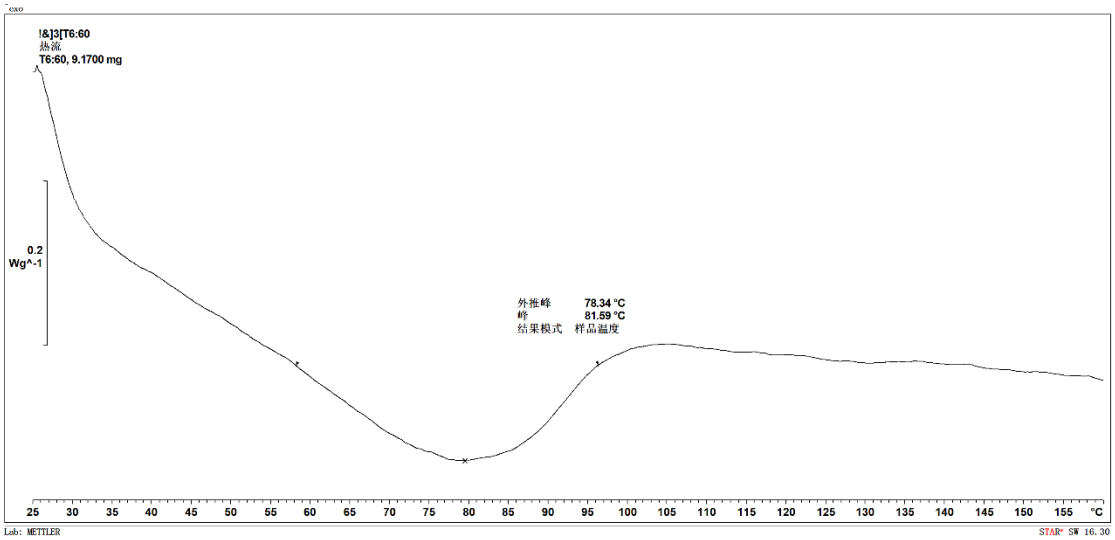

Figure S70. DSC curve of obtained polyethylene using **NiBr-Me** at 60 ℃ showing T_m (entry 13, Table 2).

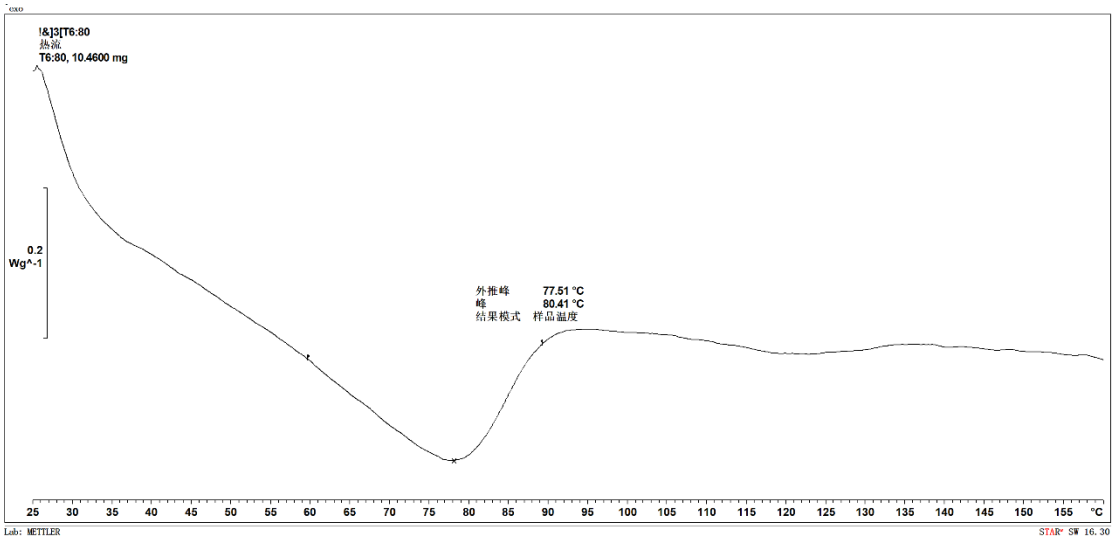

Figure S71. DSC curve of obtained polyethylene using **NiBr-Me** at 80 ℃ showing T_m.(entry 14, Table 2).

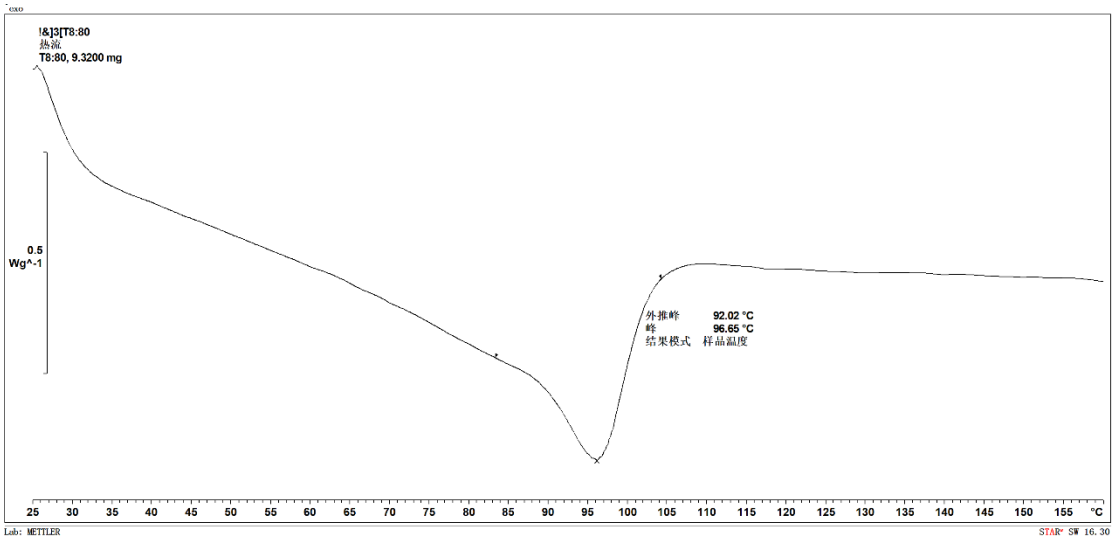

Figure S72. DSC curve of obtained polyethylene using **NiBr-Cl** at 80 °C showing T_m (entry 18, Table 2).

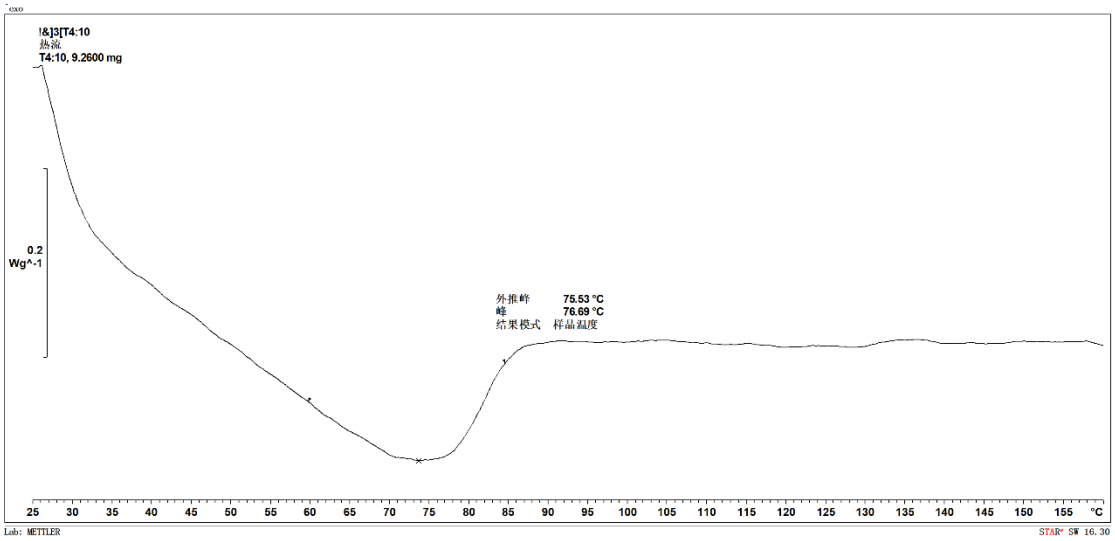

Figure S73. DSC curve of obtained polyethylene using **NiBr-Cl** at 100 °C showing T_m (entry 19, Table 2).

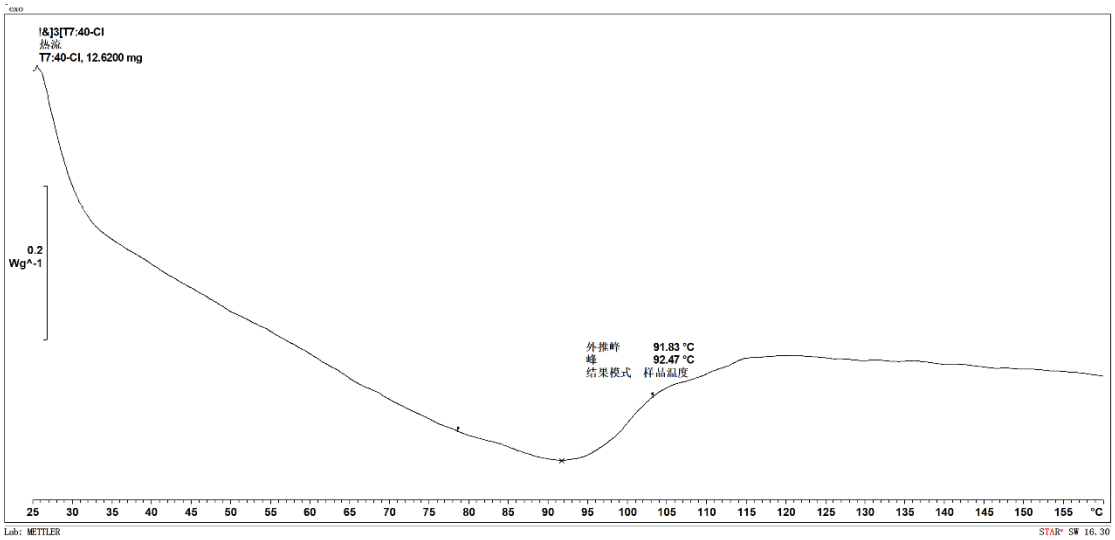

Figure S74. DSC curve of obtained polyethylene using **NiCl-Et** at 40 °C showing T_m (entry 25, Table 2).

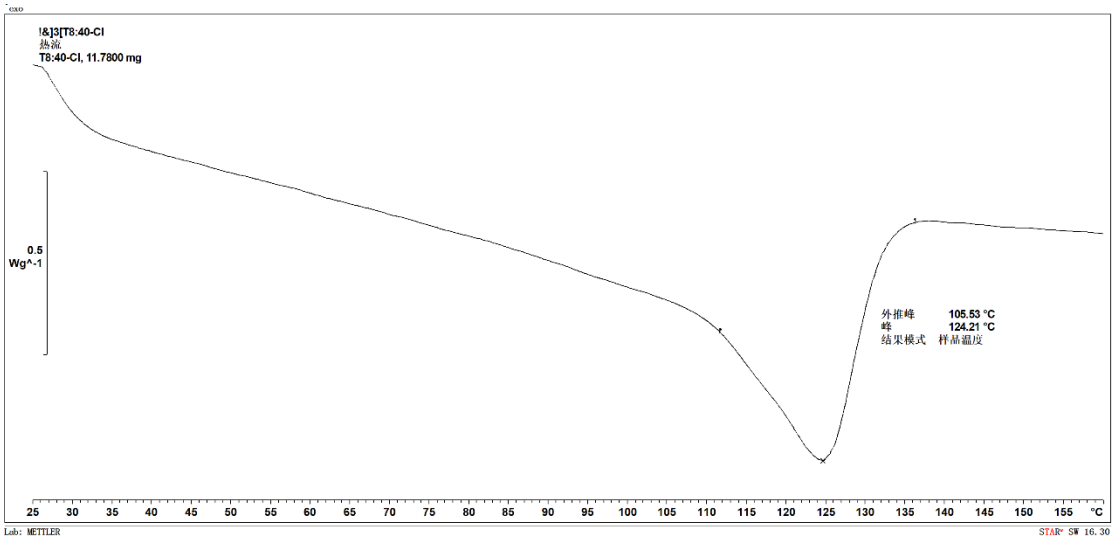

Figure S75. DSC curve of obtained polyethylene using **NiCl-Cl** at 40°C showing T_m (entry 27, Table 2).

11. Wide-angle X-ray diffraction (WAXD) spectra of the polyethylene

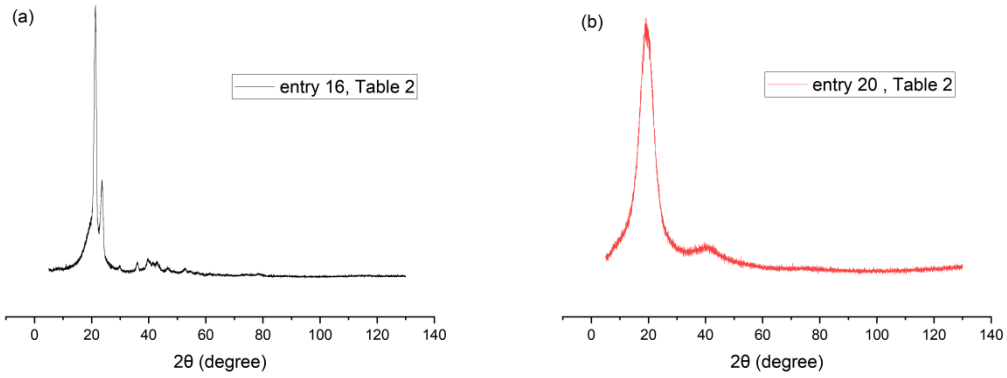

Figure S76. Wide-angle X-ray diffraction (WAXD) spectra of the polyethylene produced by (a) NiBr-Cl (entry 16, Table 2) and (b) NiBr-iPr3 (entry 20, Table 2).

12. ESI-MS spectra of ligands, and their nickel complexes

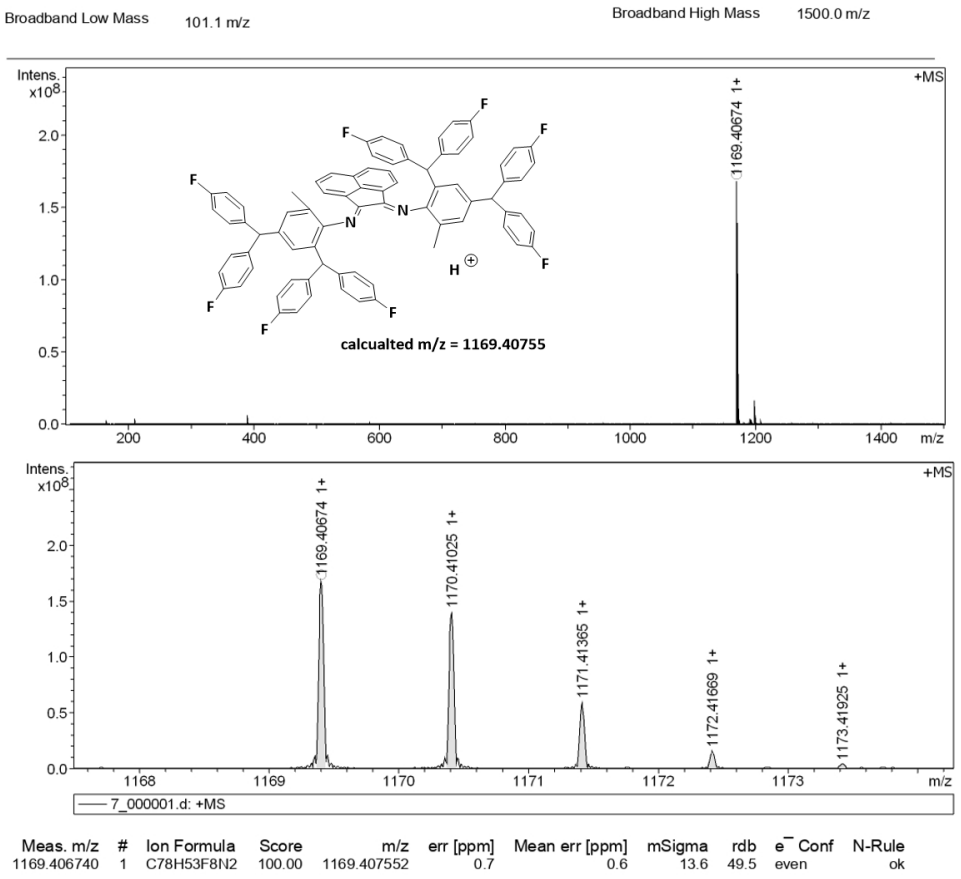

Figure S77. ESI-MS spectrum of L-Me

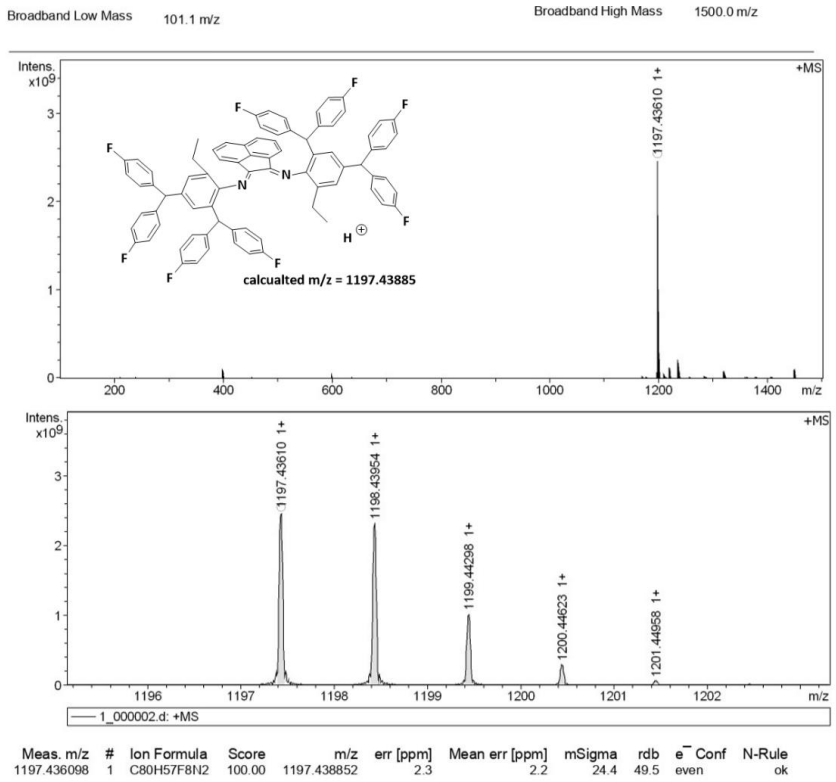

Figure S78. ESI-MS spectrum of L-Et

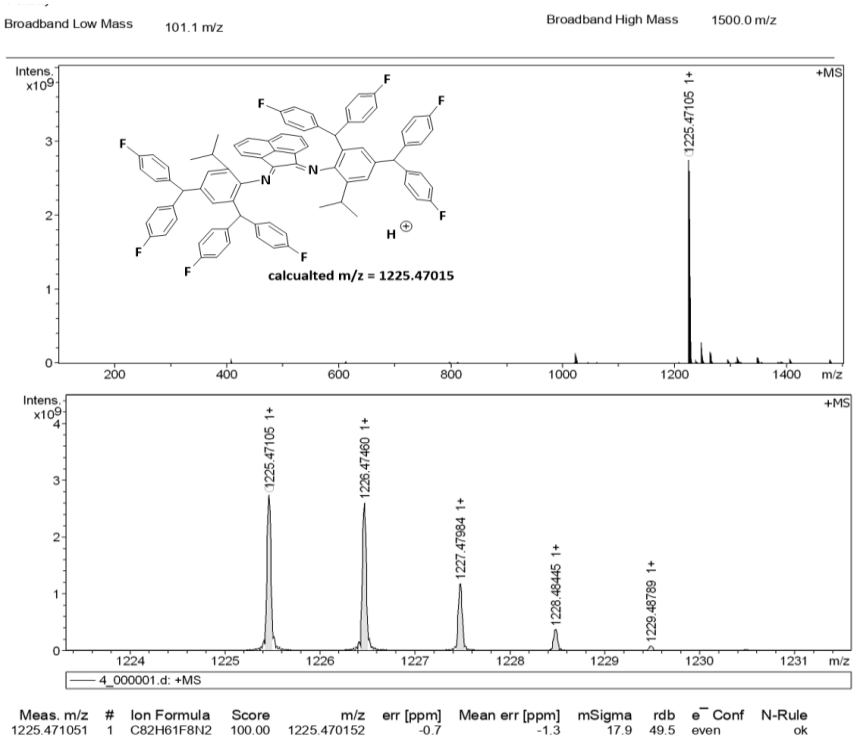

Figure S79. ESI-MS spectrum of L-iPr

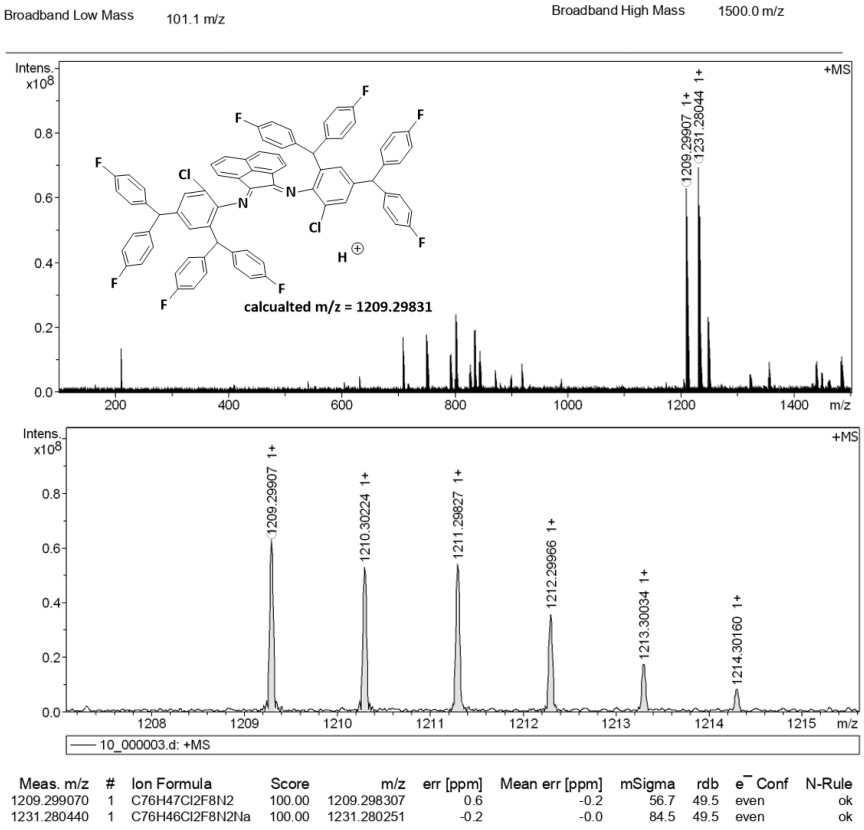

Meas. m/z	#	Ion Formula	Score	m/z	err [ppm]	Mean err [ppm]	mSigma	rdb	e⁻ Conf	N-Rule
1209.299070	1	C76H47Cl2F8N2	100.00	1209.298307	0.6	-0.2	56.7	49.5	even	ok
1231.280440	1	C76H46Cl2F8N2Na	100.00	1231.280251	-0.2	-0.0	84.5	49.5	even	ok

Figure S80. ESI-MS spectrum of L-Cl

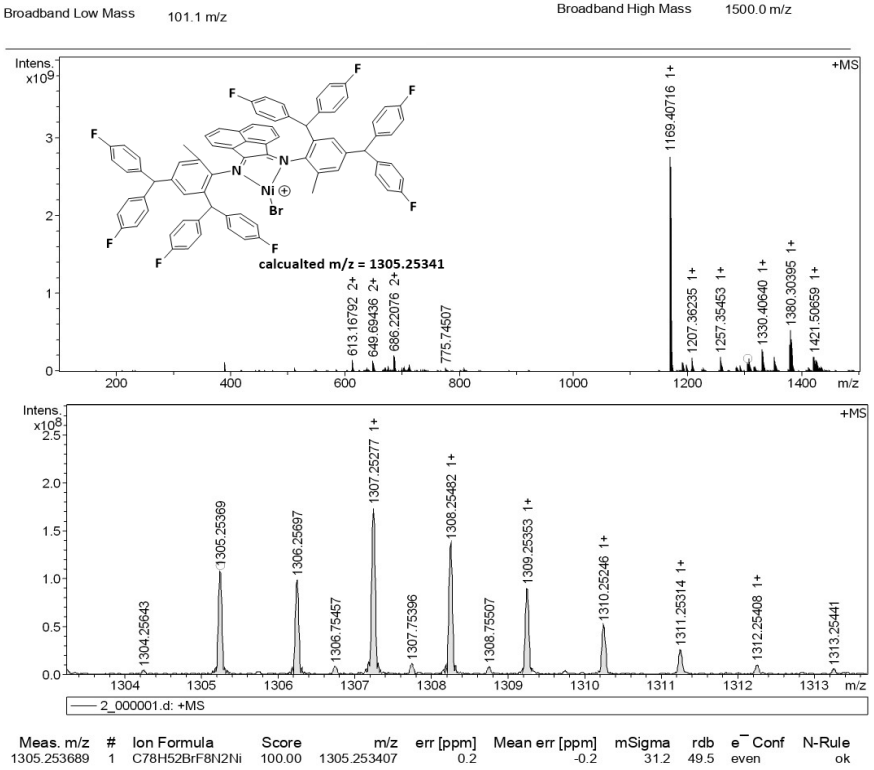

Meas. m/z	#	Ion Formula	Score	m/z	err [ppm]	Mean err [ppm]	mSigma	rdb	e⁻ Conf	N-Rule
1305.253689	1	C78H52BrF8N2Ni	100.00	1305.253407	0.2	-0.2	31.2	49.5	even	ok

Figure S81. ESI-MS spectrum of NiBr-Me

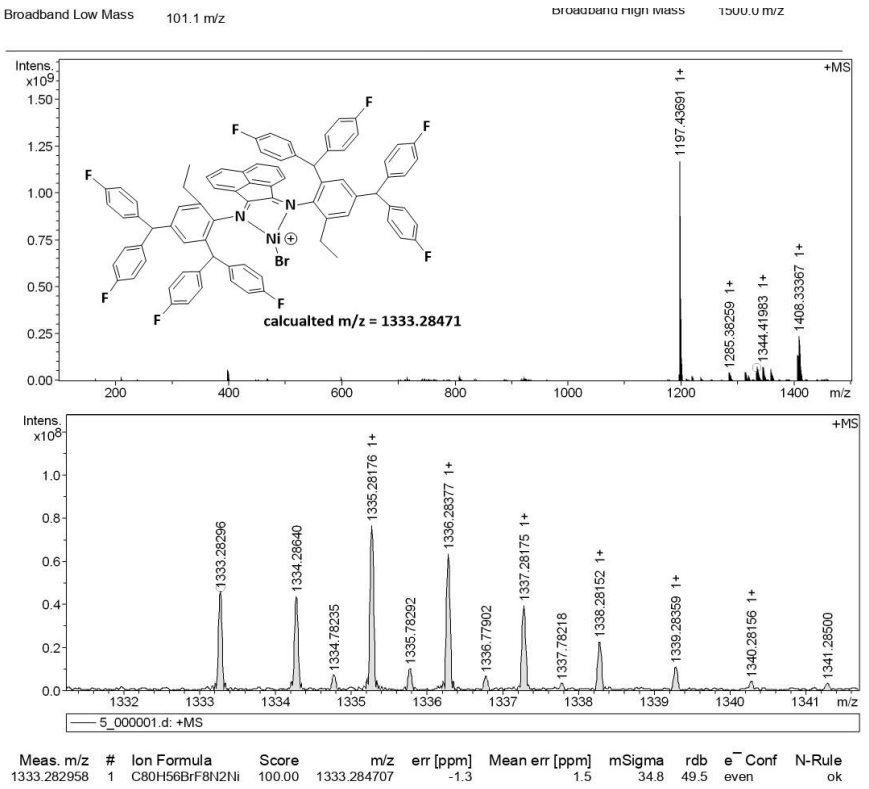

Figure S82. ESI-MS spectrum of NiBr-Et

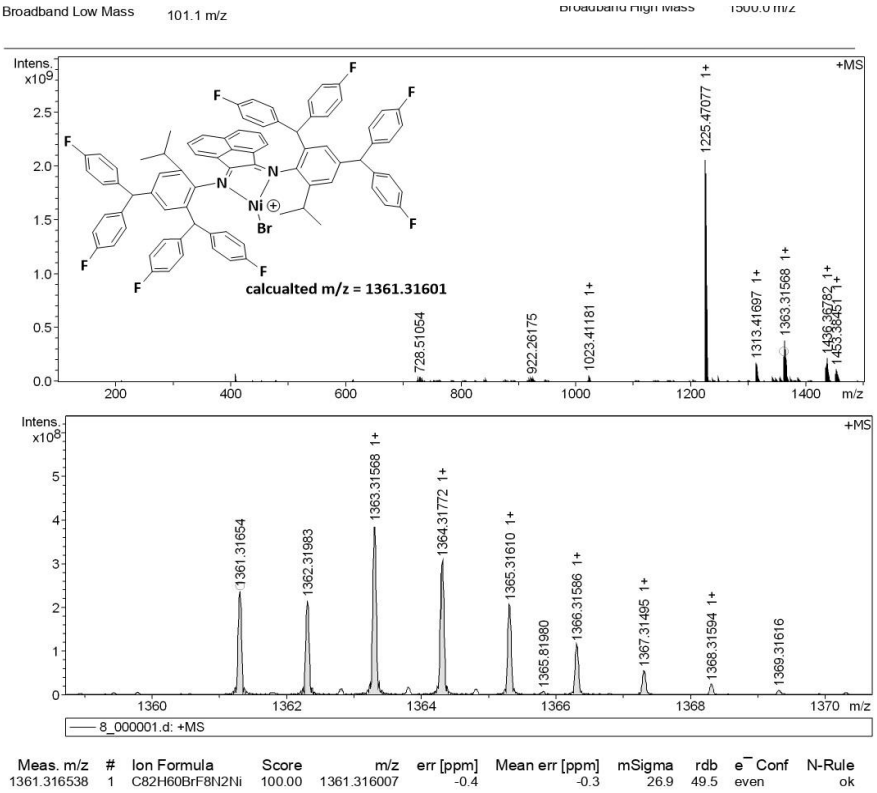

Figure S83. ESI-MS spectrum of NiBr-iPr

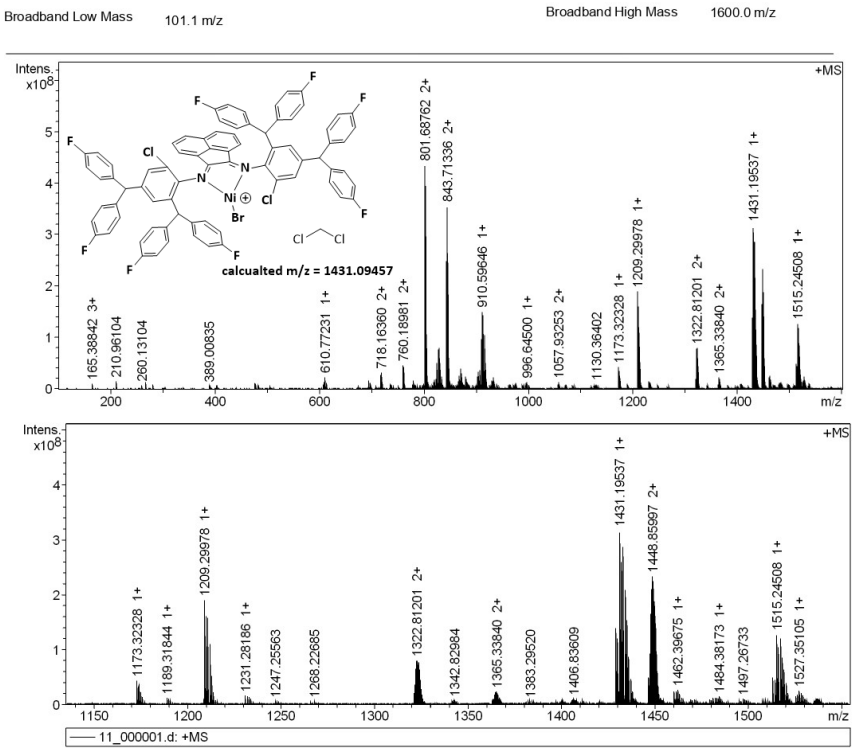

Figure S84. ESI-MS spectrum of NiBr-Cl

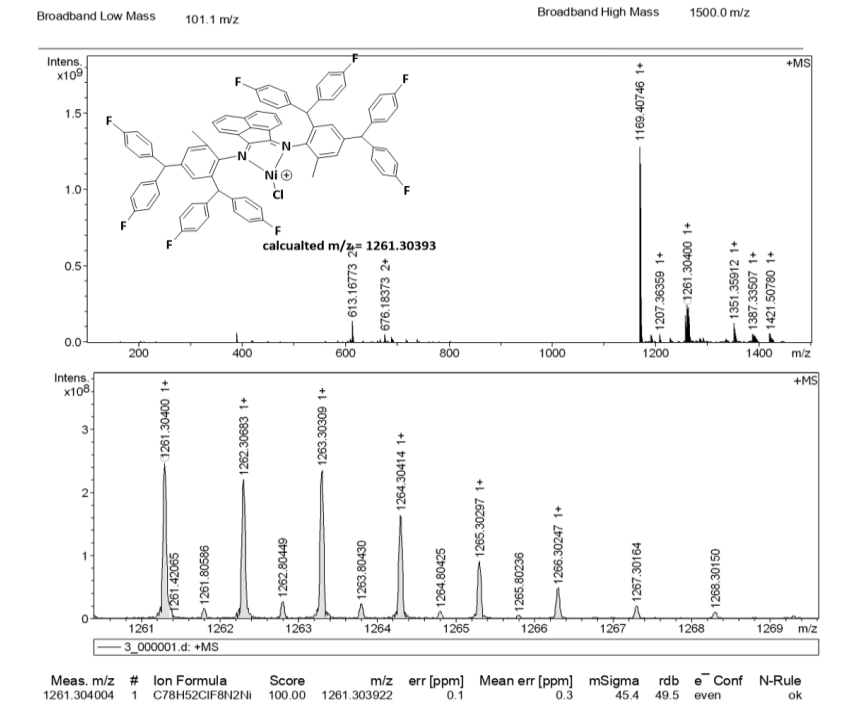

Figure S85. ESI-MS spectrum of NiCl-Me

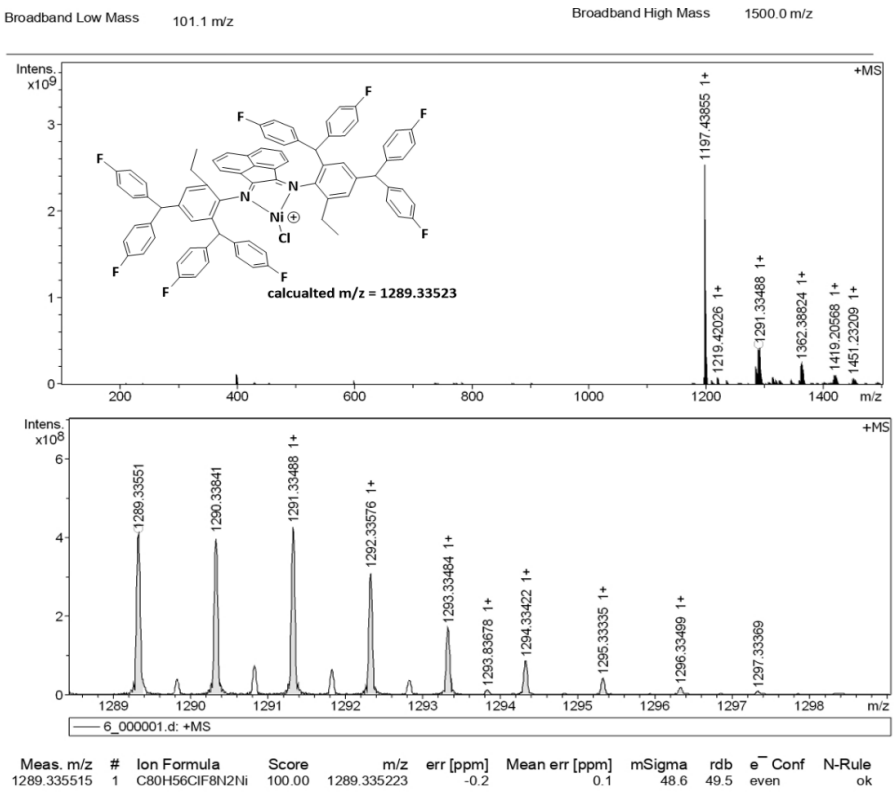

Figure S86. ESI-MS spectrum of NiCl-Et

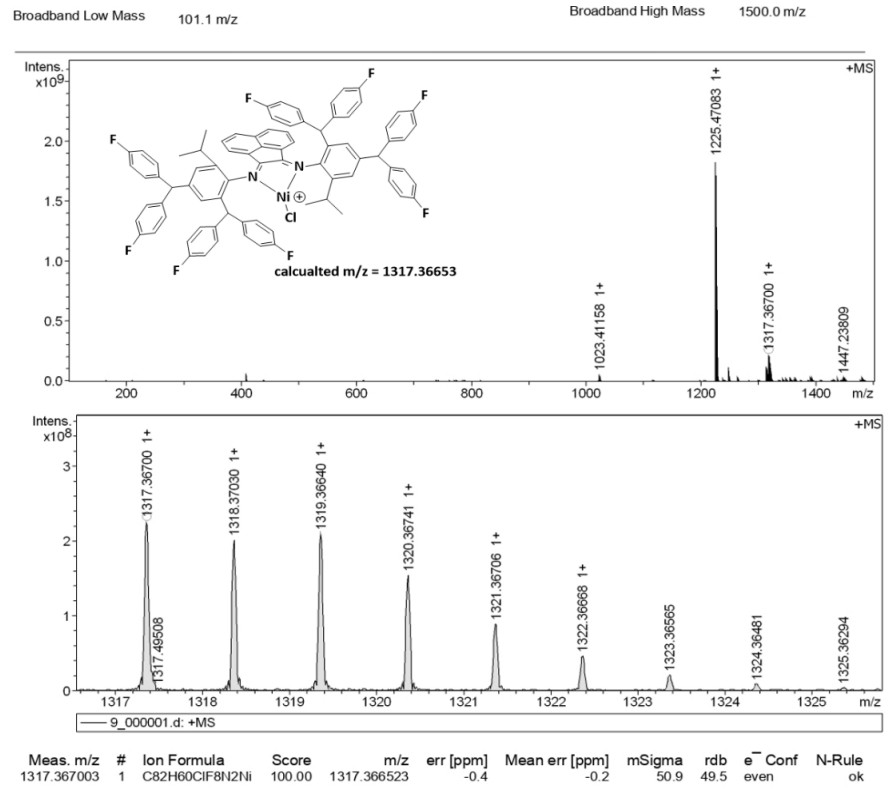

Figure S87. ESI-MS spectrum of NiCl-iPr

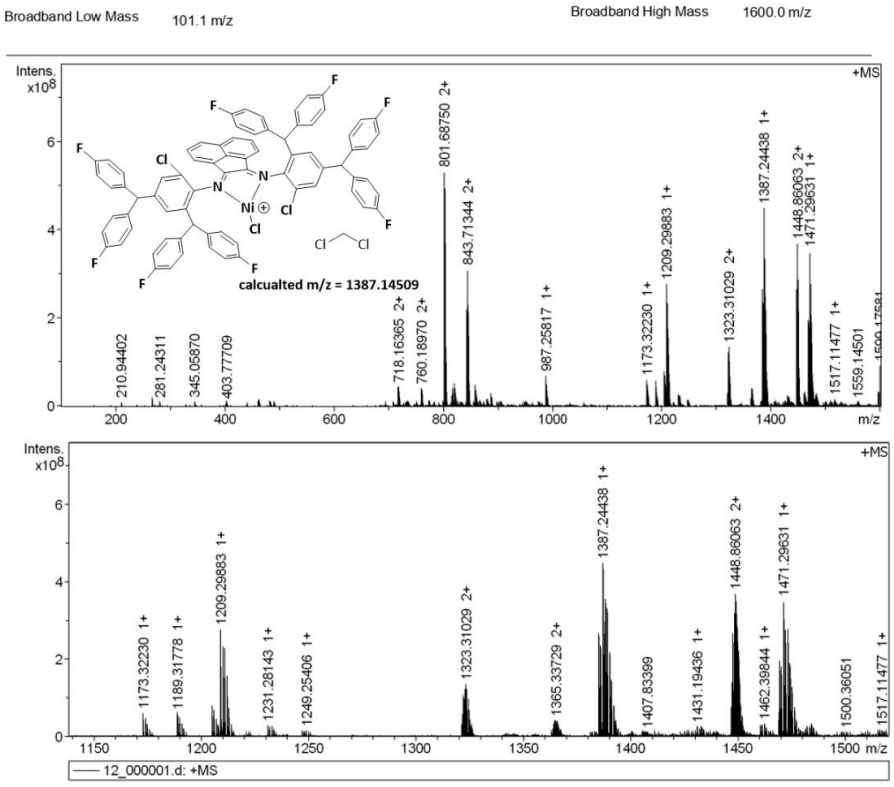

Figure S88. ESI-MS spectrum of NiCl-Cl

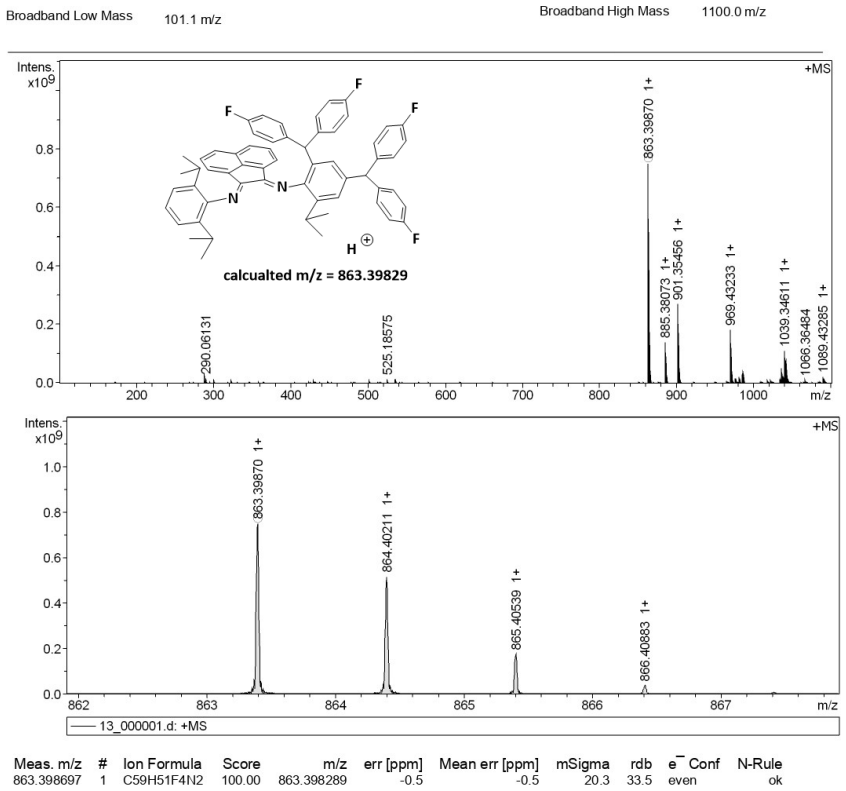

Meas. m/z	#	Ion Formula	Score	m/z	err [ppm]	Mean err [ppm]	mSigma	rdb	e⁻ Conf	N-Rule
863.398697	1	C59H51F4N2	100.00	863.398289	-0.5	-0.5	20.3	33.5	even	ok

Figure S89. ESI-MS spectrum of L-iPr$_3$

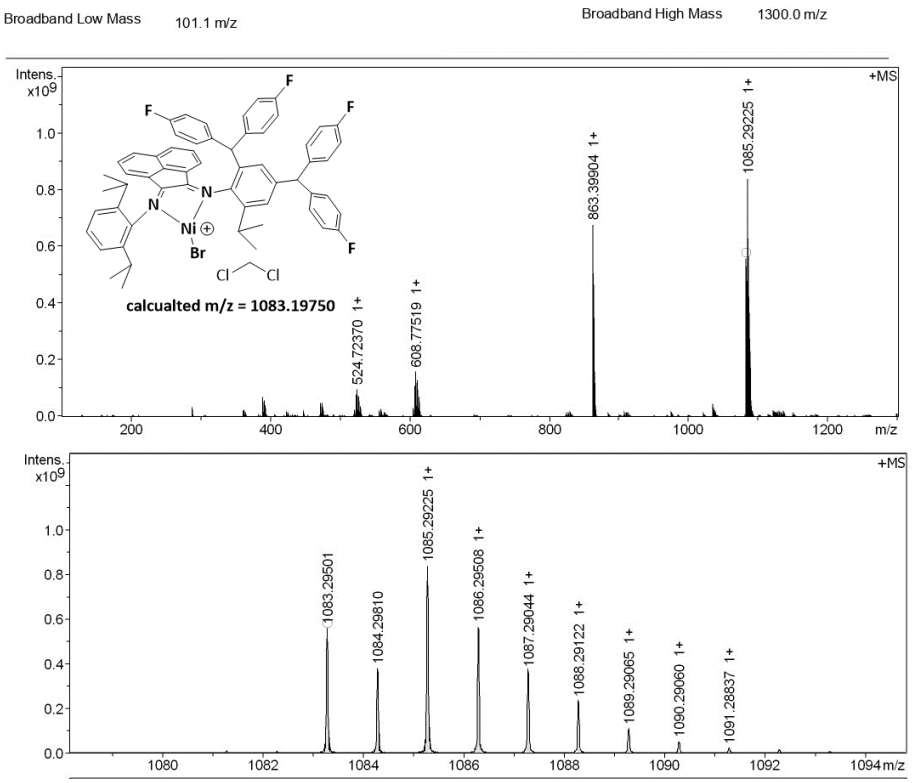

Figure S90. ESI-MS spectrum of NiBr-iPr$_3$

13. References

[1] Q. Muhammad, C. Tan and C. Chen, Concerted steric and electronic effects on α-diimine nickel- and palladium-catalyzed ethylene polymerization and copolymerization, Sci. Bull. 65 (2020) 300-307.

[2] G, M.; Sheldrick, SHELXTL-97, Program for the Refinement of Crystal Structures, University of Göttingen, Göttingen, Germany (1997).